PHYLOGENY OF GEOPHAGINE CICHLIDS FROM SOUTH AMERICA

(PERCIFORMES: LABROIDEI)

A Dissertation

by

HERNÁN LÓPEZ FERNÁNDEZ

Submitted to the Office of Graduate Studies of
Texas A&M University
in partial fulfillment of the requirements for the degree of

DOCTOR OF PHILOSOPHY

August 2004

Major Subject: Wildlife and Fisheries Sciences

PHYLOGENY OF GEOPHAGINE CICHLIDS FROM SOUTH AMERICA

(PERCIFORMES: LABROIDEI)

A Dissertation

by

HERNÁN LÓPEZ FERNÁNDEZ

Submitted to Texas A&M University
in partial fulfillment of the requirements
for the degree of

DOCTOR OF PHILOSOPHY

Approved as to style and content by:

Kirk O. Winemiller (Co-Chair of Committee)	Rodney L. Honeycutt (Co-Chair of Committee)
Melanie L. J. Stiassny (Member)	John D. McEachran (Member)
James B. Woolley (Member)	Lee A. Fitzgerald (Member)

Robert D. Brown
(Head of Department)

August 2004

Major Subject: Wildlife and Fisheries Sciences

ABSTRACT

Phylogeny of Geophagine Cichlids from South America (Perciformes: Labroidei).

(August 2004)

Hernán López Fernández, B.S., Universidad de Los Andes, Venezuela

Co-Chairs of Advisory Committee: Dr. Kirk O. Winemiller
Dr. Rodney L. Honeycutt

Three new species of cichlid fishes of the genus *Geophagus*, part of the Neotropical subfamily Geophaginae, are described from the Orinoco and Casiquiare drainages in Venezuela. Phylogenetic relationships among 16 genera and 30 species of Geophaginae are investigated using 136 morphological characters combined with DNA sequences coding for the mitochondrial gene NADH dehydrogenase subunit 4 (ND4) and the nuclear Recombination Activating Gene 2 (RAG2). Data from previous studies are integrated with the new dataset by incorporating published DNA sequences from the mitochondrial genes cytochrome *b* and 16S and the microsatellite flanking regions *Tmo-M27* and *Tmo-4C4*. Total-evidence analysis revealed that Geophaginae is monophyletic and includes eighteen genera grouped into two major clades. In the first clade, the tribe Acarichthyini (genera *Acarichthys* and *Guianacara*) is sister-group to a clade in which *Gymnogeophagus*, '*Geophagus' steindachneri*, and *Geophagus* sensu stricto are sister to '*Geophagus' brasiliensis* and *Mikrogeophagus*; all these are in turn sister-group to *Biotodoma*, *Dicrossus* and *Crenicara*. In the second clade, *Satanoperca*, *Apistogramma* (including *Apistogrammoides*), and *Taeniacara* are sister to *Crenicichla* and *Biotoecus*. Monophyly and significantly short branches at the base of the phylogeny indicate that genera within Geophaginae differentiated rapidly within a relatively short period. High morphological, ecological, and behavioral diversity within the subfamily suggest that geophagine divergence may be the result of adaptive radiation.

In memory of Mom, to Dad, to Diego

In memory of “El Chino” Foong

To Don Taphorn

ACKNOWLEDGEMENTS

I am indebted to a large number of people and institutions without whom this dissertation would remain just an idea. Above all, Kirk Winemiller, Rodney Honeycutt, and Melanie Stiassny have been involved to such extent that I feel this work is as much theirs as it is mine, although all mistakes and opinions are product of my stubbornness. Kirk started it all when he invited me to be his student some seven years ago, and since then, he has been advisor, professor, colleague, and friend. In Texas, and from Venezuela to West Africa, the times spent with Kirk will remain some of the best and more stimulating of my life. Rodney has been gracious enough to frequently exchange mammals for cichlids with an enthusiasm and passion that turns research into an adventure. Working with him has been one of the most fortunate and inspiring turns of this research. Melanie took this project as her own from the beginning and has made sure that everything I ever needed was there for me, from lessons on anatomy and systematics to lessons on life. It has been an honor to work with all of them and to come to see them as colleagues, friends, and role models. John McEachran, Jim Woolley, and Lee Fitzgerald formed the rest of a superb committee. Thoughts from classes and many conversations with all of them are present everywhere in this dissertation, and have shaped many of my thoughts about fish, systematics, and evolution.

Working with a group of fishes that spans an entire continent was possible only through the help of many museums and willing friends and colleagues that loaned specimens and/or collected tissues. For the loan of specimens from their collections, I am grateful to Melanie Stiassny (American Museum of Natural History, New York), Donald Taphorn (Museo de Ciencias Naturales de Guanare, Venezuela), Erica Pellegrini Caramaschi and Paulo Buckup (Museu Nacional do Rio de Janeiro, Brazil), Patrice Pruvost and Yves Fermon (Museum National d'Histoire Naturelle, Paris), Patrick Campbell (The Natural History Museum, London), John McEachran (Texas Cooperative Wildlife Collection, College Station), Frank Pezold (Northeastern Louisiana University, Monroe), and Roberto Reis (Museu de Zoologia do PUCRS, Porto Alegre, Brazil). For

providing tissue samples for DNA sequencing, I am indebted to Nate Lovejoy and Stuart Willis (University of Manitoba, Canada), Izeni Farias (Universidade do Amazonas, Brazil), Angela Ambrosio and Eloísa Revaldaves (Universidade Estadual de Maringá, Brazil), and Yves Fermon (Museum National d'Histoire Naturelle, Paris). Collections in the field were possible thanks to the help of Kirk Winemiller, Albrey Arrington, Stuart Willis, Craig Layman, Tom Turner, José Vicente Montoya, David Hoeinghaus, Carmen Montaña, Leslie Kelso-Winemiller, Jennifer Arrington, and Hugo López. Fishing permits in Venezuela were granted by the Servicio Autónomo para los Recursos Pesqueros y Acuícolas of the Venezuelan Ministerio del Ambiente.

Funding for the field portion of this research came mostly through grants from the National Geographic Society and the National Science Foundation to Kirk Winemiller. DNA sequencing and other laboratory research was funded partially by a Jordan Endowment Fund from the American Cichlid Association, a faculty mini-grant from Texas A&M University to Kirk Winemiller, and grants from the National Science Foundation to Rodney Honeycutt. Research on cichlid morphology was partially possible thanks to a Collection Study Grant from the American Museum of Natural History and two Axelrod Fellowships from the Department of Ichthyology at the American Museum.

I have been fortunate to interact with many friends and colleagues that made this experience much more than just graduate school. In the Winemiller lab, years of morning coffee with Albrey Arrington were an intellectual treat and built a strong friendship. Stuart Willis was partner of many an adventure and remains an unconditional friend and colleague. I benefited enormously from the time spent with David Jepsen, José Vicente Montoya, David Hoeinghaus, Craig Layman, Senol Akin, Jenny Birnbaum, and Steve Zeug. In the Honeycutt lab, I could not have done anything if April Harlin and Diane Rowe had not been willing to drop everything to help a clumsy beginner to grasp the basics of PCR and DNA sequencing. Joe Gillespie offered invaluable help with the alignment of mitochondrial ribosomal sequences. Discussions with April Harlin, Anthony Cognato, Diane Rowe, Iván Castro, Stuart Willis, Joe

Gillespie, Isabel Landim, Brian Langerhans, Cliff Rhuel, Bob Schelly, Izeni Farias, José Vicente Montoya, Thom DeWitt, Larry Frabota, Colleen Ingram, the Systematics Discussion Group, and the Ecology of Adaptive Radiations seminar at Texas A&M have benefited my work and shaped many ideas.

Over the years in College Station I met some truly brilliant people and some have become very close friends. April Harlin and Anthony Cognato, Dawn Sherry, Iván Castro, Kirk and Leslie Winemiller, Don, Lyn and Anne Willis, Al and Pat Gillogly, and Duane and Judy Schlitter have treated me like family. For their friendship of years, I am especially grateful to José Vicente Montoya, Alexandre Garcia, Scott Brandes, Dave Jepsen, Tammy McGuire, Rob Powell, Gage Dayton, Rebecca Belcher, Lance and Eve Fontaine, Magui Mieres, Stacey Allison, and Damion Marx.

Finally, my family and friends from Venezuela have been always close and supportive during this long process. I am deeply grateful to my father, Hugo, and my brother Diego, who saw the beginning of all this, and have believed in me even when I doubted. Don Taphorn started my formal education as an ichthyologist, and has always made sure that I do not stray from the path. María Alexandra Rujano, Luis Gabaldón, Cecilia Rodríguez, Saberio Pérez, Josmary Muñoz, Tatiana Páez, Alfonso Llobet, Mariana Escovar, Ximena Daza, and Jesús Molinari have managed to be close, despite the long distance.

TABLE OF CONTENTS

LIST OF FIGURES

FIGURE Page

FIGURE Page

LIST OF TABLES

CHAPTER I

INTRODUCTION

Cichlid fishes are one of the largest and most diverse families of vertebrates. Their explosive radiations in the East African Great Lakes are some of the most astonishing examples of adaptive radiation among vertebrates (e.g. Barlow 2000; Schluter 2000), and have rightfully become models in the study of evolutionary biology (e.g. Meyer 1993; Stiassny and Meyer 1999; Kornfield and Smith 2000; Verheyen et al. 2003). Unfortunately, interest in the East African radiations has largely eclipsed the study of riverine cichlids, and little is known about the evolution of this large portion of the family. Fluviatile cichlids are highly diverse, and new species are continually described from West and Central Africa (e.g. Lamboj and Snoeks 2000; Lamboj and Stiassny 2003; Lamboj 2004;), and especially from the Neotropics (e.g. Kullander 1980; 1986; 1988; 1989; 1990; Kullander et al. 1992; Lucena and Kullander 1992; López-Fernández and Taphorn 2004). According to Reis et al. (2003), 406 species of Neotropical cichlids were described by the end of the year 2002, and they estimated another 165 remaining to be described.

This dissertation provides a systematic analysis of the Neotropical cichlid subfamily Geophaginae, offering the most resolved genus-level phylogeny available to date. Clarification of phylogenetic relationships within the geophagine clade is required for studying the evolutionary biology of these ecologically and morphologically diverse cichlids. The present work establishes the systematic foundation for comparative study of the evolution of geophagine diversity. Chapter I summarizes the status of systematic knowledge of geophagine cichlids, briefly describes geophagine taxonomic diversity, and introduces the remarkable ecological, behavioral, and morphological diversity of the clade. This chapter aims to highlight the potential of geophagines as a model system for

---

This dissertation follows the style and format of Evolution.

the study of evolutionary ecology of riverine tropical fishes. Chapter II provides a description of 3 new species of *Geophagus* from the Orinoco and Casiquiare drainages of Venezuela (López-Fernández and Taphorn 2004). This chapter underscores the need for intense taxonomic work on geophagine cichlids, and provides an example of how to use taxonomic descriptions as summaries of knowledge about particular taxa. When presented in this manner, species descriptions provide a starting point for future biological research. The establishment of a phylogeny provides an interpretive framework for detailed studies of geophagine evolution, therefore, chapters III and IV pertain to the reconstruction of phylogenetic relationships within Geophaginae. Chapter III is a molecular study of phylogenetic relationships derived from analyses of combined mitochondrial and nuclear DNA sequences. This chapter also includes a comparison of relative rates of molecular evolution among Neotropical cichlid clades, especially among geophagine genera. Finally, the phylogenetic evidence is used to evaluate the hypothesis that patterns of divergence within these Neotropical riverine cichlids provide evidence of an adaptive radiation. Chapter IV explores geophagine relationships with the combined analysis of molecular and morphological characters. This is the first comprehensive total-evidence analysis of a Neotropical cichlid clade. The relative contribution of different kinds of data and congruence among partitions are analyzed, and a provisional, but completely resolved, phylogeny of Geophaginae is proposed. Finally, taxonomic and evolutionary implications of the proposed phylogeny are addressed, as well as aspects of cichlid evolution that may affect our ability to recover a strongly supported geophagine phylogeny. Chapter V summarizes the main conclusions of this study, and suggests an integrative approach for studying the evolutionary history of the geophagine adaptive radiation.

SYSTEMATICS OF NEOTROPICAL CICHLIDS

Several informal attempts have been made to classify the genera of the American Cichlidae (e.g. Kullander 1983; 1986; 1996; Kullander and Nijssen 1989; Kullander and Silfvergrip 1991). Only recently, however, formal cladistic analyses of the Neotropical clades have been carried on by Kullander (1998) and Farias et al. (1998; 1999; 2000; 2001), leading to some understanding of high-level relationships among major groups (see also Stiassny 1991; Casciotta and Arratia 1993). Using a morphology-based phylogeny, Kullander (1998) subdivided the Neotropical Cichlidae and the African genus *Heterochromis* into six subfamilies and several tribes. The subfamilies Retroculinae (genus *Retroculus*) and Cichlinae (*Cichla*, *Crenicichla*, and *Teleocichla*) constituted the basal clades of the American assemblage. Heterochromidinae (*Heterochromis*) was nested between these two and Astronotinae (*Astronotus* and *Chateobranchus*), which constituted the sister group to the rest of the Neotropical assemblage. The more derived subfamilies, Geophaginae and Cichlasomatinae, included all the remaining genera within the American cichlids. Cichlasomatinae comprised three tribes (Acaroniini, Heroini, and Cichlasomatini), and included more than 25 genera. Geophaginae were divided into three tribes: Acarichthyini (genera *Acarichthys* and *Guianacara*), Crenicaratini (*Biotoecus, Crenicara, Dicrossus*, and *Mazarunia*), and Geophagini (*Geophagus, Mikrogeophagus, 'Geophagus' brasiliensis, 'Geophagus' steindachneri, Gymnogeophagus, Satanoperca, Biotodoma, Apistogramma, Apistogrammoides* and *Taeniacara*). Recent molecular (Farias et al. 1999) and total evidence analyses including Kullander's morphological data (Farias et al. 2000; 2001) showed *Heterochromis* to be part of a monophyletic African clade, which in turn is sister to the entire Neotropical assemblage. Additionally, *Crenicichla* was nested within Geophaginae, and *Chaetobranchus* and *Chaetobranchopsis* were weakly placed between Geophaginae and Cichlasomatinae. Despite the contribution of these analyses to the clarification of higher-level relationships, the lack of relevant taxa limits the phylogenetic resolution of these studies and leaves many questions of geophagine

relationships unanswered. Although geophagine monophyly seems indisputable, there is considerable disagreement between morphological and molecular evidence when analyzed separately, and the relationships within Geophaginae are not clear.

Kullander (1998) defined Geophaginae based on the combination of six ambiguous morphological synapomorphies that appear together only in that clade but are individually observed in other Neotropical taxa. Within the subfamily, the tribe Crenicaratini is diagnosed by seven non-unique synapomorphies and contains small species with many autapomorphic characters and loss of osteological features (Kullander 1990). This condition may be related to the small size, and difficulties in determining homology could complicate the establishment of valid relationships (Buckup 1993). Unfortunately, Farias et al.'s studies (2000; 2001) included either *Crenicara* or *Biotoecus*, but never analyzed them together, and failed to include *Dicrossus*, thus leaving Crenicaratini monophyly untested. Kullander's Acarichthyini were characterized by two unique synapomorphies, and monophyly is supported by most molecular and combined evidence (Farias et al. 1999; 2000). The tribe Geophagini was characterized by the combination of four synapomorphies, two of them unambiguous. This clade was relatively well supported by morphological features (Kullander 1998), especially by the possession of an epibranchial lobe, a laminar, anteroventral expansion of the first epibranchial bone, supporting a connective tissue pad (Kullander's character 5, state 1). No other group of cichlids or any other fish group is known to bear such a structure (Kullander 1998). The epibranchial lobe of the Geophagini is probably present in the Crenicaratini, but it is not clear from Kullander's (1998) character descriptions if he considers the structures in both groups as homologous. Kullander's analysis was based on an extensive taxon sampling of cichlids, and his proposed geophagine relationships were based on the analysis of 13 genera of geophagines (sensu Kullander) plus *Crenicichla* and *Teleocichla*. The studies of Farias et al. (1999; 2000; 2001) are not suited for testing Kullander's hypothesis, because taxon sampling is insufficient. Farias et al. (2000) included only 11 genera in their molecular total evidence analysis and 9 in the combined analysis of molecular and morphological data. Their second (Farias et al.

2001) study included just 8 of the 18 genera of Geophaginae. All their total evidence analyses lacked the genera *Satanoperca*, *Biotoecus*, *Crenicara, Dicrossus*, and the *'Geophagus' steindachneri* group, and several additional genera were present in some analyses but absent in others (Farias et al. 2000; 2001). Clearly, exclusion of these taxa makes it impossible to test the monophyly of Kullander's (1998) tribes Crenicaratini and Geophagini, and impedes further resolution of internal relationships within the subfamily. Better taxon sampling and incorporation of new data are requisites to clarify relationships within Geophaginae.

TAXONOMIC, ECOMORPHOLOGICAL, AND REPRODUCTIVE DIVERSITY OF GEOPHAGINAE

Geophaginae is a mostly South American clade that includes 18 genera and over 180 described species (Kullander 2003), with many remaining to be described (Weidner 2000). Only two species in the *'Geophagus' steindachneri* group (*'G.' pellegrini* and *'G.' crassilabris*) reach the southern portion of Panama, and the genus as a whole has a trans-Andean distribution, with the Lake of Maracaibo being its eastern-most limit. All other genera are exclusively South American. Only *Satanoperca* (7 described species), *Crenicichla* (74), and *Apistogramma* (53) are common in the Orinoco, Amazonas, La Plata, and the Guianas basins, with the remaining genera having more restricted ranges. *Geophagus* sensu stricto (14), *Biotodoma* (2), *Biotoecus* (2), *Dicrossus* (2), and *Mikrogeophagus* (2) are present in both the Orinoco and Amazonas basins, although the latter has a disjunct distribution, being in the Orinoco and the upper Madeira drainages, but not in the main Amazon stem. *Guianacara* (4) is present in black waters of the Orinoco basin and in the Guianas. *Acarichthys* (1) is widespread in the Amazon and the Guianas, and *Crenicara* (2) and *Apistogrammoides* (1) are restricted to the Amazon. The *'Geophagus' brasiliensis* group (4) is restricted to the Atlantic drainages of Brazil and Uruguay, and *Gymnogeophagus* (9) is present only in the La Plata basin (i.e. Paraguay, Uruguay and Paraná drainages). The remaining genera have very localized

distributions, with *Taeniacara* (1) being known only from the Rio Negro (Brazil), *Mazarunia* from the Mazaruni river (Guyana), and *Teleocichla* (7) from the Rio Xingu (Brazil) (see Kullander 2003 for more details on distribution).

A common phenomenon in the history of geophagine taxonomy was the description of genera and species with broad distributions, sometimes spanning almost all of South America (e.g. *Geophagus* Heckel, *Geophagus surinamensis* (Bloch 1791), *Satanoperca jurupari* (Heckel 1840), see Gosse 1975). Recent taxonomic work, however, has revealed that these widely distributed genera and species actually included large numbers of unrecognized taxa (e.g. Kullander 1983; 1986; Kullander and Nijssen 1989; López-Fernández and Taphorn 2004). Although taxonomic knowledge of geophagine cichlids has improved significantly in the last three decades (e.g. Kullander 1986, 1988, 1989, 1998; Kullander and Nijssen 1989), a thorough description of geophagine diversity is not available. For example, Kullander's (1986) partial revision of the genus *Geophagus* (sensu Gosse 1975) resurrected the genus *Satanoperca*. Kullander also restricted *Geophagus* to taxa with paired caudal extensions of the swim bladder lined by epihemal ribs, leaving some species of *Geophagus* without formal generic assignment. These species are part of two distinct genera in need of description and, in this study, are treated as the *'Geophagus' steindachneri* and *'Geophagus' brasiliensis* groups, which are distinguished from *Geophagus* sensu stricto (Kullander 1986). Species-level taxonomy also has improved significantly (e.g. references), but large numbers of species are still in need of description. Apparent lack of morphological variation among species seems to be an important factor disguising the high species richness of some genera. For example, the species *Geophagus surinamensis* was thought to be largely distributed over the Orinoco, Amazon and Guianas drainages, but recent revisions have revealed a complex of 10 described species (Kullander and Nijssen 1989; Kullander et al. 1992; López-Fernández and Taphorn 2004) with many more still in need of description. Recent revisions of museum collections and field exploration in relatively inaccessible places are revealing additional diversity, and many species are known that have not yet been described. Current knowledge of geophagine diversity is

sufficient to establish the generic relationships within the group, and to begin unraveling their potentially complex evolutionary history, but this work needs a parallel and continuous effort of basic taxonomic research, oriented both towards a better understanding of the clade's biology and to its conservation.

In addition to their taxonomic diversity, geophagine cichlids are highly versatile in their ecology, morphology, and reproductive strategies. Much of geophagine morphological variability may be associated with feeding mode and habitat use. The typical geophagine feeding behavior involves sifting of the substrate using the branchial apparatus in a "winnowing" behavior (Laur and Ebeling 1983; Drucker and Jensen 1991), expelling the sand or mud through the opercular openings while food particles are ingested. The epibranchial lobe of some geophagine taxa has been hypothesized to be an adaptation involved in benthic invertebrate feeding, but has never been studied from a functional or ecomorphological point of view (Lowe-McConnell 1991). Other morphological features, such as the ventrally flattened body, and the relatively dorsal position of the eyes are also indication of geophagine substrate-based feeding (e.g. Winemiller et al. 1995). Broad morphological variation exists among substrate-sifting geophagines (e.g. *Geophagus*, *Satanoperca*, *Biotodoma*), and this variation may reflect diversity in feeding mechanics. Some taxa deviate significantly from the general geophagine plan, and have undergone body-size reduction (e.g. *Apistogramma*, *Biotoecus*, *Dicrossus*), possibly involving a change from substrate sifting to invertebrate picking. *Crenicichla* has an elongate body and its feeding habits are predatory, with many piscivorous species. Most Geophaginae are generally found in shallow, clear, or black waters with muddy or sandy bottoms throughout tropical and subtropical South America (e.g. Lowe-McConnell 1969; 1991; Goulding 1988; Weidner 2000). Within this general kind of habitat, however, there is extensive variation. Large bodied substrate sifters are usually associated to relatively open waters with little structure and slow currents (e.g. *Geophagus*, *Satanoperca*), whereas dwarf taxa tend to be associated with very shallow water and highly complex structure formed by leaf-litter and woody debris (e.g. *Biotoecus*, *Apistogramma*). Some taxa inhabit clear, relatively deep waters

in association with rocky shores (e.g. *Guianacara*) or fast currents (e.g. *Teleocichla*). Life histories among geophagines are also highly variable, and their reproductive biology and parental care behaviors include numerous variations of a generalized equilibrium strategy involving high reproductive investment (Winemiller and Taphorn 1989; Winemiller and Rose 1993). Typical monogamous pairs with substrate spawning are found in *Crenicichla*, *Biotodoma*, *Guianacara*, and several species of other genera (e.g. Cichocki 1976; 1977; Weidner 2000). *Geophagus*, *Gymnogeophagus*, *'Geophagus' brasiliensis*, and some species of *Satanoperca* take either the eggs or larvae into one or both parents' mouth for incubation (e.g. Weidner 2000; López-Fernández and Taphorn 2004). Species of the *'Geophagus' steindachneri* group are polygynous, and the eggs are fertilized after the female takes them in her mouth (Weidner 2000). "Dwarf" geophagines can be typical substrate spawners (e.g. *Biotoecus*) or polygynous harem-forming (*Apistogramma*) (e.g. Linke and Staeck 1984; Barlow 2000). *Crenicara punctulatum* is a protogynous species in which social structure may influence sex change (Carruth 2000). Integration of geophagine morphological, ecological, and behavioral diversity into a coherent picture of the group's evolutionary history can only be done in an explicit phylogenetic context, and providing this context is the central goal of this dissertation.

CHAPTER II

Geophagus abalios, G. dicrozoster AND *G. winemilleri* (PERCIFORMES: CICHLIDAE), THREE NEW SPECIES FROM VENEZUELA*

INTRODUCTION

Gosse (1975) divided the South American genus *Geophagus* Heckel into several genera based on the number of supraneural bones. *Biotodoma* Eigenmann & Kennedy has 2 supraneurals, *Gymnogeophagus* de Miranda-Ribeiro has 0 and *Geophagus* has 1. Gosse's definitions were later revised by Kullander (1986), who resurrected *Satanoperca* (Heckel) as distinct from *Geophagus*, and restricted the latter to include only species with paired caudal extensions of the swim bladder lined by 6-12 epihemal "ribs", and more caudal than precaudal vertebrae (see also Kullander & Nijssen 1989; Kullander et al. 1992). Kullander's generic assignments have been corroborated by recent phylogenetic analyses of geophagine cichlids (Kullander 1998; Farias et al. 1999, 2000, 2001). As currently recognized, the genus *Geophagus* sensu stricto (Kullander 1986; Kullander & Nijssen 1989) includes eleven described species, and numerous others remain unnamed (e.g. Kullander 1986; Kullander & Nijssen 1989; Kullander et al. 1992; Weidner 2000).

Since Kullander (1986) and Kullander and Nijssen (1989), most populations of *Geophagus* referred to as *G. surinamensis* (Bloch) (Gosse 1975) have been recognized as different taxa. The *Geophagus surinamensis* "complex" includes 7 described species (*G. surinamensis*, *G. brokopondo* Kullander and Nijssen, *G. brachybranchus* Kullander and Nijssen, *G. camopiensis* Pellegrin, *G. proximus* (Castelnau), *G. megasema* Heckel and *G. altifrons* Heckel) and an undetermined number of undescribed species with deep

---

*Reprinted with permission from "*Geophagus abalios*, *G. dicrozoster* and *G. winemilleri* (Perciformes: Cichlidae), three new species from Venezuela," by Hernán López-Fernández and Donald C. Taphorn. Zootaxa 439:1-27. 2004 by Magnolia Press.

bodies and heads, a mid-flank spot of variable size, and either with infraorbital stripe absent (e.g. *G. surinamensis*) or limited to a preopercular black mark (e.g. *G. brachybranchus*). *Geophagus* species outside the *G. surinamensis* complex have a complete infraorbital stripe, including *G. grammepareius* Kullander and Taphorn, *G. taeniopareius* Kullander and Royero, *G. argyrostictus* Kullander *G. harreri* Gosse and probably several undescribed species known to the aquarium trade (Weidner 2000).

Originally described from Surinam (Kullander & Nijssen 1989), *Geophagus brachybranchus* was identified from the Cuyuní drainage by S. O. Kullander and DCT (Taphorn et al. 1997), and is the only described species of the *G. surinamensis* complex known to occur in Venezuela. Other populations of *Geophagus* in the country have traditionally been identified as *G. surinamensis* (e.g. Mago-Leccia 1970; Axelrod 1971; Machado-Allison 1987), which is restricted to the Surinam and Marowijne rivers in eastern Surinam (Kullander & Nijssen 1989), or *G. altifrons* (Royero et al. 1992; Machado-Allison et al. 1993), which has an Amazonian distribution (Kullander 1986). These populations actually represented three undescribed species: two were identified by S. O. Kullander and D. C. Taphorn (1996 unpubl.) and the third by HLF and D. C. Taphorn (2002 unpubl.) during recent surveys of collections at the Museo de Ciencias Naturales de Guanare. Specimens of these three species appear to have been known for some time in the German aquarium trade, and two of them were referred to as *Geophagus* 'stripetail' or *G.* 'Rio Negro I', and *G.* sp "Columbia", respectively (Weidner 2000). In this paper, we described these three new species from the Orinoco and Casiquiare drainages of Venezuela; provide maps of their known distribution, and a key for the identification of the Venezuelan species of *Geophagus*.

MATERIALS AND METHODS

All measurements were taken using dial calipers to the nearest 0.1 mm when linear distance was less than 130 mm, and with a tape measure to the nearest mm when more than 130 mm. Counts of fin rays and scales were made under a dissecting scope.

Counts and measurement procedures follow those described in Kullander (1986) and Kullander and Nijssen (1989). Following Kullander et al. (1992) and Kullander (1996), scales in a horizontal row were counted on the row immediately above that one containing the lower lateral line (E1); rows above E1 (epaxial scales) are numbered E2 and higher, and rows below E1 are numbered H1 (hypaxial scales) and higher (Figure 2.1). Vertebral counts were made from x-rayed and/or cleared and stained specimens following protocols in Dingerkus and Uhler (1977) or Taylor and Van Dyke (1985).

Museum abbreviations: MCNG, Museo de Ciencias Naturales de Guanare, Guanare; AMNH, American Museum of Natural History, New York.

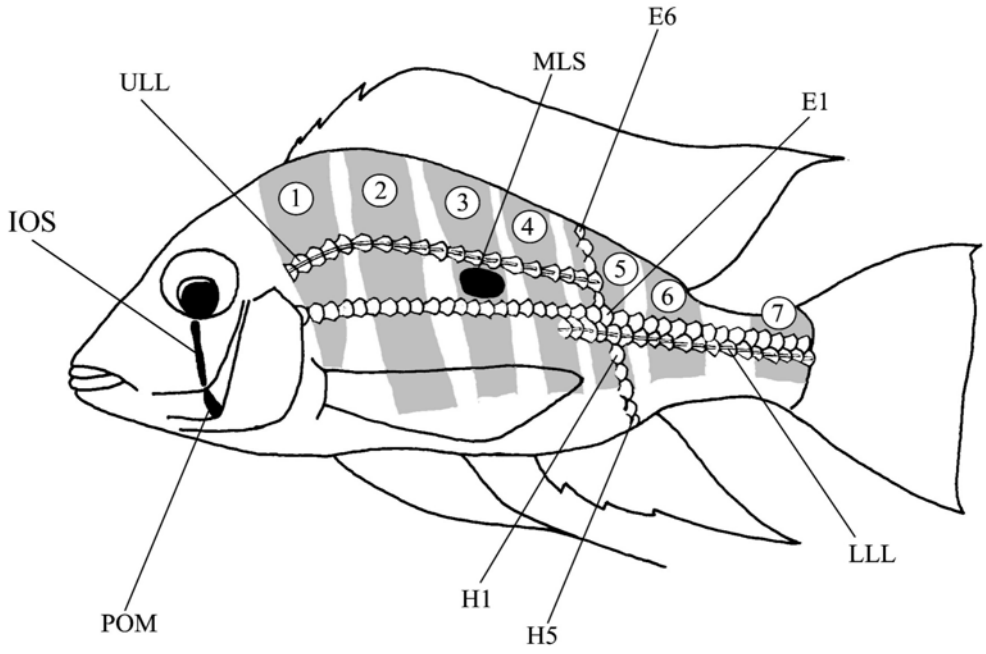

FIG. 2.1. Diagrammatic representation of scale nomenclature, head markings, and lateral bar patterns of *Geophagus* as used in this paper. Abbreviations are as follows: E1, first epaxial longitudinal series of scales, used to count number of longitudinal scales; E6, last epaxial longitudinal series of scales; H1-H5, hypaxial longitudinal series of scales; IOS, infraorbital stripe; MLS, mid-lateral spot; POM, preopercular mark; ULL, upper lateral line; LLL, lower lateral line; 1-7, lateral bars. Scale nomenclature after Kullander (1992, 1996). Infraorbital, preopercular and mid-lateral black markings are observable both in live and preserved specimens; lateral bar patterns are generally visible only on preserved specimens, and sometimes on stressed live specimens.

Geophagus abalios N. SP

Holotype

MCNG 47600, 163.0 mm SL; Venezuela: Apure: Río Cinaruco: Laguna Larga (6.5339°N 67.4150°W); K. Winemiller, H. López-Fernández, D.A. Arrington, L. Kelso-Winemiller, H. López-Chirico and J. Arrington, 1-3 Jan 1999.

Paratypes

MCNG 30939, 3, 86.0-115.0; Venezuela: Anzoátegui: Río Orinoco: Laguna Tineo (8.1903°N 63.4722°W); M.A. Rodríguez, 04 April 1987. - MCNG 33723, 3, 54.3-132.0; Venezuela: Bolívar: Río Orinoco: Laguna Bartolico (7.6417°N 66.1167°W); M.A. Rodríguez, 13 Jan 1987. - MCNG 35035, 1, 74.4 mm SL; Venezuela: Amazonas: Río Casiquiare: Playa Macanilla (2.4331°N 66.4547°W); K.O. Winemiller and D. Jepsen, 31 Jan 1997. - MCNG 40878, 1, 112.1 mm SL; Venezuela: Apure: Río Cinaruco: Laguna Guayaba; D.A. Arrington and J. Arrington, 12 April 1999. - MCNG 41124, 2, 45.5-55.5 mm SL; Venezuela: Apure: Río Cinaruco; D.A. Arrington and J. Arrington 14 April 1999. – AMNH 233634 (ex-MCNG 44865), 1, 96.3 mm SL; Venezuela: Apure: Río Cinaruco (6.5333°N 67.4164°W); D.A. Arrington and J.A. Arrington, 16 March 1999. - MCNG 47602 (ex-MCNG 6278), 1, 151.0 mm SL; Venezuela: Apure: Rio Cinaruco: Hato Las Delicias (6.5750°N 67.2361°W); D.C. Taphorn, C. Lilyestrom and B. Stergios, 11 Jan 1982. – MCNG 47601, 2, 96.3-160.0 mm SL; collected with holotype. - AMNH 93052, 2, 132.9-150.0 mm SL; Venezuela: Amazonas: Río Mavaca: small tributary on left bank; C.J. Ferraris and R. Royero, 10 March 1989.

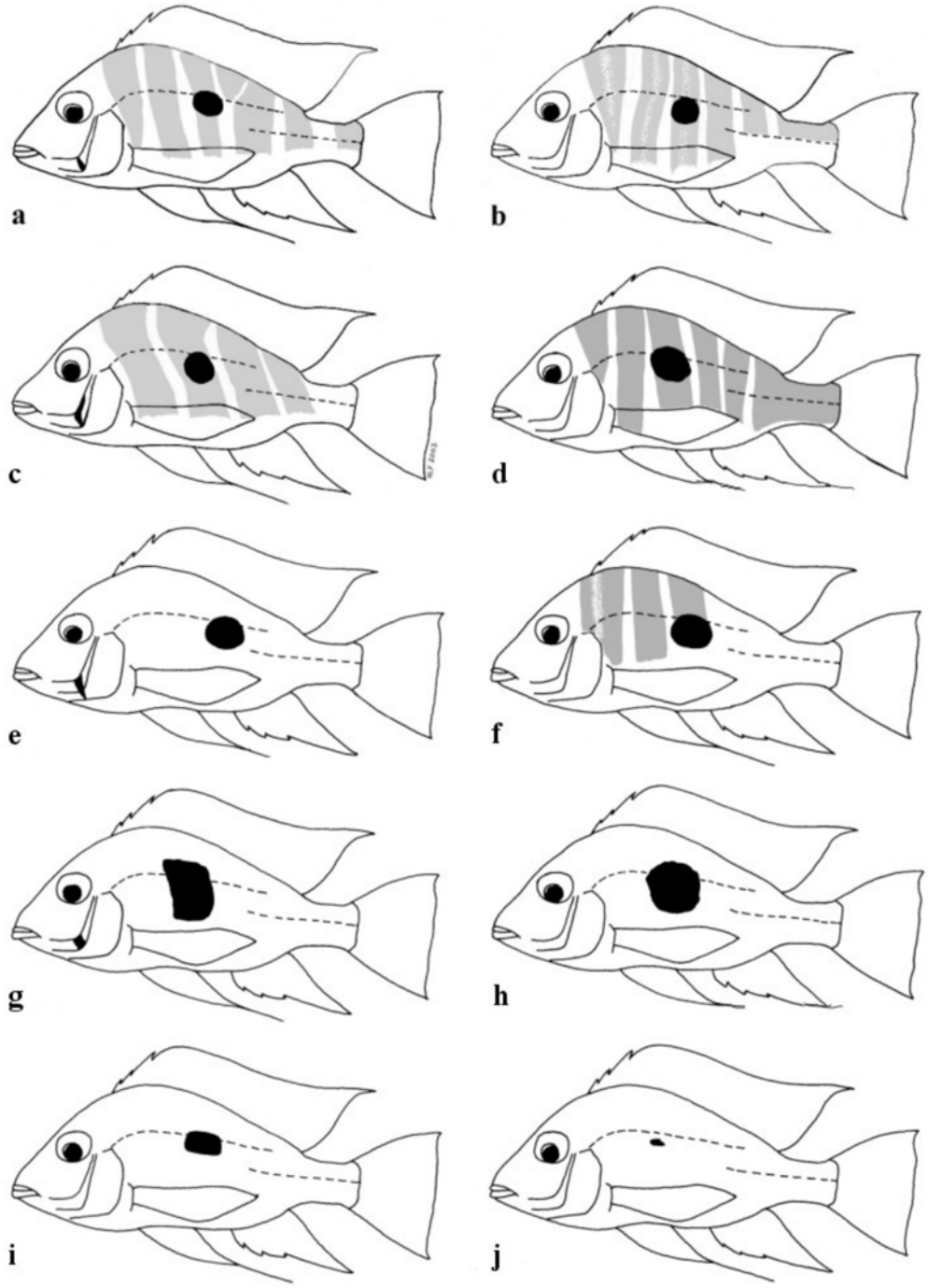

FIG. 2.2. Diagrammatic representation of preopercular markings and lateral bars distinguishing *Geophagus* species within the *G. surinamensis* complex. **a,** *G. dicrozoster*, n. sp.; **b,** *G. abalios* n. sp.; **c,** *G. winemilleri* n. sp.; **d**, *G. brokopondo*; **e**, *G. brachybranchus*; **f**, *G. surinamensis*; **g**, *G. proximus*; **h**, *G. megasema*; **i**, *G. camopiensis*, and **j**, *G. altifrons*. Preopercular markings are visible in both live and preserved individuals; lateral bar patterns are generally visible only in preserved specimens.

FIG. 2.3. *Geophagus abalios* Holotype. MCNG 47600, 163.0 mm SL; Venezuela: Apure: Río Cinaruco: Laguna Larga (6.5339°N 67.4150°W).

FIG. 2.4. *Geophagus abalios*. Uncatalogued specimen, adult in breeding coloration immediately after capture at the type locality: Laguna Larga, Río Cinaruco, Apure State, Venezuela. 6.3335°N, 67.2471°W.

Diagnosis

The lack of head markings distinguishes *G. abalios* n. sp. (Figures 2.2, 2.3 and 2.4) from *Geophagus grammepareius, G. taeniopareius, G. harreri* and *G. argyrostictus*, which have a complete infraorbital stripe, and from *G. dicrozoster* n. sp., *G. winemilleri* n. sp., *G. brachybranchus* and *G. proximus*, which have a black preopercular marking. Preserved specimens of *Geophagus abalios* can be distinguished from all other *Geophagus* species without head markings except *G. brokopondo* by the possession of six vertical, parallel bars on the flank (Figures 2.1 and 2.2); it can be distinguished from *G. brokopondo* by the anterior three bars, which are medially bisected by a clearer area, giving the impression of two thinner bars, whereas in the latter species all bars are solid; additionally, the sixth bar in *G. abalios* is elongate and restricted to the dorsal half of the caudal peduncle, above the lower lateral line, and in *G. brokopondo* the line covers the entire caudal peduncle (Figures 2.2b and 2.2d).

TABLE 2.1. Morphometrics of *Geophagus winemilleri*, *G. abalios*, and *G. dicrozoster*. Numbers in bold highlight morphometric differences among the species.

	Geophagus abalios					*Geophagus dicrozoster*					*Geophagus winemilleri*				
	n	Mean	Min	Max	Stdev	n	Mean	Min	Max	Stdev	n	Mean	Min	Max	Stdev
SL	17	107.9	45.5	192.0	42.5	20	129.7	44.8	202.0	51.0	15	86.6	37.0	195.0	54.7
Percent SL															
Head length	17	31.3	31.0	34.0	0.7	20	31.1	29.5	32.5	0.8	15	31.9	30.3	33.8	1.2
Body depth	17	**40.7**	36.0	46.2	2.9	20	38.8	32.6	42.4	2.4	15	38.9	34.3	44.6	3.7
Caudal peduncle depth	17	**12.8**	11.9	13.7	0.5	20	12.0	10.6	13.0	0.6	15	12.0	11.1	13.1	0.5
Caudal peduncle length	17	19.2	16.7	21.8	1.5	20	**20.9**	16.7	24.4	1.5	15	19.3	17.5	21.2	0.9
Pectoral fin length	17	**35.2**	31.9	40.5	2.9	20	33.9	28.6	39.0	2.8	15	33.6	27.5	39.8	4.0
Pelvic fin length	17	45.3	27.2	79.4	13.1	20	42.8	24.1	64.9	13.8	15	39.6	27.3	69.4	15.0
Last D spine length	17	17.4	14.1	19.6	1.4	19	17.0	11.6	20.2	2.8	15	**15.8**	12.2	20.2	2.5
Percent HL															
Snout length	17	46.5	38.2	59.7	5.4	20	46.7	36.4	54.9	4.9	15	**43.4**	34.1	54.8	5.8
Orbital diameter	17	31.1	26.8	41.6	3.9	20	31.3	25.8	38.6	3.6	15	**33.8**	28.3	39.6	3.3
Head depth	17	100.0	91.9	113.0	6.6	20	100.7	84.3	112.3	8.8	15	**98.6**	80.8	120.3	12.6
Head width	17	41.6	39.5	45.7	1.7	20	42.2	40.1	44.4	1.1	15	43.0	40.5	46.2	1.8
Interorbital width	17	25.3	20.8	28.3	2.3	20	25.7	19.3	29.9	3.0	15	**23.1**	17.7	33.0	4.3
Preorbital depth	17	**35.6**	25.0	43.8	5.9	20	35.3	**22.9**	43.0	6.2	15	**29.0**	19.2	42.1	7.7

Description

Based on holotype (163.0 mm SL) and 16 paratypes 45.5-192.0 mm SL with notes on variation among smaller specimens. Measurements and counts are summarized in Table 2.1. Sexes appear to be isomorphic.

Shape. Moderately elongate; dorsal outline more convex than ventral outline; head slightly broader ventrally than dorsally, chest flat; specimens 45.0 mm SL and smaller more elongate, with rounder nape; interorbital area moderately concave. Dorsal head profile straight, slightly concave in front of orbit, straight or slightly convex in specimens smaller than 112.0 mm SL, then sloping to dorsal-fin origin; dorsal-fin base descending, slightly convex to last ray, dorsal caudal peduncle forming a moderately concave curve to caudal-fin base. Ventral head profile straight, slightly descending to pelvic-fin insertion; chest slightly convex in one specimen 192.0 mm SL; straight, horizontal from pelvic-fin insertion to origin of anal fin; anal-fin base straight, ascending; ventral caudal peduncle straight to slightly concave, slightly ascending or horizontal in specimens 45.0 mm SL and smaller; ventral caudal peduncle 1.5-1.6 times in dorsal. Lips moderately wide, lower without caudally expanded fold (see Kullander et al. 1992; Figure 3). Maxilla reaching at most one third of the distance between nostril and orbit; ascending premaxillary process reaching slightly above midline of orbit. Opercule, preopercule, cleithrum, postcleithrum, and post-temporal lacking serration.

Scales. E1 33(4), 34(10), 35(3); scales between upper lateral line and dorsal fin 5.5-7.5 anteriorly, 2.5 posteriorly. Scales between lateral lines 2. Scales on upper lateral line 21(1), 22(4), 23(9), 24(1) and lower lateral line 13(1), 14(3), 15(6), 16(5). Anterior 1/3-1/2 of cheek naked, remainder with ctenoid scales; cheek scale rows 8-9. Opercule and subopercule covered with ctenoid scales. Interopercule with ctenoid scales caudally, otherwise naked. Single postorbital column of cycloid scales. Occipital and flank scales ctenoid. Circumpeduncular scale rows 7 above upper, 9 below lower lateral lines, ctenoid.

Fin scales. Pectoral and pelvic fins naked. Dorsal fin with double or triple columns of ctenoid scales along interradial membranes to one third to one half of fin

height. Scaly pad at base of dorsal fin formed by irregularly arranged small, ctenoid scales extending from first spine to fifth to seventh soft ray; specimens 55.5 mm SL or smaller, pad scales are cycloid or moderately ctenoid. Anal fin scaled on anterior section of soft portion, scales ctenoid, arranged in a single column along interradial membranes to one quarter to one third of fin height; anal fin naked in specimens 55.5 mm SL or less. Scaly pad on base of anal fin, scales small, ctenoid. Caudal fin entirely scaled except the tip of rays, and membranes between D3 and V3, scales ctenoid. Accessory caudal fin extension of lateral line between V4-V5, absent on dorsal lobe.

Fins. Dorsal XVII-11(1), XVII-12(1), XVIII-10(2), XVIII-11(6), XVIII-12(5), XIX-11(2); anal III-8(14), III-9(3). Spines increasing in length from first to sixth, equal length to ninth, then slightly shorter; lose membranes behind spine tips (lappets) acutely pointed, up to 1/3 the length of spines. Soft portion moderately expanded and pointed, reaching about 1/3 of caudal-fin length, rays 3-6 longest but not produced into filaments; specimens 56.0 mm SL and smaller with rounded soft portion, not quite reaching caudal-fin base. Anal fin pointed, with 2nd and 3rd soft rays slightly produced, not reaching caudal fin or barely beyond its base in specimens 90.6 and 192.0 mm SL. Caudal fin emarginate with lobes of approximately the same length and without filaments; one specimen 112.1 mm SL with slightly produced rays D8 and V8. Pectoral fin elongate, more or less triangular, longest at 4th ray, reaching 1st or 2nd anal-fin soft rays, then progressively shorter ventrally. Pelvic fin triangular, first ray produced into a filament reaching 5th anal-fin soft ray; in one specimen 112.1 mm SL reaching over 1/2 of caudal-fin length; specimens 45.5 mm SL or less with rays only slightly produced, reaching at most 1st spine of anal fin.

Teeth. Outer row of upper jaw with 10-28, blunt, slightly recurved unicuspid teeth; much larger than in inner rows, extending along most of premaxillary length. 2-3 inner rows, separated by a clear gap from outer row; teeth very thin, pointed, straight or slightly recurved unicuspids. Inner rows parallel to outer over its length, not forming a tight pad. Outer row of lower jaw with 6-25 unicuspid, blunt, slightly recurved unicuspids; medial 4-5 teeth larger than rest on outer row, cylindrical, slightly recurved,

blunt and more labially positioned than rest of row. Inner rows 3-4, only on medial third of dentary, separated from outer row by distinct gap; teeth long, thin, straight or slightly recurved, much smaller than outer row.

Gills. External rakers on first gill arch; 9(5), 10(3) on epibranchial lobe, 1 in angle and 12(7), 13(2) on ceratobranchial, none on hypobranchial. Microbranchiospines on the outer face of second to fourth arches. Gill filaments with narrow basal skin cover.

Tooth plates. Lower pharyngeal tooth plate elongate; width of bone 80% of length; dentigerous area 80% of width; 30 teeth in posterior row, 10 in median row. Anteriormost teeth subconical or subcylindrical, erect; most teeth laterally compressed and with small, low ridge rostrally, cusps on caudal half of teeth; lateral marginal teeth on anterior half like anteriormost, on caudal half smaller and thinner; posteromedial teeth much larger, nearly round in circumference, posterior cusps, almost blunt (Figure 2.5). Ceratobranchial 4 with 4 toothplates with 11, 28, 6 and 4 teeth.

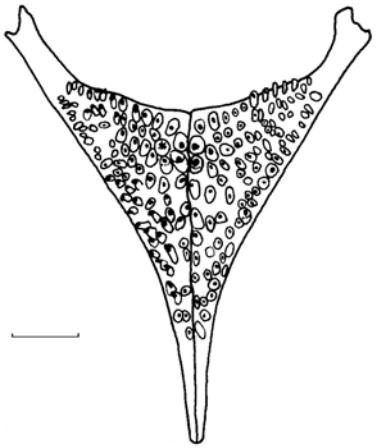

FIG. 2.5. *Geophagus abalios*, lower pharyngeal toothplate on occlusal view. From MCNG 40636, 70.5 mm SL; scale bar 1 mm.

Vertebrae. 14+18=32(1), 14+19=33(1), 15+18=33(3), 15+19=34(5), 15+20=35(1), 16+18=34(4); 11-13 epihemal ribs.

Color pattern in alcohol (Figure 2.3)

Base color grayish yellow; nape, snout and upper lip darker gray, fading caudally to base color towards cheek; lower lip yellowish white. No markings on the head, preopercule immaculate. Opercule darker on dorsal third; lower half of opercule and subopercule dusky yellow; silvery white in some specimens, probably depending on preservation. Ventrally, gill cover yellowish white; white in some specimens; branchiostegal membrane grayish. Chest white laterally and ventrally; in best preserved specimens white extends ventrally to base of caudal fin and to scale row H3 on caudal peduncle (Figure 2.1). Flanks with 6, dorso-ventrally directed, yellowish-gray bars fading or disappearing ventrally (Figure 2.2b). Bar 1 expands from the 4th or 5th predorsal scale to the base of the 4th dorsal-fin spine; its anterior edge delimited by the extrascapular and its posterior edge descending vertically and disappearing ventrally at the pectoral-fin insertion. Bar 2 extends between the 6th and 8th dorsal-fin spines, and runs vertically to H7. Bar 3 extends between the 10th and 13th dorsal-fin spines, and runs parallel to bar 2, fading ventrally at H6-H7. Bars 1-3 are generally bisected dorso-ventrally by a lighter column about 1 scale wide, giving the appearance of being two narrow bars in some specimens; this feature may be lost on poorly preserved specimens. A diffuse, blackish medial spot coincides with bar 3, extending rostro-caudally between scales 11-12 and 14-15 of E3 and dorso-ventrally between E3 and E1, such that the upper lateral line traverses the upper-most row of scales of the spot. Bar 4 extends between the bases of dorsal-fin spines 13-14 to 16-18, descends vertically and fades at H4-H5. Bar 5 extends between the first soft ray and ray 4-5 of dorsal fin, it descends vertically and disappears at H3-H4; in other specimens the bar is located between the last dorsal-fin spine and ray 3. Bar 6 extends from the base of the 6-7 (4-5 in some specimens) dorsal-fin rays and extends to the base of the caudal fin; bar is restricted to

dorsal portion of caudal peduncle, above lower lateral line, and is longer horizontally than vertically (Figure 2.2b).

Dorsal fin dusky, lappets dark gray or blackish, forming a dark edge along fin; soft and posterior third of spinous portion white-spotted on interradial membranes; four distinguishable longitudinal, parallel, grayish stripes alternate with light stripes along most of fin, turning almost hyaline rostrally; number of stripes increases with size to 6 in a 192.0 mm SL specimen. Anal fin hyaline to slightly dusky; 4 longitudinal, parallel gray stripes along soft portion of fin (5 in largest specimen). Caudal fin dusky, with round, whitish spots increasing in size towards dorsal edge; spots develop into horizontal stripes in larger specimens and a 192.0 mm SL specimen shows virtually no spots; specimens 55.5 mm SL and smaller with 4 dark, vertical bars. Pectoral fin immaculate. Pelvic fin whitish gray, dusky distally; dusky in largest specimen (192.0 mm SL), spine and first ray whitish gray to dusky.

Live colors (Figure 2.4)

Background color greenish gray, breeding specimens more metallic gray. Head without markings except for iridescent blue on the upper lip, continued as a stripe extending to the corner of the preopercule, and a slight marking of the same color on the ventral edge of orbit. A variable number of iridescent blue spots on the preopercule apparently limited to breeding specimens. Six yellow stripes extend between the base of dorsal and H4-5; in adult, breeding specimens, dorsal-most stripes appear as brownish-orange vermiculations and spots. Ventrum distinctly white; breeding adults with bright orange or red chest. Dorsal and anal fins reddish with faint iridescent blue horizontal banding that turns brighter during breeding; caudal brownish red with iridescent blue spots and bands in no clear pattern; pelvic reddish orange with iridescent blue banding, first ray white or very light blue. An aquarium photograph in Weidner (2000: 148, Figure 2.1) of an unidentified *Geophagus* from Venezuela is undoubtedly of a mature adult of *G. abalios*.

Distribution and habitat (Figure 2.6)

Geophagus abalios is commonly found in black or clear water rivers in the llanos, and is known from the Apure, Cinaruco-Capanaparo, and Aguaro-Guariquito drainages. Its current northern-most collection locality is "Las Majaguas" dam in the Río Cojedes, where it was probably introduced by recommendation of the Venezuelan ichthyologist A. Fernández-Yépez. According to his account (Fernández-Yépez and Anton 1966), *Geophagus* species were not naturally present in the reservoir, and he recommended the introduction of "*Geophagus surinamensis*" along with some other species, presumably for sport fishing purposes. *G. abalios* reaches the Andean piedmont to the west, and is the only *Geophagus* found in clear to white water seasonal lagoons along the main-stem of the Orinoco to the east (Rodríguez and Lewis Jr. 1990, 1994). The species appears restricted to the Caura drainage on the Guyana Shield, but it extends into the tributaries of the middle and upper Orinoco, including the Ventuari, Mavaca, and along the Río Casiquiare, nearly to the headwaters of the Río Negro.

Etymology

From the Greek *a*, not or without and *balios*, spotted. In reference to the lack of preopercular markings. To be regarded as an adjective in masculine form.

Geophagus dicrozoster N. SP.

Holotype

MCNG 40996, 193.0 mm SL; Venezuela: Apure: Río Cinaruco: Laguna Larga (6.5339°N 67.4150°W); D.A. Arrington and J. Arrington, 13 April 1999.

Paratypes

MCNG 30020, 7, 44.8-138.0 mm SL; Venezuela: Bolívar: Río Caroní: Campamento Guri; J.D.Williams and K.M. Ryan, 14 April 1994. – AMNH 233636 (ex-MCNG 40853), 1, 154.0 mm SL; Venezuela: Apure: Río Cinaruco: Laguna Oheros;

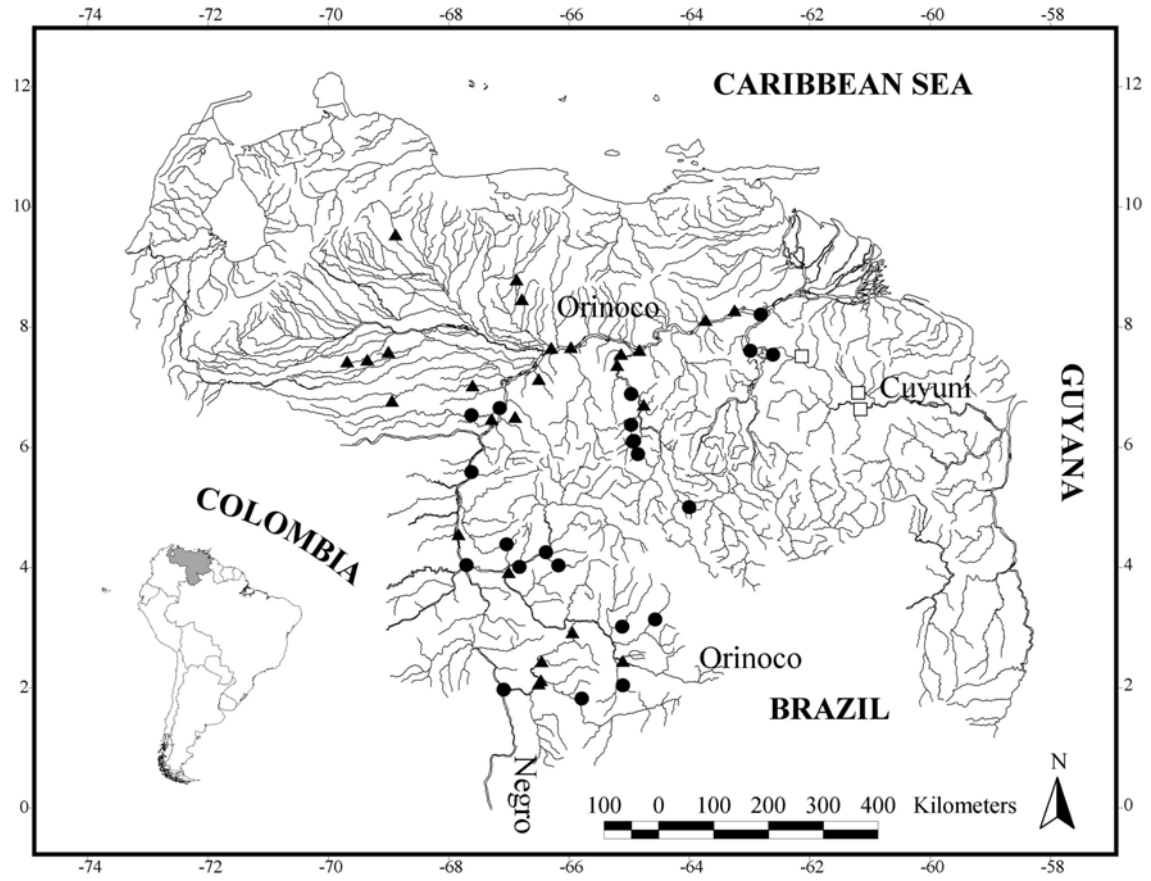

FIG. 2.6. Known distribution area of *Geophagus abalios* n. sp. (▲), *G. dicrozoster* n. sp.(●), and *G. brachybranchus* (□) in Venezuela. One dot may represent more than one collection locality.

D.A. Arrington and J. Arrington, 12 April 1999. - MCNG 40311, 22, 12.2-84.6 mm SL (2 measured); Venezuela: Apure: Rio Cinaruco: Laguna Guayaba (6.5897°N 67.2400°W); D.A. Arrington and J. Arrington, 16 March 1999. – AMNH 233635 (ex-MCNG 47603), 5, 109.6-178.0 mm SL; Venezuela: Apure: Río Cinaruco: Laguna Larga (6.5339°N 67.4150°W); K. Winemiller, H. López-Fernández, A. Arrington, L. Kelso-Winemiller, H. López-Chirico and J. Arrington, 1-3 Jan 1999. – MCNG 47604, 4, 177.0-202.0 mm SL; Venezuela: Apure: Río Cinaruco.

FIG. 2.7. *Geophagus dicrozoster* Holotype. MCNG 40996, 193.0 mm SL; Venezuela: Apure: Río Cinaruco: Laguna Larga (6.5339°N 67.4150°W).

Diagnosis

A preopercular mark distinguishes *Geophagus dicrozoster* n. sp. (Figures 2.2, 2.7 and 2.8) from *G. grammepareius*, *G. taeniopareius*, *G. argyrostictus* and *G. harreri*, which have a complete infraorbital stripe (Figure 2.1), and from *G. abalios* n. sp., *G. brokopondo*, *G. surinamensis*, *G. megasema*, *G. camopiensis*, and *G. altifrons*, which lack head markings. Preserved specimens of *G. dicrozoster* can be distinguished from other species with preopercular mark by the possession of seven vertical, parallel lateral bars, as opposite to *G. winemilleri* n. sp. (4 bars) and *G. brachybranchus* and *G. proximus* (no bars) (Figure 2.2).

Description

Based on holotype (120.2 mm SL) and the 19 paratypes 63.4 -202.0 mm SL with notes on variation among smaller specimens. Measurements and counts are summarized in Table 2.1. Sexes appear to be isomorphic.

Shape. Moderately elongate; dorsal outline more convex than ventral outline; head broader ventrally than dorsally; specimens 63.4 mm SL and smaller more elongate; interorbital area moderately concave. Dorsal head profile moderately convex, ascending to dorsal-fin origin, except in front of orbit where slightly concave, in specimens smaller than 65.0 mm SL, straight from orbit to dorsal-fin origin; dorsal-fin base descending, arched to last ray, then forming a horizontal, moderately concave line to caudal-fin insertion. Ventral head profile straight, slightly descending to chest; slightly convex to pelvic-fin insertion; straight, horizontal from pelvic-fin insertion to origin of anal fin; anal-fin base slightly convex, ascending; ventral caudal peduncle moderately concave, slightly ascending or horizontal in specimens 64.0 mm SL and smaller.

FIG. 2.8. *Geophagus dicrozoster*. Uncatalogued specimen, young adult immediately after capture at the type locality: Laguna Larga, Río Cinaruco, Apure State, Venezuela. 6.3335°N, 67.2471°W.

Lips moderately wide, lower with slightly caudally expanded fold (see Kullander et al. 1992, Figure 3). Maxilla reaching 1/3-2/3 of the distance between nostril and orbit; ascending premaxillary process reaching slightly above midline of orbit. Opercule, preopercule, cleithrum, postcleithrum, and post-temporal lacking serration.

Scales. E1 34(3), 35(7), 36(8), 38(2); scales between upper lateral line and dorsal fin 6.5-8.5 anteriorly, 2.5-3.5 posteriorly. Scales between lateral lines 2. Scales on upper lateral line 19(1), 20(7), 21(8), 22(4) and lower lateral line 14(1), 15(4), 16(3), 17(9), 18(3). Anterior half of cheek naked, remainder with ctenoid scales; cheek scale rows 9-10. Opercule covered with ctenoid scales. Caudo-ventral area of subopercule naked, remainder with ctenoid scales. Interopercule with cycloid scales caudally. Single postorbital column of ctenoid scales, particularly in largest specimens. Occipital and flank scales ctenoid. Circumpeduncular scale rows 7-9 above upper, 9-11 below lower lateral line, ctenoid.

Fin scales Anal, pectoral and pelvic fins naked. Dorsal fin scaled on spinous and soft portions, scales ctenoid, and arranged in double or triple columns along interradial membranes up to one third to one half of fin height. Scaly pad at base of dorsal formed by irregularly arranged small, ctenoid scales extending from first spine to third to seventh soft ray. Anal scaleless, scaly pad on base of anal absent, at most a few small scales on base of anterior portion of fin, moderately ctenoid. Caudal fin scaled along its entire surface, except the tip of rays, and part of membranes between D3 and V3, scales ctenoid. Accessory caudal fin extension of lateral line between V4-V5, absent on dorsal lobe.

Fins. Dorsal XVI-12(2), XVI-13(1), XVII-11(2), XVII-12(9), XVII-13(1), XVIII-11(2), XVIII-12(2); anal III-7(1), III-8(18), III-9(1). Dorsal-fin spines increasing in length from first to sixth, equal length to ninth, then slightly shorter; lappets pointed, short; soft portion round, reaching just beyond caudal-fin insertion; moderately pointed in a 202.0 mm SL, and reaching about a third of caudal-fin length; rays 4-6 longest but not produced into filaments; in specimens 63.0 mm SL and smaller dorsal fin not reaching caudal-fin insertion. Anal fin round, moderately pointed in largest specimens,

with rays 2-5 longest, not reaching caudal fin or barely beyond its base in largest specimens. Caudal fin emarginate with lobes of approximately the same length and without filaments; one specimen 120.2 mm SL with slightly produced ray D8. Pectoral fin elongate, more or less triangular, longest at 4th ray, reaching 1st or 2nd anal-fin spines, then progressively shorter ventrally. Pelvic fin triangular, first ray produced into a filament reaching 3rd anal-fin soft ray; in a specimen 202.0 mm SL almost reaching caudal-fin insertion; specimens 45.5 mm SL or less with slightly or not produced rays, reaching at most 1st anal-fin spine.

Teeth. Outer row of upper jaw with 17-26 approximately cylindrical, frequently blunt, slightly recurved, unicuspid teeth; larger than in inner rows, extending along most of premaxillary length; 6-7 inner rows, separated by a clear gap from outer row; teeth on outer row thin, slightly recurved unicuspids, forming a pad. Outer row of lower jaw with 16-22 blunt, slightly recurved unicuspid teeth; median 3 teeth more labially positioned than rest of row; inner rows 6 (4 in small specimens), forming a pad, separated from outer row by distinct gap; teeth thin, slightly recurved unicuspids.

Gills. External rakers on first gill arch; 10(11), 11(1) on epibranchial lobe, 1 in angle and 12(3), 13(7), 14(2) on ceratobranchial, none on hypobranchial. Microbranchiospines on the outer face of second to fourth arches. Gill filaments with narrow basal skin cover.

Tooth plates. Lower pharyngeal tooth plate elongate (Figure 2.9); width of bone 80-82% of length; dentigerous area 80% of width; 28 teeth in posterior row, 11 in median row. Anteriormost teeth subconical, laterally compressed and erect; cusps posterior, slightly curved rostrad, small rostral edge ridge; lateral marginal teeth with same cusp pattern, teeth thinner and more laterally compressed towards caudal edge of plate; posteromedial teeth much larger, almost cylindrical, cusps posterior, almost blunt. Ceratobranchial 4 with 5 toothplates with 4-6, 5-7, 5-13, 6-11 and 3-7 teeth; one of two specimens with 7 toothplates with 6, 4, 5, 5, 4, 3 and 3 teeth on left side.

Vertebrae. 14+18=32(1), 14+19=33(10), 15+18=33(3), 15+19=34(1); 11-12 epihemal ribs.

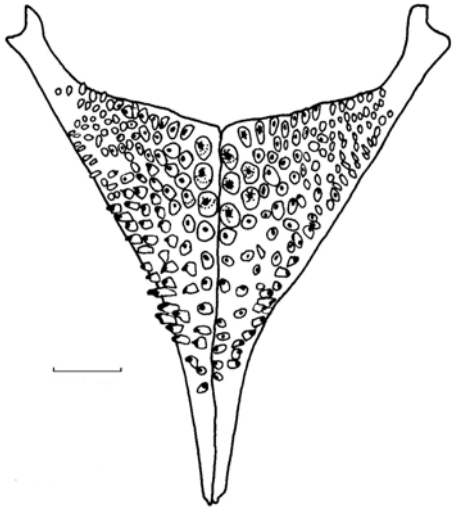

FIG. 2.9. *Geophagus dicrozoster*, occlusal aspect of lower pharyngeal tooth plate. From MCNG 40623, 88.4 mm SL; scale bar 1 mm.

Color pattern in alcohol (Figure 2.7)

Background color grayish yellow; nape, snout, upper lip and naked portion of cheek darker gray, scaled portion of cheek lighter; lower lip yellowish white. Vertical, blackish mark in the corner of the preopercule, continued into the interopercule as a faint spot; indistinguishable or faded in specimens smaller than 65.0 mm SL. Opercule with a dark, brown spot on dorsal edge, reaching first scale of upper lateral line, otherwise uniformly dusky yellow or silvery white in some specimens probably depending on preservation. Ventrally, gill cover dusky yellow or yellowish white in some specimens; branchiostegal membrane also yellowish, grayish brown in one specimen 202.0 mm SL. Chest yellow laterally and ventrally, white in many specimens, juveniles with distinctive silvery-white chest region; in best preserved specimens dusky yellow or white extends ventrally to base of caudal fin and to H3 on caudal peduncle flanks. Flanks with 7, dorso-ventrally directed, dark-gray bars fading or disappearing ventrally (Figure 2.2a). Bar 1 expands from the 7^{th}-8^{th} predorsal scale to the base of the dorsal fin between spines 4-5 forming an inverted triangle; its anterior edge roughly delimited by the extrascapular

and its posterior edge descending ventrally to the pectoral-fin insertion. Bar 2 extends between the base of dorsal-fin spines 6-7 and 9, and runs vertically to H6-7. Bar 3 extends between the base of dorsal-fin spines 10-11 and 12-13, descends ventrally and slightly caudally oriented, fading progressively to H6-7. A well-demarked, black medial spot is located on bar 3, extending rostro-caudally between scales 11 and 14-15 of E3 and dorso-ventrally between the lower half of E4 and E1, such that the upper lateral line traverses the dorsal 1/4 –1/3 of the spot. Bar 4 extends between the bases of dorsal-fin spines 14-15 to 17, and descends ventro-caudally to the upper lateral line, where it merges with bar 5 such that the two bars form a "Y" shaped figure (Figure 2.2a); in specimens 50.0 mm SL or less, bar 4 may appear as a spot on the base of the dorsal, not quite reaching bar 5. Bar 5 extends between the base of dorsal-fin spine 18 and ray 1 or rays 1-2 and rays 4-5, it descends vertically fading at H1-2. Bar 6 extends from the base of the 7-8 dorsal fin rays to the second postdorsal scale in the caudal peduncle, descends vertically and fades at H1-2. Bar 7 covers the area between the last 4-5 lower lateral line scales and the base of the caudal fin, disappearing ventrally at H2.

Dorsal fin dusky, lappets dark gray or blackish, forming a faint dark edge along fin; dorsal fin immaculate except a few indistinct whitish spots in the membranes of caudal half of soft portion; in specimens 63.0 mm SL or smaller, three dusky longitudinal, parallel, stripes alternate with light stripes along soft portion of dorsal fin. Anal fin hyaline to slightly dusky; 4 longitudinal, parallel gray bands along soft portion; largest specimen with dark gray lappets. Caudal fin gray-brown, with whitish longitudinal bands of variable length and elongate spots, forming no evident pattern; specimens up to 85.0 mm SL with 4 dark, vertical bands that gradually turn into the above described pattern with increasing size. Pectoral fin immaculate. Pelvic fin dusky, darker distally; spine and first ray whitish gray to dusky.

Live colors (Figure 2.8)

Dark markings as in alcohol specimens. Background color yellowish olive green; head silvery with yellow on gill cover, snout gray, upper lip iridescent blue extending behind lips to preopercular mark. Dorsal fin reddish with faint iridescent blue spots, especially on the soft portion; some specimens with proximal third of spiny portion yellow, probably due to breeding condition; anal fin red or reddish with distinctive iridescent blue horizontal banding; caudal fin reddish with a variable pattern of iridescent blue stripes and spots. Five to seven faint, yellow horizontal stripes alternating with olive green along body, but not always distinct.

Distribution and habitat (Figure 2.6)

Geophagus dicrozoster is common in the black waters of the Caura and Caroní drainages of the Guyana Shield; it is also present in all major tributaries of the middle and upper Orinoco, including the drainages of the Cataniapo, Ventuari, Atabapo, Ocamo, and Mavaca, as well as the Casiquiare and the headwaters of the Río Negro. In the llanos, *G. dicrozoster* is restricted to the moderately black-watered Río Cinaruco, although further collections will likely show its presence in the nearby Río Capanaparo and its tributaries. No specimens have been captured from white water, or from llanos clear water drainages as the Aguaro-Guariquito.

Etymology

From the Greek *dikros*, forked, and *zoster*, belt. Given in reference to the "Y" formed by lateral bars 4 and 5. To be regarded as an adjective in masculine form.

Geophagus winemilleri N. SP.

Holotype

MCNG 35486, 195.0 mm SL; Venezuela: Amazonas: Río Siapa: Laguna Yocuta, (2.1347° N 66.3742° W); K. Winemiller and D. Jepsen, 21 Jan 1997.

Paratypes

MCNG 12227, 9, 24.5-47.3 mm SL (4 measured); Venezuela: Amazonas: Río Casiquiare: El Porvenir, approx. 60 Km. from confluence with Río Negro (2.0833°N 66.5°W); L. Nico, E. Conde, P. Cardozo, G. Aymard and B. Stergios, 15 April 1985. – AMNH 233637 (ex-MCNG 12301), 1, 188.0 mm SL; Venezuela: Amazonas: Caño Emoni, 2 Km. upstream from confluence with Río Siapa (2.1167°N 66.3333°W); L. Nico, E. Conde, P. Cardozo, G. Aymard and B. Stergios, 17 April 1985. - MCNG 37858, 29, 19.2-149.0 mm SL (5 measured); Venezuela: Amazonas: Río Casiquiare: Isla Cuamate, past Solano (2.0083°N 66.8994°W); L. Nico, S. Walsh, A. Arrington and A. Añez 07 Jan 1998. – AMNH 233638 (ex-MCNG 42016), 13, 18.0–113.6 mm SL (2 measured); Venezuela: Amazonas: Río Negro: Punta de Barbosa community (1.9844°N 67.1183°W); L. Nico, H. Jelks and H. López-Fernández, 06 Jan 1999. - MCNG 42386, 2, 97.9-118.3 mm SL; Venezuela: Amazonas: Río Negro: Mavajaté rapids (1.9872°N 67.1233°W); L. Nico, H. Jelks, A. Barbarino, et al., 18 Jan 1999.

Diagnosis

A preopercular mark distinguishes *Geophagus winemilleri* (Figures 2.2, 2.10 and 2.11) from *G. grammepareius*, *G. taeniopareius*, *G. argyrostictus* and *G. harreri*, which have a complete infraorbital stripe, and from *G. abalios* n. sp., *G. brokopondo*, *G. surinamensis*, *G. megasema*, *G. camopiensis*, and *G. altifrons*, which lack head markings. Preserved specimens of *G. winemilleri* can be distinguished from other species with preopercular mark by the possession of 4 ventrally-inclined, parallel lateral bars, as opposite to *G. dicrozoster* n. sp. (7 bars) and *G. brachybranchus* and *G. proximus* (no bars) (Figure 2.2).

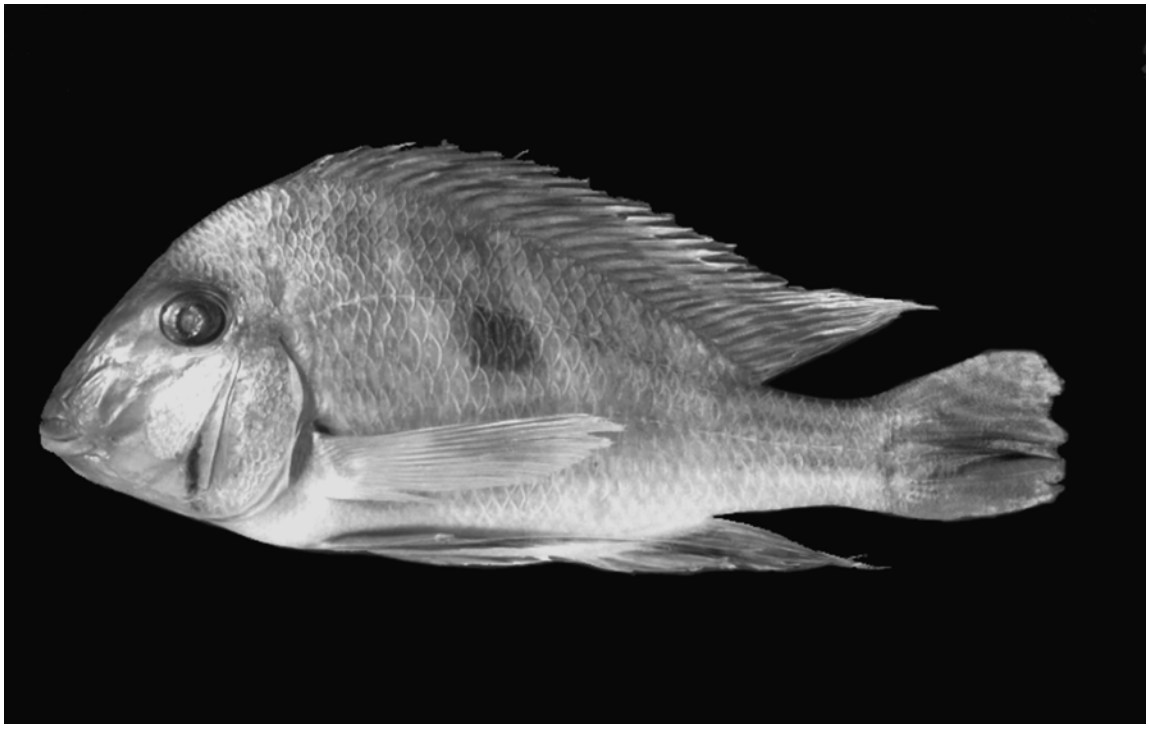

FIG. 2.10. *Geophagus winemilleri* Holotype. MCNG 35486, 195.0 mm SL. Venezuela: Amazonas: Río Siapa: Laguna Yocuta, (2.1347° N 66.3742° W).

FIG. 2.11. *Geophagus winemilleri*. AMNH 233638, adult paratype immediately after capture at comunidad Punta Barbosa, Río Negro headwaters, Amazonas State, Venezuela. 1.9844°N, 67.1183°W.

Description

Based on holotype (195.0 mm SL) with notes on variation in 14 paratypes 41.8 to 188.0 mm SL. Measurements and counts are summarized in Table 2.1. Sexes appear to be isomorphic.

Shape. Moderately elongate; dorsal outline more convex than ventral outline; head broader ventrally than dorsally; specimens 45.0 mm SL and smaller with rounder nape; interorbital area moderately concave. Dorsal head profile slightly curved above upper lip, then straight, steeply ascending to orbit, slightly convex or straight (specimens smaller than 118.0 mm SL) in front of orbit, then sloping to dorsal-fin origin; descending, slightly convex to last ray of dorsal fin, then straight, almost horizontal to caudal-fin base. Ventral head profile straight, slightly descending; chest moderately

convex; straight, horizontal from pelvic-fin insertion to origin of anal fin; anal-fin base straight, slightly ascending; ventral caudal peduncle straight, slightly ascending; caudal peduncle about 1.5 times longer ventrally than dorsally. Lips moderately wide, lower with slightly caudally expanded fold (see Kullander et al. 1992, Figure 3). Maxilla not quite reaching middle vertical line between nostril and orbit; ascending premaxillary process reaching lower half of orbit. Opercule, preopercule, cleithrum, postcleithrum, and post-temporal lacking serration.

Scales. E1 32(1), 34(5), 35(9); scales between upper lateral line and dorsal fin 6.5-7.5 anteriorly, 2.5 posteriorly. Scales between lateral lines 2. Scales on upper lateral line 21(1), 22(4), 23(5), 24(3), 25(2) and lower lateral line 13(1), 14(5), 15(5), 16(2). Anterior 1/3 to 1/2 of cheek naked, remainder with ctenoid scales; cheek scale rows 7-8. Opercule and subopercule covered with ctenoid scales; interopercule naked except caudo-dorsal region with ctenoid scales. Single postorbital column of mostly ctenoid scales. Occipital and flank scales ctenoid. Circumpeduncular scale rows 7 above upper, 9 below lower lateral lines, ctenoid.

Fin scales. Anal, pectoral and pelvic fins naked. Dorsal fin scaled in spinous and soft portions, scales ctenoid, arranged in double or triple columns along interradial membranes to ¼-½ of fin height. Scaly pad at base of dorsal fin formed by irregularly arranged, small, ctenoid scales extending from 2nd or 3rd spine to 5th or 6th ray. Reduced scaly pad on anterior portion of base of anal fin, from second spine to second or third ray, scales small, ctenoid. Caudal fin scaled in its entire surface, except the tip of rays, and membranes between D2 and V2, scales ctenoid. Accessory caudal fin extensions of lateral line between D3-D4 and V4-V5.

Fins. Dorsal XVIII-10(1), XVIII-11(4), XVIII-12(2), XIX-10(2), XIX-11(5), XIX-1(1); anal III-7(2), III-8(13). Spines increasing in length from first to sixth, equal length to ninth, then slightly shorter; lappets acutely pointed, up to ¼ the length of spines. Soft portion pointed, reaching the base of caudal fin, except for rays 4-5, reaching about ½ of caudal-fin length; specimens smaller than 76.3 mm SL with rounded soft portion, not quite reaching caudal-fin insertion. Anal fin with 3rd soft ray

moderately produced, reaching about ¼ of caudal-fin length, otherwise scarcely reaches base of caudal fin. Caudal fin emarginate with lobes of approximately the same length and without filaments in studied specimens. Pectoral fin elongate, more or less triangular, longest at 4th ray, reaching 1st or 2nd anal-fin soft rays, then progressively shorter ventrally. Pelvic fin triangular, first ray produced into a filament reaching 1/3 of caudal peduncle length; in one specimen 149.0 mm SL reaching 1/3 of caudal-fin length; specimens 45.5 mm SL or less without produced rays, not reaching base of anal fin.

Teeth. Outer row of upper jaw with 19-31, slightly recurved, unicuspid teeth; slightly larger than in inner rows, extending along most of premaxillary length. Three to four inner rows with no clear gap separating them from outer row; teeth unicuspid, very thin, pointy, straight or slightly recurved. Inner rows parallel to outer on all its length, not forming a pad. Outer row of lower jaw with 7-28 unicuspid, blunt, slightly recurved, unicuspids; outer row restricted to median 1/3 of dentary length in holotype and large specimens, but extending farther in specimens 118.0 mm SL and smaller. Inner rows 3-4, separated from outer row by distinct gap; teeth long, thin, straight or slightly recurved unicuspids, smaller than outer row, and forming a pad on median region of dentary.

Gills. External rakers on first gill arch; 9(2), 10(4), 11(4) on epibranchial lobe, 1 in angle and 11(1), 12(6), 13(3) on ceratobranchial, none on hypobranchials. Microbranchiospines on the outer face of second to fourth arches; gill filaments with narrow basal skin cover.

Tooth plates. Lower pharyngeal tooth plate elongate (Figure 2.12); width of bone 84% of length; dentigerous area 76% of width; 30 teeth in posterior row, 11 in median row. Anteriormost teeth subconical, erect, laterally compressed; cusps on caudal half, slightly curved anteriorly, small rostral edge ridge; lateral marginal teeth as anteriorly on rostral edge, gradually flatter and smaller caudally; posteromedial teeth much larger, nearly round in circumference, medial or slightly posterior cusps, almost blunt. Ceratobranchial 4 with 5 toothplates with 4, 14, 6, 6 and 2 teeth.

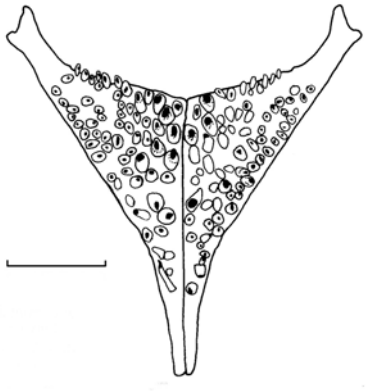

FIG. 2.12. *Geophagus winemilleri*, lower pharyngeal toothplate in occlusal view. From MCNG 12227, 41.7 mm SL; scale bar 1 mm.

Vertebrae. 14+19=33(1), 14+20=34(1), 15+19=34(13); 11-13 epihemal ribs.

Color pattern in alcohol (Figure 2.10)

Base color grayish yellow; nape, snout and upper lip dark gray, fading caudally to base color towards cheek; lower lip yellowish white. The only marking on the head is a vertical, dark mark in the corner of the preopercule, roughly parallel to its caudal edge, fading ventrally but continued into the interopercule in large specimens; indistinguishable or faded in specimens smaller than 70 mm SL. Gill cover slightly darker than base color. Flanks with four, broad, ventro-caudally directed, yellowish-gray bars running from dorsal to ventral regions and disappearing below the lower lateral line (Figure 2.2c). Bar 1 expands from the 4th or 5th scale, anterior to dorsal-fin origin, to the base of the 5th or 6th dorsal-fin spine, extends over the anterior portion of the flank and disappears in the region caudal to the pectoral-fin insertion. Bar 2 extends from the 7th or 8th to the 11th or 12th dorsal-fin spine, runs parallel to bar 1 and disappears approximately at the level of H1. A blackish medial spot coincides with bar 2, extending rostro-caudally between the scales 10 and 13 of E3 and dorso-ventrally between the lower half of E3 and E1, such that the upper lateral line borders the dorsal edge of the

spot. Bar 3 extends between the 13th or 14th dorsal-fin spine to the 1st or 2nd soft ray, and runs parallel to bar 2 to H1 or H2, where it fades. Bar 4 extends between the base of the 3rd and the last dorsal-fin ray, and disappears in H1; in some specimens bar 4 can start at the base of the 1st or 2nd dorsal-fin ray and then appears merged with bar 3 at its base, but it is clearly separated ventrally (Figs. 1, 2c). A fifth, faded vertical bar can generally be distinguished covering the caudal-most 4 or 5 columns of scales of the caudal peduncle, but this bar tends to turn into a grayish colored area in larger specimens.

Dorsal fin hyaline to smoky, lappets dark gray or blackish; soft portion with white spotting on the interradial membranes, forming a more or less parallel pattern of horizontal stripes; in specimens 149.0 mm SL and smaller, 3 longitudinal, parallel, grayish stripes alternate with hyaline stripes along most of the dorsal fin, fading into an increasingly indistinguishable pattern rostrally. Anal fin dusky to grayish; two longitudinal, parallel darker stripes along soft portion of fin. Caudal fin dusky, with indistinct pattern ranging from round spots to longitudinal, whitish stripes, or a combination of both; specimens 45.5 mm SL and smaller with 2 or 3 blackish, vertical bands. Pectoral fin immaculate. Pelvic fin dusky to dark gray, spine and first ray whitish to slightly dusky.

Live colors (Figure 2.11)

Live specimens show the same dark markings as described for preserved individuals. Snout gray turning bluish gray in the cheek, gill cover yellow with iridescent blue spots on each scale, lips yellowish white. Flanks are bluish silver with five longitudinal yellow stripes between base of dorsal fin and H1. Dorsal and anal fins brownish red with iridescent blue longitudinal banding; pelvic fin bright red with iridescent blue banding, first ray white; caudal fin red, with large iridescent blue to white spots. An aquarium picture in Weidner (2000: 125, Figure 3: *Geophagus* sp. "Rio Negro I") shows unpaired fins and pelvic with a much brighter red than specimens photographed shortly after capture in the wild (HLF pers. obs.).

Distribution and habitat (Figure 2.13)

Geophagus winemilleri is an uncommonly caught species (a revision of nearly 400 lots of *Geophagus* at MCNG resulted in only 6 lots of this species), known only from the black waters of the lower Casiquiare drainage and the headwaters of the Río Negro in southern Venezuela (Figure 2.13). The scarcity of collections does not allow determining whether the species reaches the Orinoco main-stem. Individuals of this species are commonly sold in the market at the town of Barcelos, Brazil, in the middle-course of the Río Negro (HLF pers. obs.). An undescribed species known in the German aquarium trade as *G*. sp. "Rio Negro I" or *G*. sp. "stripetail" (Weidner 2000) corresponds well with the characters of *G. winemilleri*; according to Weidner's locality data, the species might extend as south as the Archipelago das Anavilhanas, near the confluence of the Rio Negro with the Amazonas.

Etymology

Named for Dr. Kirk O. Winemiller, who led the field expeditions to the Río Casiquiare region during which most of the type specimens of *G. winemilleri* were collected, and in recognition of his nearly two decades of contributions to ecology and tropical fish biology, many of which have been based on Venezuelan fishes.

FIG. 2.13. Known distribution area of *Geophagus winemilleri* n. sp. (▲), *G. grammepareius* (■), and *G. taeniopareius* (●) in Venezuela. One dot may represent more than one collection locality.

KEY TO THE VENEZUELAN SPECIES OF *GEOPHAGUS*

1 Infraorbital stripe complete (Figure 2.1), extending from ventral edge of orbit to edge of preopercule or dorsal half of interopercule ……..……..……..…….2

- Infraorbital stripe absent, or reduced to dark mark on preopercule (Figure 2.1) …..……...…...3

2 Dorsal fin base with sheath of scales; faint horizontal stripes on flank ……..……..…… *G. taeniopareius*

- Dorsal fin base without sheath of scales; no horizontal markings on flank ……..……..…… *G. grammepareius*

3 Base of gill filaments on first gill arch largely covered by broad flap of skin; no discernible lateral bars on preserved specimens (Figure 2.2e); Cuyuní river drainage …….…… *G. brachybranchus*

- Base of gill filaments on first gill arch with narrowly covered with skin at base; 4 to 7 lateral bars on preserved specimens; Orinoco or Río Negro drainages ……..……..…….4

4 Seven dark pes on flank, with pes 4 and 5 forming a "Y" pattern; ventral caudal peduncle contained 1.1 to 1.3 times in dorsal caudal peduncle; subopercule caudoventrally naked (Figure 2.2a)……..……..….. *G. dicrozoster*

- Fewer than seven bars on flank; ventral caudal peduncle contained 1.5 to 1.6 times in caudal peduncle; subopercule fully scaled ...…….……5

5 Dorsal lobe of caudal fin with accessory lateral line extension between rays D3 and D4; preopercular mark present; four, broad and parallel, caudo-ventrally inclined lateral bars on flank (Figure 2.2c)……...…….…….……. *G. winemilleri*

- Dorsal lobe of caudal fin without accessory lateral line extension; preopercular mark absent; six, vertical and parallel bars on flank (Figure 2.2b)..……....…. *G. abalios*

DISCUSSION

Three species of *Geophagus* from the "*surinamensis* complex" are described, elevating the described species in the genus to fourteen, and the known Venezuelan species to six. The new species *Geophagus abalios*, *G. dicrozoster* and *G. winemilleri*

are diagnosable from species outside the *G. surinamensis* complex by the lack of a complete infraorbital stripe (Figs. 1, 2), which can be absent (*G. abalios*) or reduced to a preopercular mark (*G. dicrozoster*, *G. winemilleri*). The combination of coloration and squamation characters distinguishes the three species from each other, and from the other seven described species within the *G. surinamensis* complex (Figure 2.2). Lateral bar patterns have been used as diagnostic characters in other genera of Neotropical cichlids, notably *Mesonauta* (Kullander & Silfvergrip 1991; Schindler 1998) and *Apistogramma* (e.g. Kullander 1980). It is clear from the present paper that some species of *Geophagus* present well-defined and stable patterns of lateral bars, and these can be used as diagnostic characters. Color photographs of aquarium specimens suggest that double-bar patterns and the lack of a preopercular mark, as observed in *G. abalios* n. sp., occur together in yet undescribed species (e.g. Weidner 2000, *Geophagus* sp. "Maicuru", *G.* sp. "Porto Franco", *G.* sp. "Tapajós Orange Head"). This apparent consistency may reflect underlying phylogenetic relationships within *Geophagus*, and may provide useful sets of characters for future phylogenetic analysis within the genus.

Although little is known of the ecology of *Geophagus abalios* and *G. dicrozoster*, it appears that they share many essential aspects of their biology. Field observations in the Río Cinaruco (south-western Venezuelan llanos) indicate that both species are mouthbrooders (HLF unpubl.). Both species are among the most abundant in samples from lagoon, or to a lesser extent, channel habitats over bare sandy bottoms, although they can be abundant in structured habitats with submerged wood or rocks (Arrington 2002). On at least one occasion, *G. dicrozoster* was captured in rapids near the headwaters of the Río Negro (K. Winemiller et al. unpubl.). Preliminary diet analyses indicate that, at least qualitatively, both species share a diet of benthic insect larvae dominated by chironomids (Diptera), trichopterans and ephemeropterans (HLF unpubl.). Given the great similarity of these species in overall morphology, color patterns, feeding modes, and probably reproductive behavior, it is remarkable that they seem to share the same habitats in an extensive manner. The ecology of *G. winemilleri* is almost entirely unknown: all available records and observations indicate that it

inhabits black waters with sandy bottoms, and it probably is a "larvophilous" mouth brooder (Weidner 2000).

Geophagus abalios and *G. dicrozoster* are sympatric in most of their known distribution, and frequently are found in the same habitats, particularly in the Cinaruco river, southern Apure State (HLF unpubl.). Their syntopy will probably be shown to be more extensive once they are distinguished in collections, where they are commonly referred to as *G. surinamensis* or *G. altifrons* (e.g. Mago-Leccia 1970; Machado-Allison 1987; 1993; Royero et al. 1992). The broad distribution of both species in the Orinoco basin suggests they should be as common in Colombia as they are in the Venezuelan portion of the basin. It is not clear from current distributional knowledge whether the range of *G. abalios* and *G. dicrozoster* extends further south than the headwaters of the Río Negro. The known distribution of *G. winemilleri* is restricted to the lower Casiquiare and the upper Río Negro, but the species may be present in the Río Ventuari drainage of the middle Orinoco basin (D. C. Taphorn and C. Montaña unpubl.). The fish diversity of the middle Orinoco and its tributaries is poorly known, and further collections are needed to clarify whether *G. winemilleri* is present in the upper Casiquiare and upper-middle Orinoco region. *G. winemilleri* is known to occur in the middle Río Negro (HLF pers. obs.). Weidner (2000) indicates that all aquarium imports come from the Río Negro and refers to a case in which the species was caught in the Archipelago das Anavilhanas, just north of Manaus. Further taxonomic, phylogenetic and distributional studies in the Río Negro will be necessary before a fruitful discussion of the biogeographic history of *Geophagus* in this region is possible.

CHAPTER III

MOLECULAR PHYLOGENY AND RATES OF EVOLUTION OF GEOPHAGINE CICHLIDS FROM SOUTH AMERICA (PERCIFORMES: LABROIDEI)

INTRODUCTION

The Neotropical cichlid subfamily Geophaginae encompasses 18 genera and over 180 described species (Kullander 2003), with many more in need of description (e.g. Kullander 2003; López-Fernández and Taphorn 2004). Although knowledge of geophagine biology is limited, this group of fishes displays diverse ecology, morphology, and reproductive behavior. Their overall morphological and behavioral diversity suggests ecomorphological specialization for feeding and habitat use (e.g. Winemiller et al. 1995; López-Fernández unpubl.). For instance, some taxa share a common feeding mode based on sifting of benthic invertebrates (e.g. Lowe-McConnell 1991; Winemiller et al. 1995), while others are strict piscivores. Geophagines also exhibit a variety of reproductive modes, from typical substrate spawners to mouthbrooding, and are the only riverine cichlids approaching the reproductive versatility of lacustrine cichlids (e.g. Wimberger et al. 1998; Barlow 2000; Weidner 2000). Several genera and species of geophagines are syntopic in South American rivers (e.g. Winemiller et al. 1995; Arrington and Winemiller 2003), thus ecomorphological and behavioral specialization may facilitate niche partitioning within species-rich ecological communities. Such extensive ecological specialization may constitute an adaptive radiation. According to Schluter (2000), an adaptive radiation results from the fast divergence of a monophyletic lineage into multiple, ecologically specialized descendants. In an adaptive radiation, relationships among taxa should display short branch lengths at the base of the phylogeny, reflecting rapid differentiation. Therefore, a phylogeny for Geophaginae is required to determine if the subfamily constitutes an

adaptive radiation, and to frame investigations of ecological and morphological divergence within the adequate phylogenetic context.

Recent phylogenetic analyses of the Cichlidae (Kullander 1998; Farias et al. 1999, 2000, 2001) have improved understanding of high-level relationships within the Neotropical clade (e.g., definition of subfamilies), yet even here there are disagreements. Using a morphology-based phylogeny, Kullander (1998) subdivided the Neotropical Cichlidae and the African genus *Heterochromis* into six subfamilies. The Retroculinae (genus *Retroculus*) and Cichlinae (*Cichla*, *Crenicichla*, and *Teleocichla*) constituted the basal clades of the American assemblage. The African Heterochromidinae (*Heterochromis*) was nested between the latter two and Astronotinae (*Astronotus* and *Chateobranchus*), thus rendering the Neotropical cichlids paraphyletic. The more derived subfamilies Geophaginae and Cichlasomatinae included all the remaining genera within the American cichlids. Geophaginae included 16 genera and were divided into three tribes: Acarichthyini (*Acarichthys* and *Guianacara*), Crenicaratini (*Biotoecus, Crenicara, Dicrossus*, and *Mazarunia*), and Geophagini (*Geophagus, Mikrogeophagus, `Geophagus` brasiliensis, `Geophagus` steindachneri, Gymnogeophagus, Satanoperca, Biotodoma, Apistogramma, Apistogrammoides* and *Taeniacara*). Cichlasomatinae included two large, sister subclades: the Cichlasomini and the Heroini.

In disagreement with the definition of Kullander, molecular studies (Farias et al. 1998, 1999) and total evidence analyses (Farias et al. 2000, 2001), including Kullander's morphological data, found the Neotropical Cichlidae to be monophyletic and *Heterochromis* to be basal to the African clade. Farias et al. (1999, 2000, 2001) also found the genera *Crenicichla* and *Teleocichla* nested within Geophaginae, expanding the subfamily to 18 genera, and challenging the previously proposed relationship between *Crenicichla, Teleocichla* and the basal genus *Cichla* (Stiassny 1987, 1991; Kullander 1998). Although Farias et al.'s studies have convincingly supported monophyly of Geophaginae, suprageneric arrangements of taxa are unclear, and the internal relationships within the subfamily are currently not established. Farias et al. (1999, 2001) also found that geophagine cichlids had significantly faster rates of molecular

evolution than other Neotropical cichlids. However, the focus of their analysis was on the higher-level relationships within the Cichlidae, and their sampling of Geophaginae was limited. Thus far, no comprehensive assessment has been provided for either the relationships among geophagine genera, or the degree of rate heterogeneity observed among taxa. If such rate heterogeneity is extensive within the group, the derivation of phylogenies with some techniques can be difficult (Felsenstein 1978, 2004).

A molecular phylogeny of Geophaginae was reconstructed by integrating published molecular data from four loci and including new sequences from the mitochondrial gene ND4 and the nuclear gene RAG2. In addition, taxon sampling was expanded with respect to previous studies to include 16 of the 18 genera and 30 species of geophagines. These data are used to: (1) evaluate relationships among genera of Geophaginae; (2) explore the extent of rate heterogeneity within geophagine cichlids; and (3) evaluate the evidence supporting an adaptive radiation for the group.

MATERIALS AND METHODS

Taxon sampling

DNA sequence data were collected for a fragment of the mitochondrial ND4 (NADH dehydrogenase subunit 4) gene and of the nuclear RAG 2 (Recombination Activating Gene 2) gene. Specimens examined included 21 genera and 38 species of Neotropical cichlids, and when possible, sequences were obtained from two individuals of each species. Ingroup samples included 16 of 18 genera and 30 species (Table 3.1) of Geophaginae *sensu* Farias et al. (1999, 2000, 2001), excluding only the genera *Teleocichla* and *Mazarunia*, for which tissue samples could not be obtained. The genus *Geophagus* sensu lato actually includes three distinct genera, of which two are in need of description (e.g. Kullander 1986; Kullander and Nijssen, 1989). Each of these genera is represented by one species in this study, and they are referred to as *'Geophagus' brasiliensis* and *'Geophagus' steindachneri*, which must not be confused with the genus *Geophagus* sensu stricto. One species of each of the genera *Cichlasoma*, *Mesonauta* and

TABLE 3.1 List of taxa for which ND4 and RAG2 were sequenced in this study with collection localities and accession numbers to GenBank. More detailed locality data are available from HLF on request. Taxa and accession number for sequences of 16S, cytochrome *b*, *Tmo-M27* and *Tmo-4C4* used to build the supermatrix are also given. Superscript numbers indicate the original publication of non-original sequences. References are as follows: 1: Farias et al. (2001); 2: Farias et al. (1999); 3: Farias et al. (2000); 4: Zardoya et al. (1996); 5: Kumazawa et al. (1999); 6: Streelman and Karl (1997); 7: Farias, Meyer and Ortí, Unpublished; 8: Tang (2001) and 9: Farias et al. (1998).

			Accession numbers					
	# Fish	Collection locality	ND4	16S	Cytochrome *b*	RAG2	Tmo-4C4	Tmo-M27
Outgroup taxa								
Astronotus sp.	2	Aquarium trade	AY566776	AF048998[2]	AB018987[5]	AY566740	AOU70345[6]	AOU63668[4]
				A. crassipinnis	*A. ocellatus*		*A. ocellatus*	*A. ocellatus*
Cichla intermedia	1	Río Cinaruco, Venezuela	AY566788			AY566752		
Cichla orinocensis	1	Río Cinaruco, Venezuela	AY566786	AF049018[2]	AF370643[1]	AY566751	AF113064[3]	AF112602[3]
Cichla temensis	2	Río Cinaruco, Venezuela	AY566793	AF049019[2]	AF370644[1]	AY566755		
Retroculus sp.	1	Macapá, Brazil	AY566774	AF112591[2]	AF370640[1]	AY566737	AF113061[3]	AF112599[3]
Cichlasomatinae								
Cichlasoma orinocense	2	Apure, Venezuela	AY566778	AF045845[9]	AF145128[3]	AY566747	AF113075[3]	AF112613[3]
					C. bimaculatum		*C. amazonarum*	*C. amazonarum*
Hoplarchus psittacus	1	Río Cinaruco, Venezuela	AY566789	AF045855[9]	AF370673[1]	AY566760	AF113074[3]	AF112612[3]
Mesonauta egregius	2	Caño Maporal, Venezuela	AY566782	AF045859[9]	AF370675[1]	AY566748	AF113066[3]	AF112604[3]
				M. insignis	*M. insignis*		*M. insignis*	*M. insignis*
Geophaginae								
Acarichthys heckelii	2	Aquarium trade	AY566768	AF049004[2]	AF370653[1]	AY566733	AF113083[3]	AF112621[3]
Apistogrammoides pucallpaensis	2	Río Orosa, Perú	AY566770			AY566735		
Apistogramma hoignei	1	Caño Maporal, Venezuela	AY566781	AF049006[2]	AF370656[1]	AY566746	AF113095[3]	AF112633[3]
				Apisto. sp.2	*Apisto*. sp.		*Apisto*. sp.2	*Apisto*. sp.2
Apistogramma agassizi	2	Río Orosa, Perú	AY566787	AF049005[2]		AY566749		
				Apisto. sp.1				
Biotodoma wavrini	2	Río Cinaruco, Venezuela	AY566784	AF049007[2]	AF370657[1]	AY566726	AF113082[3]	AF112620[3]
Biotodoma cupido	2	Río Orosa, Perú	AY566772			AY566723		
Biotoecus dicentrarchus	2	Río Cinaruco, Venezuela	AY566792	AF112641[7]		AY566754		
				Biotoecus sp.				
Crenicara punctulatum	2	Río Nanay, Perú	-	AF049008[2]	AF370655[1]	AY566742	AF113090[3]	AF112628[3]
				Crenicara sp.	*Crenicara* sp.		*Crenicara* sp.	*Crenicara* sp.
Crenicichla geayi	2	Río Las Marías, Venezuela	AY566771	AF045848[9]	AF370645[1]	AY566736		
				Creni. sp.	*Creni*. sp.			

TABLE 3.1 Continued

	# Fish	Collection locality	Accession numbers					
			ND4	16S	Cytochrome *b*	RAG2	Tmo-4C4	Tmo-M27
Crenicichla af. *lugubris*	2	Río Cinaruco, Venezuela	AY566785	AF049002[2] *C. lugubris*	AF370646[1] *C. regani*	AY566750	AF113087[3] *C. regani*	AF112625[3] *C. regani*
Crenicichla sveni	2	Apure, Venezuela	AY566779	AF285939[8] *C. lepidota*		AY566743	U70335[6] *C. saxatilis*	CSU63667[4] *C. saxatilis*
Crenicichla af. *wallacii*	2	Río Cinaruco, Venezuela	AY566790			AY566753		
Dicrossus sp.	2	Aquarium trade	AY566767			AY566731		
Geophagus brachybranchus	2	Río Cuyuní, Venezuela	AY566763			AY566727		
Geophagus grammepareius	1	Río Claro, Venezuela	AY566796	AF112642[7] *G. argyrostictus*		AY566724	AF113092[3] *G. argyrostictus*	AF112630[3] *G. argyrostictus*
Geophagus abalios	2	Río Cinaruco, Venezuela	AY566795	AF045850[9] *G. altifrons*		AY566757	AF113091[3] *G. altifrons*	AF112629[3] *G .altifrons*
Geophagus dicrozoster	2	Río Cinaruco, Venezuela	AY566794	AF049009[2] *G.* cf. *proximus*		AY566756		
Geophagus surinamensis	2	Haut Maroni, French Guiana	AY566777	AF112597[2] *Geophagus* sp.	AF370658[1] *Geophagus* sp.	AY566741	AF113093[3] *Geophagus*	AF112631[3] *Geophagus* sp.
'Geophagus' brasiliensis	2	Aquarium trade	AY566766	AF049016[2]	AF370659[1]	AY566732	AF113088	AF112626
'Geophagus' steindachneri	2	Aquarium trade, origin not known	AY566765		AF370660[1]	AY566730		
Guianacara n. sp. 'Caroni'	2	Río Claro, Venezuela	AY566762	AF049010[2] *Guianacara* sp.	AF370654[1] *Guianacara* sp.	AY566725	AF113084[3] *Guianacara* sp.	AF112622[3] *Guianacara* sp.
Gymnogeophagus balzanii	1	Aquarium trade, probably from Uruguay	-	AF112594[7] *G. gymnogenys*	AF370661[1] *G. gymnogenys*	AY566739	AF113085[3] *G. gymnogenys*	AF112623[3] *G. gymnogenys*
Gymnogeophagus rhabdotus	2	Aquarium trade, probably from Uruguay	AY566775	AF049011[2] *G. labiatus*	AF370662[1] *G. labiatus*	AY566738		
Mikrogeophagus altispinosus	2	Aquarium trade	AY566764	AF045857[2]		AY566729	AF113089[3]	AF112627[3]
Mikrogeophagus ramirezi	2	Caño Maporal, Venezuela	AY566780			AY566744		
Satanoperca daemon	2	Río Cinaruco, Venezuela	AY566791	AF049013[2] *S. acuticeps*	AF370663[1] *S. acuticeps*	AY566758		
Satanoperca jurupari	2	Río Orosa & R. Nanay, Perú	AY566783	AF049014[2]	AF370664[1]	AY566745		
Satanoperca mapiritensis	2	Río Pao & R. Morichal Largo, Venezuela	AY566761			AY566728		
Satanoperca pappaterra	2	Río Paraná, Brazil	AY566773			AY566759		
Taeniacara candidi	2	Aquarium trade	AY566769	AF112592[2]	AF370665[1]	AY566734	AF113094[3]	AF112632[3]

Hoplarchus were added to the ingroup to further test geophagine monophyly against its sister-group Cichlasomatinae (Kullander 1998; Farias et al. 2000, 2001). Based on previous knowledge of cichlid relationships (Oliver 1984; Stiassny 1991; Kullander 1998; Farias et al. 1999, 2000, 2001), three species of *Cichla* and one of *Astronotus* and *Retroculus* were used as outgroups. Throughout the paper, references to both ingroup and outgroup pertain to the above designation of taxa. Whenever possible, more than one species per genus were sampled to test genus-level monophyly, and to improve robustness and resolution of the analysis (e.g. Graybeal 1998; Zwickl and Hillis 2002).

In addition to new data from the ND4 and RAG2 genes, a "supermatrix" (Gatesy et al. 2002) was derived from previously published sequences of the mitochondrial protein-coding cytochrome *b* and the ribosomal 16S genes, the nuclear microsatellite flanking-region *Tmo-M27*, and the nuclear locus *Tmo-4C4* (See Table 3.1 for references and accession numbers). The supermatrix allowed for a total-evidence analysis of all molecular data available for Geophaginae. Given the objective of resolving genus-level relationships, species-level taxonomic mismatches between new data and published sequences were circumvented by creating composites of species to improve resolution at the genus level. Whenever possible, species combinations in the supermatrix (Table 3.1) were based on previous knowledge of intra-generic phylogeny as well as phylogenetic analyses from the new data, which supported genus-level monophyly. For example, *Satanoperca daemon* was combined with *S. acuticeps* following Kullander and Ferreira (1988), and *Gymnogeophagus rhabdotus* with *G. labiatus* based on Wimberger et al. (1998). However, a lack of explicit phylogenetic information often caused decisions to be based on rather arbitrary criteria that helped reduce the amount of missing data. This approach, thus, should satisfy the objective of providing a robust analysis of inter-generic relationships, but species-level relationships recovered from the supermatrix are necessarily spurious and are not being reported. When published sequences were lacking for a genus or locus, that part of the matrix was coded as missing data (?).

Molecular methods

The DNeasy kit (Qiagen) was used to extract total genomic DNA from muscle tissues stored in 95% ethanol. The mitochondrial ND4 gene (~650 bp) was amplified using standard PCR protocols (94°C denaturation, 60 sec., 48°C annealing 60 sec., 77°C extension 45 sec. for 35 cycles) and directly sequenced using primers Nap 2 (Arévalo et al. 1994) and ND4LB (Bielawsky et al. 2002) and the internal sequencing primer Geo-ND4F (5' TCCTCCCCCTRATAATTCTKGC 3'), specifically designed for this study. The nuclear RAG 2 gene (~1000 bp) was amplified using a touchdown PCR protocol (94°C, 30 sec. denaturation, 62°C, 60°C, and 58°C, 2 cycles each; then 56°C for 25 cycles, 60 sec. annealing, and 72°C 90 sec. extension). PCR products were gel extracted using the Quiaquick kit (Qiagen) before sequencing. Amplification and external sequencing primers (F2 & R7) were from Lovejoy and Collette (2001) and the internal sequencing primers Geo IF (5' AGGTCCTACATGCCTACATGC) and GeoIR (5' GGGGCTGCCTTGCARAAGC) were developed specifically for this study. Forward and reverse DNA strands were sequenced with fluorescent-labeled dideoxynucleotide terminators (BigDye, PE Biosystems) following the protocol of Sanger et al. (1977) and using an automated ABI Prism 377 or 3100 sequencer (PE Biosystems).

Alignment

All new sequences were compared to published DNA sequences using NCBI's BLAST search to confirm their identity. Since cichlid sequences of ND4 and RAG2 were not available before this study, sequences significantly matching the expected nucleotide regions in any teleosts were considered accurate and included in the analyses. Forward and reverse sequences were edited and aligned in Sequencher 4.0 (Genecodes), and a consensus sequence was constructed for each specimen of each taxon. Unambiguous sequences of the ND4 fragment could not be obtained for the geophagine taxa *Crenicara punctulatum* and *Gymnogeophagus balzanii*, thus they were removed from the ND4 matrix and treated as missing data in the combined analyses (Table 3.1). Preliminary multiple alignment of all sequences was determined with Clustal X

(Thompson et al. 1994), using default gap penalties. Several gap penalties were used to account for any indels involving codons and overall higher level of nonsynonymous substitutions observed for ND4. The 16S fragment was aligned using the secondary structural model of *Xenopus laevis* predicted by the Gutell Lab at the University of Texas at Austin (Cannone et al. 2002: http://www.rna.icmb.utexas.edu). A total of 29 base pairs in regions of ambiguous structural alignment were excluded because positional homology could not be established. The alignments of microsatellite flanking region *Tmo-M27* and nuclear locus *Tmo-4C4* were checked for unnecessary gaps or obvious alignment mistakes, but otherwise were used unmodified. GenBank accession numbers for new sequences used in this study are given in Table 3.1; a Nexus file with the alignments for all loci is available from HLF on request.

Phylogenetic analyses

A total of four different datasets were analyzed using maximum parsimony and Bayesian approaches: ND4, RAG2, ND4 and RAG2 combined (Total Evidence dataset), and all six genes (ND4, cytochrome *b*, 16S, RAG2, Tmo-4C4 and Tmo-M27) combined in the supermatrix described above and in Table 3.1. Each dataset was analyzed following the procedures described below:

Parsimony analyses. Parsimony analyses, both equally and differentially weighted, were performed in PAUP* v4.0b10 (Swofford, 2002) using 100 replicates of heuristic search with random addition sequence and Tree Bisection and Reconnection (TBR) branch swapping. As a means to partially accommodate rate heterogeneity and saturation effects at certain positions under parsimony, two-parameter step matrices were used to differentially weight transitions and transversions for each of the six aligned gene fragments. Transition/transversion ratios were estimated using ML on a Neighbor-Joining tree constructed using the HKY85 model of nucleotide substitution (Hasegawa et al. 1985) in PAUP*. Support for the parsimony-derived topologies was estimated with nonparametric bootstrap (Felsenstein 1985) and Bremer support indices (Bremer 1988, 1994) with searches performed in PAUP*. Bootstrap included 100 pseudoreplicates and

10 heuristic search replicates under the same conditions of the original search, for both the equally and differentially weighted analyses. Bremer support was estimated only for the strict consensus tree of the unweighted MP analysis with topological constraints implemented in MacClade 4.0 (Maddison and Maddison 2000) and 100 replicates of heuristic search using random addition sequences and TBR.

Bayesian analyses. Bayesian phylogenetic analyses of each of the four data sets (ND4, RAG2, Total evidence and the supermatrix) were run in MrBayes 3.0b4 (Huelsenbeck and Ronquist 2001; Ronquist and Huelsenbeck 2003). This version of MrBayes implements a modified Metropolis coupled Markov Chain Monte Carlo (MC^3) algorithm that independently samples trees and the parameters of the model of evolution from each data partition (Ronquist and Huelsenbeck 2003). The program produces topologies of the combined data, but uses separate models of evolution for each partition. Initial models of molecular evolution were selected using nested Likelihood Ratio Tests as implemented in ModelTest (Posada and Crandall 1998). Once the general model was obtained for each partition, specific parameters of nucleotide substitution were left to vary using default priors, thus each model could accommodate several possible rate models (Huelsenbeck and Imennov 2002). For each data set, phylogenetic analyses were run for 2×10^6 generations, sampling every 100 generations for a total of 20,000 samples per run (Leaché and Reeder 2002).

Log-likelihood values of each sample against the number of generations were plotted, and the Markov chain was considered to have attained stationarity when log-likelihood estimates reached a stable value (Huelsenbeck and Ronquist 2001; Leaché and Reeder 2002). All samples with likelihood values below the stationarity level were discarded as burn-in. Three methods were applied to each data set to avoid estimating phylogenies corresponding to local optima. 1) The MC^3 algorithm implemented in MrBayes was employed. This approach facilitates an efficient search of tree space by using three incrementally heated chains along with the cold chain from which parameters are derived. Heated chains reduce the height of suboptimal peaks and fill valleys between peaks; by randomly swapping with the heated chains, the cold chain can

more effectively explore tree space, reducing the chance of being trapped on local suboptimal peaks (Geyer and Thompson 1995; Huelsenbeck and Ronquist 2001; Ronquist and Huelsenbeck 2003). 2) For each data set, the MC^3 analyses were repeated with different starting trees until not less than four runs converged on the same mean stationarity value. Samples were then used from the four runs which converged on the highest likelihood. 3) For each of the four convergent analyses, 50% majority rule consensus trees were separately estimated, and mean values calculated for the parameters of nucleotide substitution.

Comparison of molecular and morphological topologies

Kullander (1998) proposed a classification of Geophaginae based on his analysis of 91 morphological characters. Likelihood-based tests of Kishino-Hasegawa (KH, Kishino and Hasegawa 1989) and Shimodaira-Hasegawa (SH, Shimodaira and Hasegawa 1999), as implemented in PAUP*, were used to compare the MP and Bayesian topologies with that of Kullander's morphological analysis. Kullander used a consensus of character states for each genus, and taxon sampling was slightly different between his analysis and this study; to make the topologies more comparable, the trees were modified such that a single branch represented each genus, and *Taeniacara candidi* was removed because it was not included in Kullander's study. Topological tests were performed using the ND4, RAG2 and total evidence datasets, but due to the amount of missing data (e.g. *Satanoperca*, *Biotoecus*), meaningful comparisons using the supermatrix dataset could not be performed. In addition, topological comparisons with Farias et al.'s (1999, 2000, 2001) molecular trees were not performed due to their reduced taxon sampling.

Rates of molecular evolution

The two cluster test (TCT) and the branch length test (BLT) of Takezaki et al. (1995) in the LINTRE program (1995, http://www.bio.psu.edu/People/Faculty/Nei/Lab) were performed. These tests offer two different approaches to test whether a group of

sequences evolves in a clock-like fashion. The TCT is a generalized version of the relative-rate test (RRT, Li and Bousquet 1992; Tajima 1993) that allows one to evaluate whether a lineage in a phylogeny evolves significantly faster than other lineages. The TCT is less sensitive to unbalanced tree topology than the original RRT (Robinson et al. 1998). The BLT tests whether the branch length of a lineage is significantly longer or shorter than the average branch length across the tree (Takezaki et al. 1995), thus detecting whether a lineage evolves significantly faster or slower than the others do. Accuracy and power of the tests increase when the tree is rooted with the nearest outgroup (Robinson et al. 1998), and when taxon sampling is increased (Robinson et al. 1998; Sorhannus and Van Bell 1999). With this in mind, *Astronotus* was used as the outgroup following the results of Farias et al. (2000), and performed the tests including all species in the phylogeny.

RESULTS

ND4

The aligned ND4 dataset included 648 base pairs. A single codon deletion was found in *Retroculus* sp. at position 126, and in all species of *Cichla* and in *Biotodoma cupido* at position 130. Homogeneity of nucleotide composition was not rejected by the X^2 test ($X^2 = 90.111$, df = 105, $p > 0.8$) as implemented in PAUP* 4.0b10 (Swofford 2002). The HKY85 model of substitution revealed an overall transition/transversion ratio of 2.23, which was used for the weighted parsimony analysis. The largest overall genetic distance (uncorrected sequence divergence = 41.52%) occurred among the geophagine taxa *Crenicichla wallacii* and *Dicrossus* sp., and the smallest divergence (4.78%) between *Geophagus brachybranchus* and *G. surinamensis*. Sequence divergence between geophagine cichlids and outgroup taxa ranged between 16.2% (*Guianacara* n. sp. 'Caroní' x *Cichla orinocense*) and 36.8% (*Crenicichla wallacii* x *Cichla intermedia*). Divergence between geophagine and cichlasomine taxa varied between 18.3% (*Cichlasoma orinocense* x *Geophagus brachybranchus*) and 37.9%

(*Mesonauta egregius* x *Crenicichla wallacii*). Saturation plots for 648 bp and 36 taxa of ND4 (Figure 3.1) showed an overall saturation of transitions beyond 15-20% divergence, a pattern mostly due to the effect of high rates of change at third positions. Transversions showed little or no overall saturation, as only third positions showed a tendency to saturate beyond 30 to 35% divergence.

Unweighted parsimony analysis of ND4 consisted of 395 informative sites for 36 taxa and produced 2 most parsimonious (MP) trees of 2770 steps with a global consistency index (CI) of 0.30, retention index (RI) of 0.39, and rescaled consistency index (RC) of 0.12. The difference between the two unweighted MP trees was the position of species within the genus *Geophagus*. Transition/transversion weighted parsimony included 403 informative sites, producing a single MP tree of 3918.91 steps and CI = 0.32, RI = 0.41 and RC = 0.13. Both unweighted and weighted parsimony analyses produced essentially the same topology (Figure 3.2A), with a weakly supported monophyletic Geophaginae. The best supported relationships within the subfamily were a clade uniting *Satanoperca*, *Apistogramma* (including *Apistogrammoides*) and *Taeniacara* (the "*Satanoperca* clade" from here on), and the monophyly of most genera. The unweighted analysis produced a paraphyletic *Mikrogeophagus*, which was monophyletic in the weighted topology. A general time reversible model of molecular evolution was used for the Bayesian analysis, including invariants and gamma-approximated site-specific rate heterogeneity (GTR + I + Γ). Four independent runs converged in the same likelihood range after approximately 25,000 generations; the first 50,000 (500 trees) were discarded as burn in. Fifty percent majority rule topologies and model parameters for each run (19,500 trees/samples per run) were identical, thus all trees were combined into the final topology (Figure 3.2B). The Bayesian analysis produced a monophyletic Geophaginae, recovered the "*Satanoperca* clade" as did the MP analysis, and supported a sistergroup relationship between *Geophagus* and *'Geophagus' steindachneri*. Most other support was given to the monophyly of various genera.

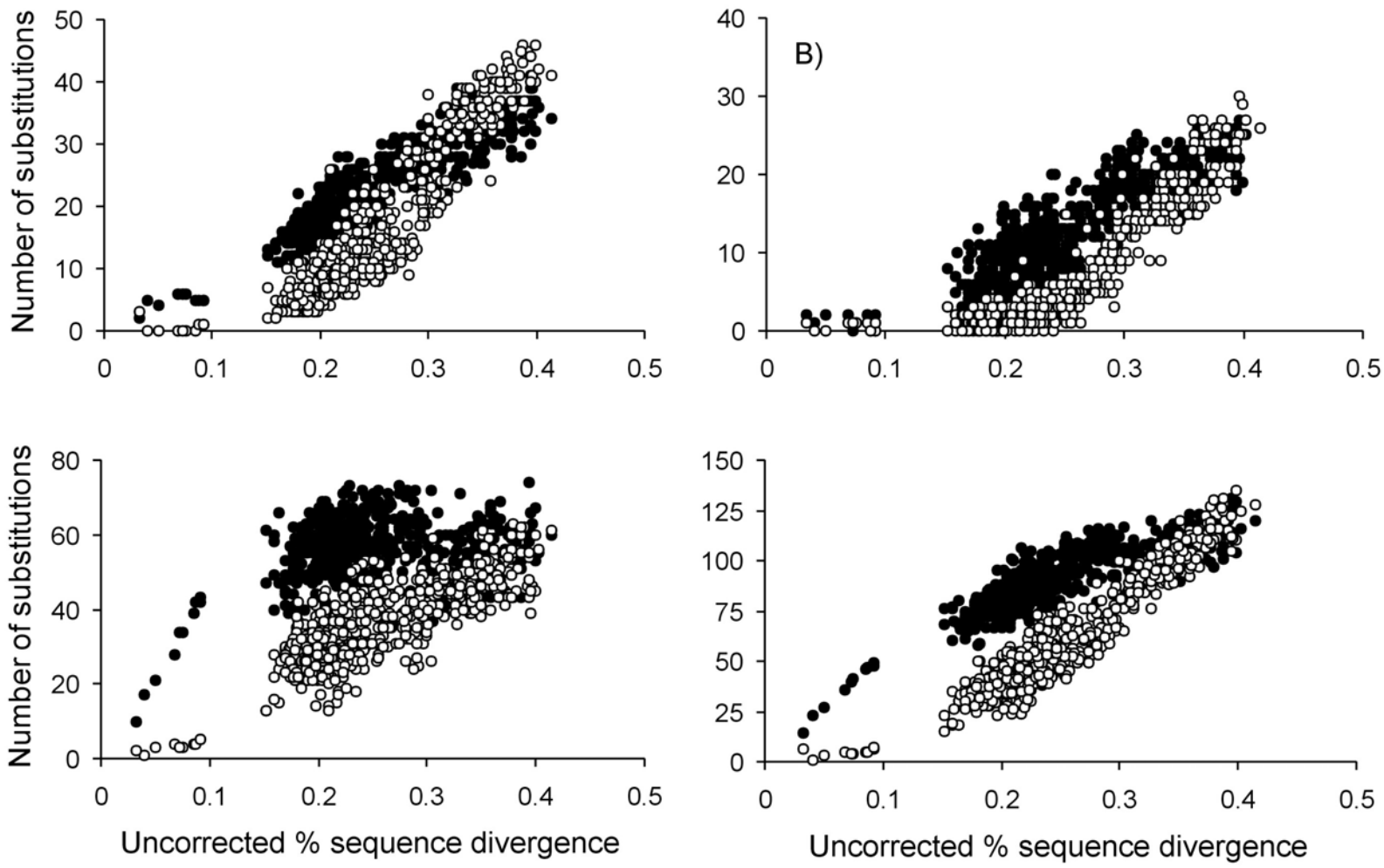

FIG. 3.1. ND4 saturation plots showing transitions (filled circles) and transversions (empty circles). A) first positions; B) second positions; C) third positions; D) all positions. Graphs represent absolute number of nucleotide substitutions against uncorrected percent sequence divergence (p-distance) from pairwise taxa comparisons.

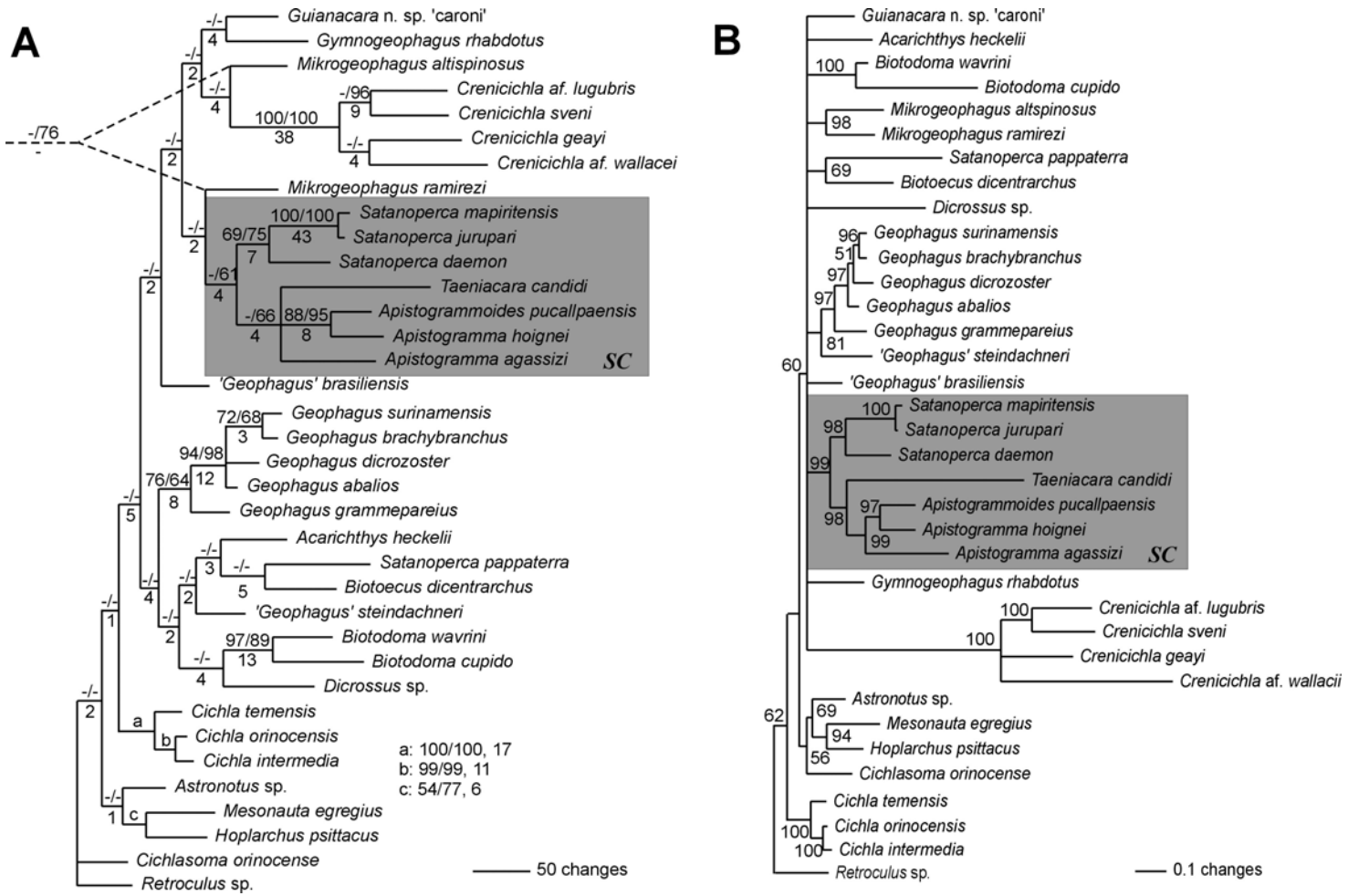

FIG. 3.2. Topologies derived from DNA sequences of the mitochondrial gene ND4. A) Consensus of most parsimonious topologies derived from equally weighted (2 MP trees) and transition/transversion weighted (1 MP tree) analysis of a 648 bp of the mitochondrial NADH dehydrogenase subunit 4 (ND4). Boostrap support, based on 100 pseudoreplicates, for unweighted/weighted analyses is given above branches (only scores >50% are shown); Bremer decay indices for the equally weighted analysis are given below branches. Support values for nodes a-c are given to the right of the tree. See text for tree statistics. B) 50% majority rule Bayesian topology derived from ND4 sequences with a GTR + I + Γ general model of evolution. The topology resulted from combining 78,000 trees from 4 independent runs of 2 x 10^6 generations sampling every 100 trees with burn in of 50,000 generations/500 trees for each analysis. Posterior probabilities are given above branches. Highlighted clade (see discussion): ***SC*** = *Satanoperca* clade.

RAG2

The RAG2 dataset included 976 base pairs, with no differences in length among the 38 taxa included. Homogeneity of base pairs was not rejected by the X^2 test (X^2 = 7.498, df = 111, p = 1.0), and the HKY85 model of nucleotide substitution resulted in a transition/transversion ratio of 2.41. The largest overall genetic distance (7.2%) occurred among the geophagine taxa *Apistogramma hoignei* and *Biotodoma cupido*, and the smallest between *Geophagus brachybranchus* and *G. surinamensis*, which showed no difference in their sequences for the RAG2 fragment. Sequence divergence between geophagine cichlids and outgroup taxa ranged between 6.7% (*Acarichthys heckelii* x *Retroculus* sp.) and 2.6% (*Acarichthys heckelii* x *Cichla temensis*). Divergence between geophagine and cichlasomine taxa varied between 6.4% (*Apistogramma hoignei* x *Mesonauta egregius*) and 3.0% (*Acarichthys heckelii* x *Hoplarchus psittacus*). Saturation plots for the aligned 976 bp from 38 taxa revealed no apparent saturation of nucleotide substitution at any codon position (plots not shown).

Unweighted parsimony analysis of RAG2 included 155 parsimony informative sites for 38 taxa, producing 152 MP trees of 483 steps and CI = 0.70, RI = 0.71 and RC = 0.50. The transition/transversion weighted analyses included 159 informative sites and produced 36 MP trees of 681.99 steps and CI = 0.71, RI = 0.73 and RC = 0.52. The strict consensus trees of both analyses were virtually identical as was overall bootstrap support (Figure 3.3A). Three multi-genus clades were unresolved at the base of a monophyletic Geophaginae: the Tribe Acarichthyini (*Acarichthys* and *Guianacara*), the "*Satanoperca* clade," and a clade including *Biotodoma*, *Mikrogeophagus*, *Geophagus* sensu lato, *Gymnogeophagus*, *Crenicara* and *Dicrossus*, referred to as the "Big clade" from here on. RAG2 Bayesian analyses were run using a GTR + I + Γ model of nucleotide substitution. Of six independent runs, two converged at a lower likelihood range than the other four and were discarded. The four analyses converging at highest likelihood values were then used for tree construction as described for ND4, but in this case the first 1,000 trees were discarded as burn in. As before, 50% majority rule consensus trees and parameters of sequence evolution for each of the four analyses were

identical, thus topologies were combined onto a single tree (Figure 3.3B). The Bayesian topology was essentially identical to the parsimony tree, except for the incorporation of *Crenicichla* and *Biotoecus* at the base of the "Big clade", thus leaving the geophagine phylogeny as a polytomy of three clades, each with at least two genera (Figure 3.3B, and see discussion)

Total evidence

The combined datasets of ND4 and RAG2 produced a matrix of 1624 bp for 38 taxa. Since ND4 sequences were not available for *Crenicara punctulatum* and *Gymnogeophagus balzanii* (see methods), these were treated as missing data. The unweighted parsimony analysis included 550 informative positions and produced 1 MP tree of length 3304 with CI = 0.36, RI = 0.42 and RC = 0.15. The transition/transversions weighted parsimony analysis consisted of 562 informative sites and produced 1 MP tree of 4667.94 steps with CI = 0.37, RI 0.44 and RC = 0.16 (Figure 3.4A). The total evidence parsimony analyses produced a monophyletic Geophaginae with poorly resolved internal relationships, but with some common elements with the independent analyses, particularly the "*Satanoperca* clade" and some components of the "Big clade". Bayesian total evidence analyses were performed under unlinked GTR + I + Γ models of nucleotide substitution for each partition. The final topology (Figure 3.4B) was derived exactly as described for ND4; parameters of sequence evolution for ND4 and RAG2 were not different from those estimated during the individual analyses. The Bayesian topology was similar to the RAG2 Bayesian tree, but completely resolved: the Tribe Acarichthyini was basal to a clade in which the "Big clade," with (weakly supported) *Crenicichla* and *Biotoecus* at its base, was sister to the "*Satanoperca* clade"..

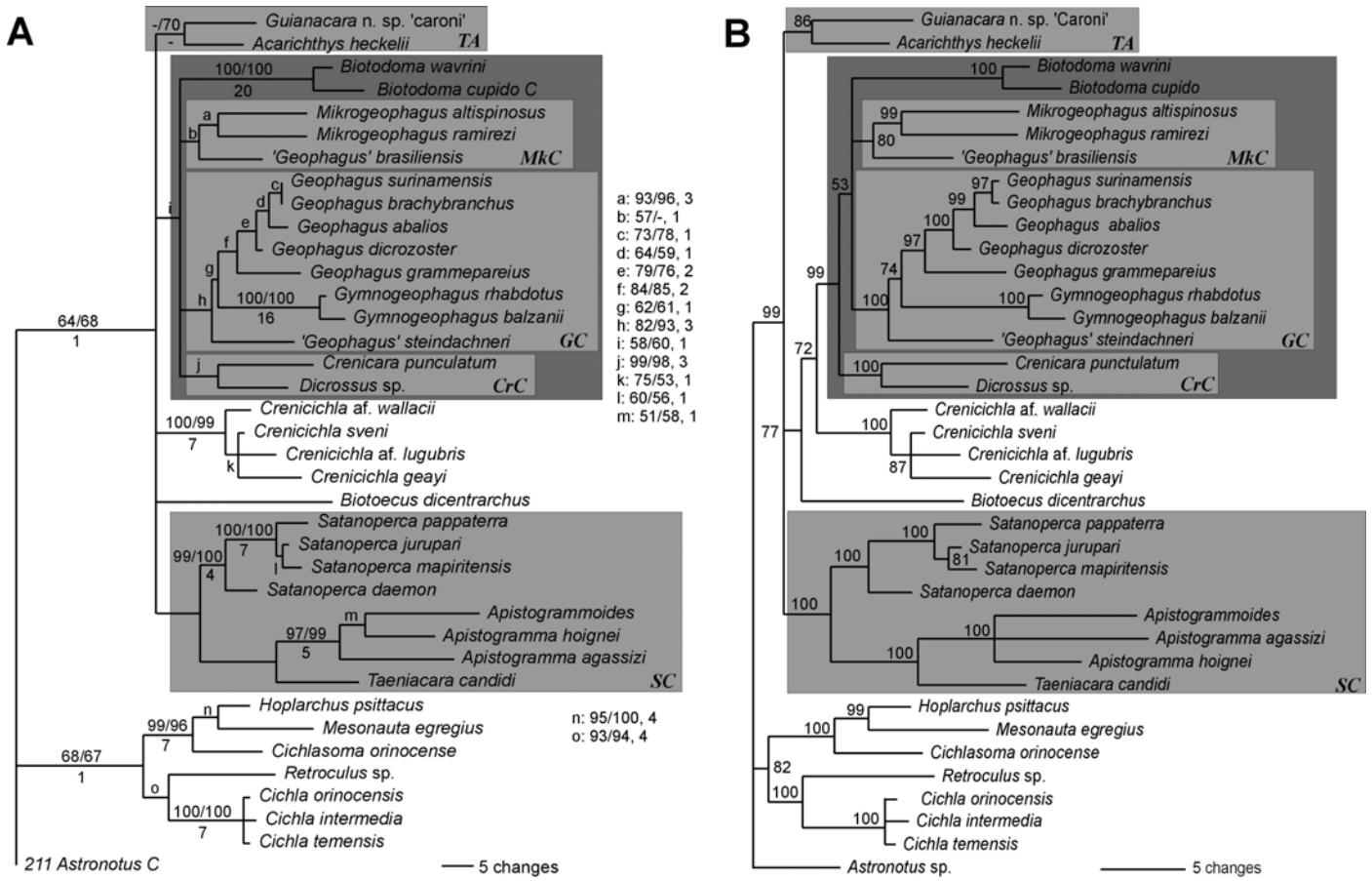

FIG. 3.3. Topologies from DNA sequences of the nuclear gene RAG2. A) Consensus of most parsimonious topologies derived from equally weighted (152 MP trees) and transition/transversion weighted (36 MP trees) analysis of a 976 bp of the nuclear Recombination Activation Gene 2 (RAG2). Boostrap support, based on 100 pseudoreplicates, for unweighted/weighted analyses is given above branches (only scores >50% are shown); Bremer decay indices for the equally weighted analysis are given below branches. Support values for nodes a-o are given to the right of the tree. See text for tree statistics. B) 50% majority rule Bayesian topology using RAG2 sequences with a GTR + I + Γ general model of evolution. The topology resulted from combining 76,000 trees from 4 independent runs of 2 x 10^6 generations sampling every 100 trees with burn in of 100,000 generations/1000 trees for each analysis. Posterior probabilities are given above branches. Highlighted clades (see discussion): ***BC*** = Big clade; ***CrC*** = Crenicarine clade; ***GC*** = *Geophagus* clade; ***MkC*** = *Mikrogeophagus* clade; ***SC*** = *Satanoperca* clade; ***TA*** = Tribe Acarichthyini.

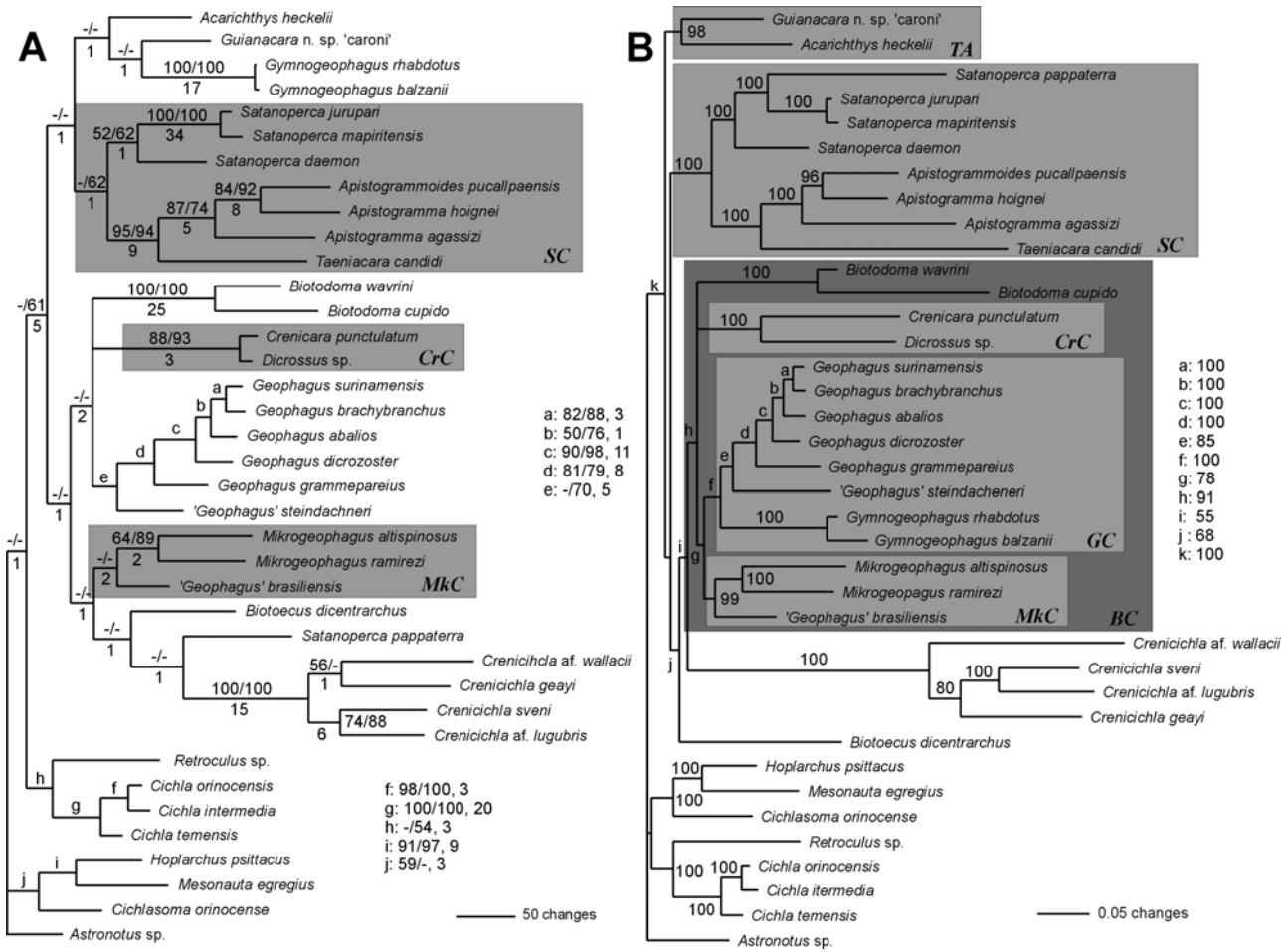

FIG. 3.4. Topologies from the combined ND4 and RAG2 datasets. A) Consensus of most parsimonious topologies derived from equally weighted (1 MP tree) and transition/transversion weighted (1 MP tree) analysis of the combined 1624 bp of the mitochondrial ND4 and the nuclear RAG2. Boostrap support, based on 100 pseudoreplicates, for unweighted/weighted analyses is given above branches (only scores >50% are shown); Bremer decay indices for the equally weighted analysis are given below branches. Support values for nodes a-j are given to the right of the tree. See text for tree statistics. B) 50% majority rule Bayesian topology using ND4 and RAG2 sequences with unlinked GTR + I + Γ general models of evolution. The topology resulted from combining 78,000 trees from 4 independent runs of 2 x 10^6 generations sampling every 100 trees with burn in of 50,000 generations/500 trees for each analysis. Posterior probabilities are given above branches. Highlighted clades (see discussion): ***BC*** = Big clade; ***CrC*** = Crenicarine clade; ***GC*** = *Geophagus* clade; ***MkC*** = *Mikrogeophagus* clade; ***SC*** = *Satanoperca* clade; ***TA*** = Tribe Acarichthyini.

Super matrix

The supermatrix (Table 3.1 and see methods) contained sequences from six molecular markers: ND4, RAG2, cytochrome *b*, 16S, *Tmo-M27* and *Tmo-4C4*, for a total of 3960 aligned base pairs from 38 taxa, of which several are composites of more than one species. The unweighted parsimony analysis contained 1161 informative sites, and recovered 2 MP trees of 6215 steps with CI = 0.40, RI = 0.39 and RC = 0.16. For ND4 and RAG2 the same transition/transversion ratios as for other analyses were used, and the following ratios were calculated for the remaining partitions: cytochrome *b* = 2.27, 16S = 2.32, *Tmo-M27* = 3.90, *Tmo-4C4* = 1.90. The weighted parsimony analysis included 1185 informative sites, producing a single MP tree of 6225 steps with CI = 0.40, RI = 0.39 and RC = 0.16 (Figure 3.5). Parsimony analysis of the supermatrix strongly supported geophagine monophyly and recovered the "*Satanoperca* clade", but otherwise failed to recover relationships found in analyses of RAG2 and the total evidence dataset; all new relationships found in the analysis were weakly supported. Bayesian analysis of the supermatrix was performed using unlinked models of nucleotide substitution for each one of the six partitions. A GTR + I + Γ model was used in all cases, except for *Tmo-M27*, for which the HKY85 + Γ model was employed. Four independent runs produced identical model parameters and partial topologies, thus all samples were combined after discarding the first 500 trees of each run as burn in (Figure 3.6). Bayesian analysis of all the molecular data produced a monophyletic Geophaginae with *Guianacara* at the base of a three-clade polytomy. This polytomy included a mildly supported clade including *Crenicichla*, *Biotoecus* and *Acarichthys*, and the "Big clade" and "*Satanoperca* clade", both with strong support.

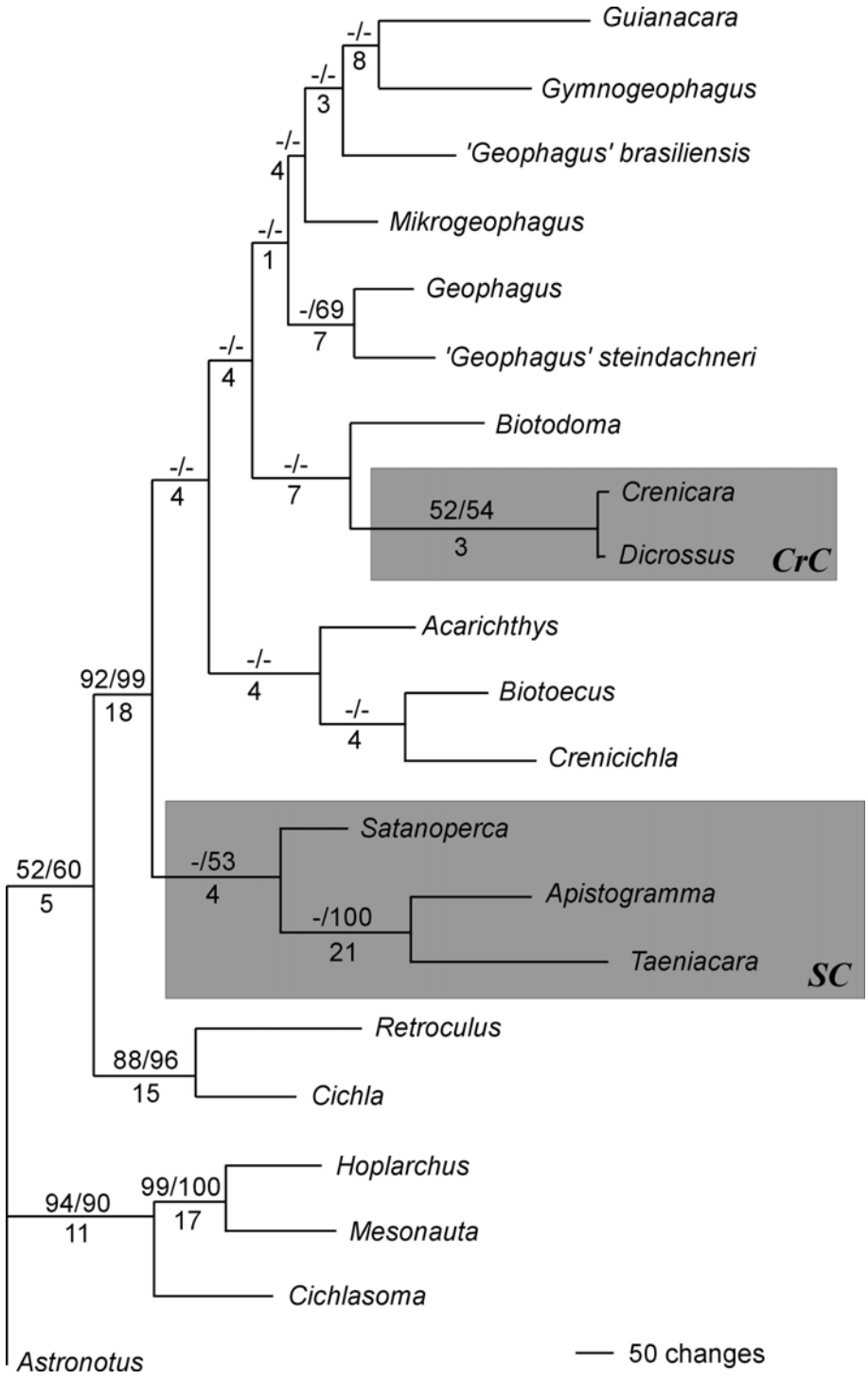

FIG. 3.5. Consensus of most parsimonious topologies derived from equally weighted (2 MP trees) and transition/transversion weighted (1 MP tree) analysis of the combined 3960 bp of the mitochondrial ND4, cytochrome *b* and 16S and the nuclear RAG2, *Tmo-M27* and *Tmo-4C4*. Boostrap support, based on 100 pseudoreplicates, for unweighted/weighted analyses is given above branches (only scores >50% are shown); Bremer decay indices for the equally weighted analysis are given below branches. See text for tree statistics. Highlighted clades (see discussion): ***CrC*** = Crenicarine clade; ***SC*** = *Satanoperca* clade.

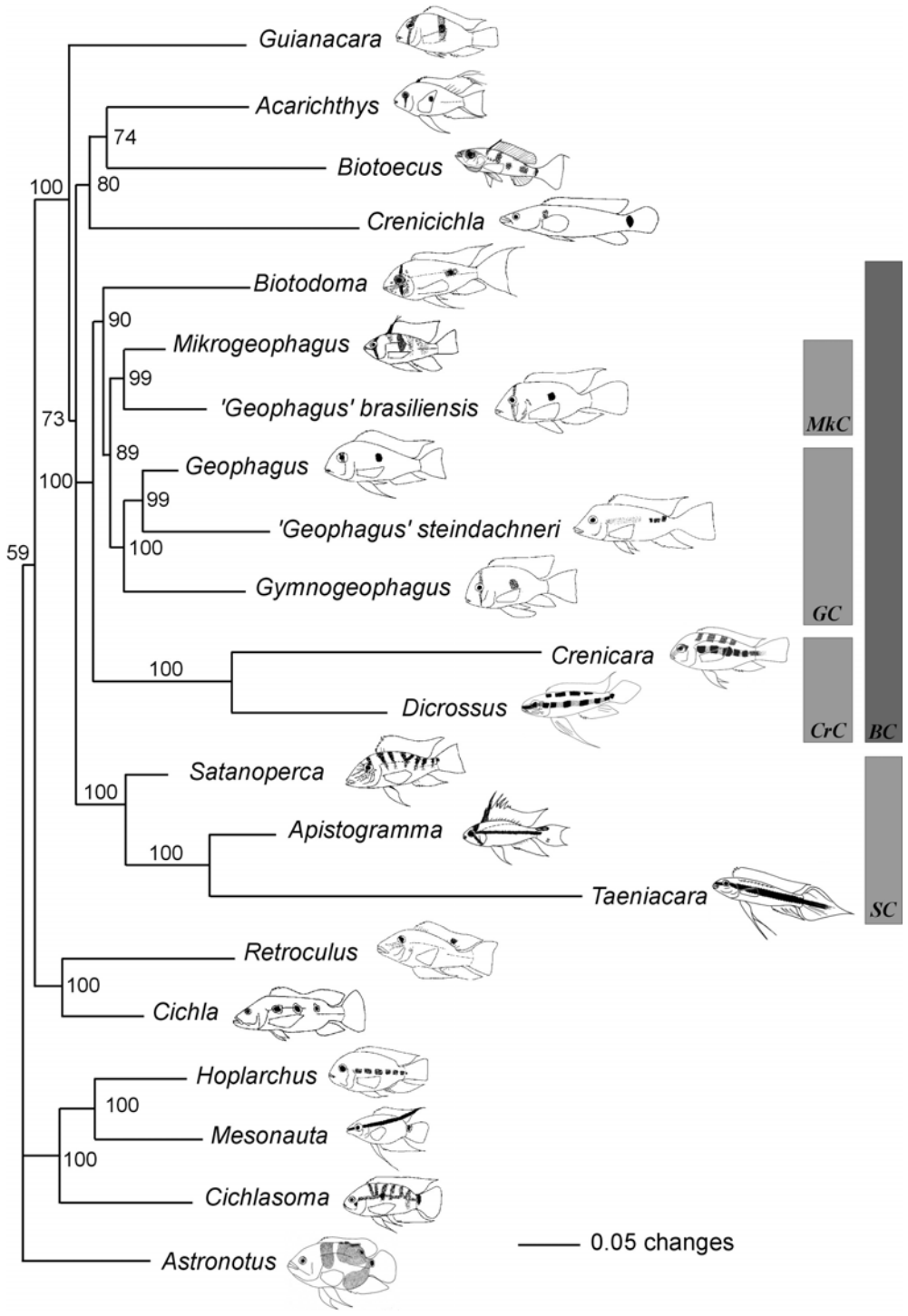

FIG. 3.6. 50% majority rule Bayesian topology derived from the combined 3960 bp of the mitochondrial ND4, cytochrome *b*, and 16S and the nuclear RAG2, *Tmo-M27*, and *Tmo-4C4*. Unlinked GTR + I + Γ general models of evolution were used for all partitions except *Tmo-M27*, for which a HKY85 + Γ model was used. The topology resulted from combining 78,000 trees from 4 independent runs of 2 x 10^6 generations sampling every 100 trees with burn in of 50,000 generations/500 trees for each analysis. Posterior probabilities are given above branches. Highlighted clades (see discussion): ***BC*** = Big clade; ***CrC*** = Crenicarine clade; ***GC*** = *Geophagus* clade; ***MkC*** = *Mikrogeophagus* clade; ***SC*** = *Satanoperca* clade.

With the exception of the most basal nodes, this analysis resolved most of the intergeneric relationships within Geophaginae, and defined three subclades within the subfamily.

Comparison of molecular and morphological topologies

The KH and SH tests indicated that all molecular phylogenies were significantly more likely than Kullander's (1998) morphological topology (Table 3.2). Based on the KH tests, of all parsimony topologies, only the ND4 tree was found to be more likely than both Kullander's and the Bayesian ND4 tree. In contrast, the Bayesian topologies of the RAG2 and TE datasets were significantly more likely than either Kullander's or the parsimony topologies. The SH tests, expected to be more conservative (Shimodaira and Hasegawa, 1999), did not reject the hypothesis of equal likelihood when Kullander's topology was compared to either of the ND4 trees. The Bayesian RAG2 and TE topologies were consistently better than Kullander's tree according to the SH test. The parsimony and Bayesian topologies based on RAG2 were not significantly different (SH test), but the TE Bayesian topology was found to be significantly more likely than the TE parsimony tree. These findings suggest an effect of ND4 in determining incongruence between the total evidence trees.

TABLE 3.2. Results of the Kishino-Hasegawa and Shimodaira-Hasegawa tests comparing Kullander's (1998) morphology-based phylogeny with the molecular phylogenies obtained in this study.

	Parameters	Kullander	MP	Bayesian
ND4	-ln L	6656.33	6642.26	6655.56
	Δ -ln L	14.07	Best	13.30
	KH-test P	< 0.05		< 0.05
	SH-test P	0.142		0.147
RAG2	-ln L	3530.65	3444.68	3438.05
	Δ -ln L	92.6	6.62	Best
	KH-test P	< 0.05	< 0.05	
	SH-test P	< 0.01	0.481	
TE	-ln L	21590.92	21566.08	21524.20
	Δ -ln L	66.72	41.89	Best
	KH-test P	< 0.05	< 0.05	
	SH-test P	< 0.05	< 0.05	

Rate heterogeneity

The TCT analysis revealed significant rate heterogeneity among lineages (ND4: $Q = 1719.5$, $df = 35$, $p < 0.0001$; RAG2: $Q = 9200$, $df = 37$, $p < 0.0001$), with numerous rate differences revealed among taxa for both ND4 and RAG2 (Table 3.3). As found by Farias et al. (1999, 2000, 2001), geophagine cichlids showed overall faster rates of molecular evolution than other Neotropical taxa in both mitochondrial and nuclear genes. It is interesting that *Retroculus*, an outgroup genus morphologically similar to large-bodied geophagines, also revealed significantly fast rates of ND4 evolution, although this was not the case for RAG2. Extensive rate heterogeneity occurred among and within genera of geophagines as well, but patterns were not always the same in both genes. *Crenicichla* and *Taeniacara* showed the fastest mitochondrial rates, whereas *Apistogramma* had the fastest nuclear rates. Rate heterogeneity was also detected within genera in both genes, particularly in *Crenicichla*, *Apistogramma*, *Satanoperca*, and *Biotodoma*. The BLT indicated that rate heterogeneity is much more extensive in ND4 than in RAG2. In ND4, the genera *Biotodoma*, *Dicrossus*, *Crenicichla*, *Apistogramma*, and *Taeniacara* showed at least one species with significantly longer branches than average (Table 3.4), indicating an accelerated rate of molecular evolution. In contrast, *Guianacara*, *Acarichthys*, *Mikrogeophagus*, and *Geophagus sensu lato* showed significantly shorter branches than average. Interestingly, all non-geophagine taxa, with the exception of *Retroculus* ($p>0.05$), showed significantly shorter branches and thus lower rates of evolution in the mitochondrial gene. RAG2 showed a less heterogeneous pattern of evolution, and only *Biotodoma* and *Apistogramma* (including *Apistogrammoides*) showed accelerated rates of molecular evolution, whereas *Guianacara*, *Acarichthys* and one species of *Geophagus* sensu stricto showed significantly lower rates. Of the non-geophagine taxa, only *Cichla* had significantly shorter branches, whereas the rest were not significantly different from the average length.

TABLE 3.3. Assessment of rate heterogeneity among clades by the Two Cluster Test (Takezaki, Rzhetsky and Nei, 1995). Q-values evaluate overall rate heterogeneity; P-values determined from the chi-square distribution. Model used for TCT was Tamura Nei + Γ as implemented in LINTRE.

Gene (df)	TCT	Clades contributing to rate heterogeneity and their rate relationships	P-value
ND4 (35)	Q = 1719.5	*Crenicichla* af. *wallacii* > *C. geayi* (26)	<0.001
	P <0.0001	*Crenicichla* af. *wallacii*, *C. geayi* > *C. sveni*, *C.* af. *lugubris*	<0.001
		Crenicichla > *Taeniacara*	<0.001
		Crenicichla, *Taeniacara* > *Retroculus*	<0.001
		Crenicichla, *Taeniacara*, *Retroculus* > All geophagines	<0.001
		All geophagines, *Retroculus* > *Hoplarchus*, *Mesonauta*	<0.001
		Mesonauta > *Cichla*	<0.05
		Biotodoma cupido > *B. wavrini*	<0.001
		Apistogramma agassizi > *Apistogrammoides*, *Apistogramma hoignei*	<0.001
		Apistogramma> *Satanoperca*	<0.001
		Satanoperca pappaterra > *Biotoecus*	<0.01
		Acarichthys > '*Geophagus' steindachneri*	<0.001
		Gymnogeophagus > *Guianacara*	<0.001
		Mikrogeophagus > *Geophagus*	<0.001
		Guianacara, *Mikrogeophagus*, *Geophagus*, *Gymnogeophagus* > *'Geophagus' brasiliensis*	<0.001

TABLE 3.3. Continued

Gene (df)	TCT	Clades contributing to rate heterogeneity and their rate relationships	P-value
		Acarichthys, *Biotodoma*, *Dicrossus*, '*Geophagus' steindachneri*, *Satanoperca*, *Apistogramma* > *Biotoecus*, *Satanoperca pappaterra*	<0.01
		Acarichthys, *Biotodoma*, *Biotoecus*, *Dicrossus*, '*Geophagus' steindachneri*, *Satanoperca*, *Apistogramma* > *Guianacara*, *Mikrogeophagus*, *Geophagus*, '*Geophagus' brasiliensis*, *Gymnogeophagus*	<0.001
RAG2 (37)	Q= 9200	*Mesonauta*> *Hoplarchus*	<0.001
	P <0.0001	*Cichla intermedia* > *C. temensis*	<0.05
		Retroculus > *Cichla*	<0.05
		All geophagines > *Retroculus*, *Cichla*	<0.001
		All other geophagines > *Acarichthys*	<0.001
		Crenicichla geayi > *C. sveni*	<0.001
		Crenicichla sveni, *C. geayi* > *C.* af. *wallacii*	<0.01
		Biotodoma, *Mikrogeophagus*, *Crenicara*, *Dicrossus*, *Geophagus*, '*Geophagus' brasiliensis*, '*G.' steindachneri*, *Gymnogeophagus* > *Crenicichla*	<0.01
		Apistogrammoides > *Apistogramma hoignei*	<0.001
		Apistogramma agassizi > *Apistogrammoides*, *A. hoignei*	<0.01
		Apistogramma, *Apistogrammoides* > *Taeniacara*	<0.001
		Satanoperca > *S. daemon*	<0.001

TABLE 3.3. Continued

Gene (df)	TCT	Clades contributing to rate heterogeneity and their rate relationships	P-value
		Satanoperca, *Apistogramma*, *Taeniacara* > *Guianacara*, *Biotoecus*	<0.001
		Biotoecus > *Guianacara*	<0.001
		Crenicara > *Dicrossus*	<0.01
		Biotodoma cupido > *B. wavrini*	<0.01
		Biotodoma > '*Geophagus' brasiliensis*	<0.001
		Biotodoma , '*Geophagus' brasiliensis* > *Mikrogeophagus*, *Geophagus* , '*Geophagus' steindachneri*	<0.001
		Gymnogeophagus > '*Geophagus' steindachneri*	<0.01
		'*Geophagus' steindachneri*, *Gymnogeophagus* > *Geophagus*	<0.001
		Geophagus grammepareius > *Geophagus*	<0.01
		Guianacara, *Biotoecus*, *Satanoperca*, *Apistogramma*, *Taeniacara* > *Biotodoma*, *Mikrogeophagus*, *Crenicara*, *Dicrossus*, *Geophagus*, '*Geophagus' brasiliensis*, '*G.' steindachneri*, *Gymnogeophagus*, *Crenicichla*	<0.001

TABLE 3.4. Branch Length Test of rate heterogeneity (Takezaky, Rzhetsky and Nei, 1995). P-values are reported followed by a sign indicating rate increase (+) or rate decrease (-) in comparison with the average rate for all taxa. Model used for BLT was Tamura Nei + Γ as implemented in LINTRE

.

	BLT, P-value, Rate of evolution			
	df = 35		df = 37	
Taxon name	ND4		RAG2	
Guianacara n.sp. 'Caroní'	<0.001	-	<0.05	-
Acarichthys heckelii	<0.01	-	<0.001	-
Biotodoma wavrini	NS		NS	
Biotodoma cupido	<0.001	+	<0.05	+
Mikrogeophagus altispinosus	NS		NS	
Mikrogeophagus ramirezi	<0.05	-	NS	
Biotoecus dicentrarchus	NS		NS	
Crenicara punctulatum	N/A		NS	
Dicrossus sp.	<0.01	+	NS	
Geophagus surinamensis	<0.001	-	NS	
Geophagus brachybranchus	<0.001	-	NS	
Geophagus abalios	<0.001	-	NS	
Geophagus dicrozoster	<0.001	-	<0.05	-
Geophagus grammepareius	<0.001	-	NS	
'Geophagus' brasiliensis	<0.001	-	NS	
'Geophagus' steindachneri	<0.001	-	NS	
Satanoperca pappaterra	NS		NS	
Satanoperca jurupari	NS		NS	
Satanoperca mapiritensis	NS		NS	
Satanoperca daemon	NS		NS	
Gymnogeophagus rhabdotus	NS		NS	
Gymnogeophagus balzanii	N/A		NS	
Crenicichla af. *wallacii*	<0.001	+	NS	

TABLE 3.4. Continued

	BLT, P-value, Rate of evolution			
	df = 35		df = 37	
Taxon name	ND4		RAG2	
Crenicichla sveni	<0.001	+	NS	
Crenicichla af. *lugubris*	<0.001	+	NS	
Crenicichla geayi	<0.001	+	NS	
Apistogrammoides pucallpaensis	NS		<0.001	+
Apistogramma agassizi	<0.001	+	<0.001	+
Apistogramma hoignei	NS		<0.01	+
Taeniacara candidi	<0.001	+	NS	
Hoplarchus psittacus	<0.001	-	NS	
Mesonauta egregius	<0.001	-	NS	
Cichlasoma orinocense	<0.001	-	NS	
Retroculus sp.	NS		NS	
Cichla orinocensis	<0.001	-	<0.001	-
Cichla intermedia	<0.001	-	<0.05	-
Cichla temensis	<0.001	-	<0.001	-

DISCUSSION

Phylogenetic relationships of Geophaginae

Under both parsimony and Bayesian analyses, the ND4 matrix produced a monophyletic Geophaginae, albeit with questionable support (Figure 3.2); analyses of all other datasets, both MP and Bayesian, indicated stronger support for geophagine monophyly (Figures 3.3-3.6). With the exception of ND4, all analyses recovered a monophyletic cichlasomatine clade in which *Hoplarchus* and *Mesonauta* were grouped in accordance with previous studies of the tribe Heroini (Kullander 1998; Farias et al. 1999, 2000, 2001). Analyses of ND4 supported monophyly of most geophagine genera, and a sister-group relationship between *Geophagus* sensu stricto and *'Geophagus' steindachneri*, but failed to provide any other well-supported intergeneric associations. Within the geophagine clade, most combined analyses consistently found two monophyletic groups including 12 of the 16 genera in this study and a weakly supported clade including the remaining four genera. The overall arrangement of taxa in the molecular trees (Figs. 2-6) is in disagreement with the topology described by Kullander (1998, see KH and SH tests in Table 3.2). For convenience of discussion, each major group diagnosed by the molecular data will be examined separately in the following paragraphs.

The "*Satanoperca* clade." The relationship uniting *Satanoperca* with the sister-taxa *Apistogramma* and *Taeniacara* (the "*Satanoperca* clade") was consistent in all analyses, and support for it was generally high (Figures 3.2-3.6). Farias et al. (1999, 2000, 2001), using 16S and cytochrome *b* sequences, observed a similar pattern in independent analyses, but found an alternative arrangement of *Apistogramma* grouping with *Crenicichla* in their total evidence analysis (Farias et al. 2000, 2001). In contrast to the molecular data, a "*Satanoperca* clade" was not supported by previous morphological analyses (Kullander 1998). The consistency and high support for the "*Satanoperca* clade" in all of this study's analyses, however, provides strong support for the monophyly of this clade. Within *Apistogramma*, the ND4, RAG2 and total evidence

analyses (i.e. those with no missing data) coincided in grouping *A. hoignei* with the monotypic *Apistogrammoides*, suggesting the latter includes an exceptional, autapomorphic species of *Apistogramma* that does not warrant separate generic status. One point of incongruence between the ND4 and RAG2 datasets is the placement of *Satanoperca pappaterra* as sister to *Biotoecus* by the ND4 gene (Figure 3.2), whereas both the RAG2 and total evidence analyses place this taxon as part of a monophyletic *Satanoperca* (Figures 3.3-3.4). There are at least three explanations for this incongruence. First, the sequence shared between *S. pappaterra* and *Biotoecus* is the result of a pseudogene. This seems unlikely. Base composition of ND4 sequences for these two taxa is similar to that of other taxa examined, as well as to previously reported data for ND4 in fish (Bielawski et al. 2002). In addition, no electropherograms revealed evidence of multiple sequences, and all primers (external and internal), when used in independent combinations of PCR amplifications, resulted in similar sequences. Second, the close ND4 relationship may have resulted from contamination. This also appears unlikely. Uncorrected genetic distance between *S. pappaterra* and *Biotoecus* (p = 24.9%) is not very different from the distance between *Biotoecus* and the other species of *Satanoperca* (*S. daemon* = 22.3%, *S. mapiritensis* = 25.2%, *S. jurupari* = 24.6%). Third, it is possible that *S. pappaterra* and *Biotoecus* are more similar in rates of ND4 evolution relative to other species of *Satanoperca*. Although the BLT for rate heterogeneity does support this hypothesis (Table 3.4), comparisons with the TCT revealed a slower rate of change in *S. pappaterra* and *Biotoecus* relative to the other species of *Satanoperca* (Table 3.3). In such cases of heterogeneity, relationships can be obscured (i.e. highly heterogeneous rates, frequent non-synonymous amino acid substitutions). This notion is reinforced by the fact that the unweighted parsimony analysis of ND4 was unable to recover a monophyletic *Mikrogeophagus*, whereas the weighted and the Bayesian analyses did find the genus to be monophyletic. Finally, ND4 may simply be too noisy for comparisons involving high levels of divergence as in the case of *Satanoperca pappaterra* relative to its congeners.

The "Big clade." Supported by parsimony and Bayesian results from RAG2 and most combined analyses, the "Big clade" included *Biotodoma*, *Mikrogeophagus*, *Geophagus* sensu lato, *Gymnogeophagus*, *Crenicara,* and *Dicrossus* (Figures 3.3, 3.4B-3.6). Four elements, with various degrees of resolution depending on the analysis, are contained within this group. 1) A monophyletic genus *Biotodoma*, 2) a "*Mikrogeophagus* clade" in which that genus is sister to *'Geophagus' brasiliensis*, 3) the "*Geophagus* clade," including a basal *'Geophagus' steindachneri* and a sister-group relationship to *Gymnogeophagus*, and 4) the "crenicarine clade" containing *Crenicara* and *Dicrossus*. Highest resolution of relationships within the "Big clade" were obtained from the Bayesian analysis of the supermatrix (Figure 3.6), with a pectinate arrangement of the "crenicarine clade" at the base, followed by *Biotodoma* and then a clade containing the sister "*Mikrogeophagus*" and "*Geophagus*" clades. The "crenicarine clade" partially corresponds to the tribe Crenicaratini of Kullander (1998), but he had originally included *Biotoecus*, which appeared elsewhere in this study's analyses. Based these results, recognition of a separate tribe seems unwarranted, as crenicarines group within a larger clade containing other genera. The relationship between "*Mikrogeophagus*" and "*Geophagus brasiliensis*" represents an association not found by other studies. Given this study's increased taxon sampling and overall increase in sequence data, one might expect more resolution within Geophaginae.

Acarichthys, *Guianacara*, *Crenicichla* and *Biotoecus.* The sister-group relationship between *Acarichthys* and *Guianacara* (tribe Acarichthyini in Kullander's classification) has been repeatedly proposed, both by morphological (Kullander 1998), molecular (Farias et al. 1999), and some (Farias et al. 2000), but not all (Farias et al. 2001), total evidence analyses. Although supported by both RAG2 and the Bayesian total evidence results, the ND4, parsimony total evidence, and supermatrix analyses failed to support the monophyly of this clade. Failure to recover this clade could be due to scarcity of data, as *Acarichthys* is a monotypic genus, and only one species of *Guianacara* was included. Therefore, better taxon sampling may provide better support for the relationship (Graybeal 1998; Zwickl and Hillis 2002). Nonetheless, when other

studies have identified this clade, support has been comparatively low with respect to other relationships (e.g. Farias et al. 1999, Figure 3; Farias et al. 2001, Figure 4). In the final Bayesian analysis, *Guianacara* occurred at the base of Geophaginae, and *Acarichthys* weakly grouped with *Biotoecus*, as sister to *Crenicichla*. Interestingly, a sister-group relationship of *Crenicichla, Teleocichla* and the Acarichthyini was observed by Farias et al (1999) in their 16S phylogenetic analysis. A clear pattern emerged in which *Guianacara* and *Acarichthys* appear as "peripheral" genera, not immediately related to the bulk of the geophagine diversity found in the "*Satanoperca* clade" and in the "Big clade". The same scenario seems likely for *Crenicichla* and *Biotoecus*. The phylogenetic position of these two genera within Geophaginae remains elusive. The Bayesian RAG2 and total evidence analyses grouped them at the base of the "Big clade" with moderate support (55 to 77% posterior probability), but this arrangement disappeared in the 6-gene analysis, where they grouped with *Acarichthys*. Although the general morphology of both genera is superficially similar (e.g. elongate, shallow bodies), there is no clear indication that they are closely related. In previous studies, *Crenicichla* sometimes grouped with *Apistogramma* (e.g. Farias et al. 2000, 2001, total evidence), but the consistency of the "*Satanoperca* clade" seems to rule out that possibility. Resolution of relationships of these four genera likely will require increased taxon sampling, especially for *Crenicichla* and *Guianacara*, as *Acarichthys* is monotypic and *Biotoecus* has only two known species.

In summary, the most resolved molecular phylogeny of Geophaginae was obtained by Bayesian analysis of the supermatrix dataset, including six different molecular markers (Figure 3.6). Within the monophyletic Geophaginae, two lineages were well supported; the first was the "Big clade," with the crenicarine clade at the base, followed by *Biotodoma* as sister to a dichotomy in which the "*Mikrogeophagus* clade" was sister to a pectinate "*Geophagus* clade" with *Gymnogeophagus* at the base. The second strongly supported clade was the consistently recovered "*Satanoperca* clade". The "Big clade" and the "*Satanoperca* clade" found in this study include most of the taxa formerly assigned to the Tribe Geophagini (Kullander 1998), but also contain

genera from Kullander's Tribe Crenicaratini. Finally, a third, weakly supported clade included a sister relationship between *Crenicichla* and a dichotomy of *Acarichthys* and *Biotoecus*. In agreement with previous molecular and total evidence work (Farias et al. 1998, 1999, 2000, 2001), the genus *Crenicichla* was found to be part of the geophagine clade, but no clear support for its position within the subfamily was found. Kullander's tribe Acarichthyini was not consistently recovered in this analysis, and *Guianacara* was left either at the base of the geophagine clade (Bayesian tree) or as sister to *Gymnogeophagus* (MP tree) in the six-gene analyses. In conclusion, two, well-supported supra-generic groupings within Geophaginae were found, but the relationships of the genera *Crenicichla*, *Biotoecus*, *Acarichthys* and *Guianacara* remain uncertain and demand further study. Newly observed relationships in this analyses are probably the combined result of increased datasets and taxon sampling. The general tendency in this study was to find improved resolution in the combined, larger datasets, and additional data should further resolve geophagine relationships.

ND4 versus RAG2 and Parsimony versus Bayesian analysis

A strikingly different pattern was observed between ND4 and RAG2. Whereas ND4 yielded comparatively low resolution and parsimony and Bayesian analyses were inconsistent with each other (Figure 3.2), RAG2 was highly consistent and offered high resolution at deep levels within the geophagine phylogeny (Figure 3.3). ND4 alone was able to recover a monophyletic Geophaginae and the "*Satanoperca* clade," but it was otherwise limited to establishing genus-level monophyly. Basal relationships within Geophaginae were unresolved, and resolution outside the group was poor. On the other hand, RAG2 recovered not only geophagine monophyly, but also the major clades within it. RAG2 was the only dataset generating a hypothesis of relationship for *Crenicichla* and *Biotoecus*, albeit with low support.

The lack of resolution and inconsistency found in ND4 are likely the result of saturation effects and/or rate heterogeneity. ND4 showed saturation of third position transitions and overall transitional saturation beyond 15% divergence (Figure 3.1), a

pattern congruent with observations in cichlid cytochrome *b* (Farias et al. 2001) and characiform 16S (Ortí and Meyer 1997). Saturation at third positions reduces resolution at deep levels in the phylogeny, but can still be informative on relationships among closely related, recently diverged lineages (Farias et al. 2001), thus the relatively well supported monophyly of most genera. The extensive rate heterogeneity found in ND4 (Tables 3.3 and 3.4) showed short (e.g. *Geophagus*) and long branches (e.g. *Crenicichla*) within the geophagine tree. This situation potentially can create long branch attraction, making parsimony analyses inherently inconsistent (Felsenstein 1978, 2004). RAG2 showed no evidence of nucleotide saturation, and its rates of molecular evolution were less heterogeneous (Table 3.4). RAG2 produced highly resolved, consistent, and well supported topologies both under parsimony and Bayesian methods.

Parsimony-derived topologies of the different datasets were incongruent, and with the exception of RAG2 (Figure 3.3), they were inconsistent with the Bayesian topologies. Results consistently showed that, whenever mitochondrial genes were involved (particularly ND4 and cytochrome *b*), parsimony performed poorly due to the effects of saturation and extensive rate heterogeneity in the mitochondrial genes (see Tables 3.3 and 3.4, and Farias et al. 2001). Bayesian analyses were congruent among themselves, and resolution and support generally increased with the amount of data. Because Bayesian analyses incorporate explicit models of nucleotide substitution, they should present the advantages of maximum likelihood analysis when confronted with non-homogeneous patterns of molecular evolution (e.g. Holder and Lewis 2003; Felsenstein 2004). Although not completely resolved, the Bayesian topology derived from the 6-gene matrix (Figure 3.6) offered the most resolved and best-supported hypothesis of geophagine relationships.

Implications of the molecular phylogeny: Are geophagine cichlids an adaptive radiation?

According to Schluter (2000), adaptive radiations are characterized by four features: common ancestry, rapid speciation, phenotype-environment correlation, and trait utility. Based on this definition, Geophaginae may provide an example of an adaptive radiation of Neotropical cichlids. Geophaginae clearly are a monophyletic clade, both according to the results presented in this paper and to previous research (e.g. Farias et al. 2000). More revealing is the fact that, judging from the Bayesian phylograms, their phylogeny is characterized by short basal branches (Figures 3.2B, 3.3B, 3.4B and 3.6). These short branches can indicate either lack of information to resolve basal relationships, or fast differentiation at the base of the tree (e.g. Kontula et al 2003). Considering that we used nearly 4,000 base pairs from six different genes and obtained a robust topology with the combined analysis, it seems unlikely that the short basal branches are due only to lack of data. Instead, it seems reasonable to assume that a short period of fast diversification characterized the origin of geophagine diversity, allowing little time for character fixation, and thus resulting in small amounts of phylogenetic information associated with that period. Geophagines thus seem to fulfill Schluter's requirements of monophyly and rapid divergence.

It is also interesting that patterns of molecular evolution in the group are characterized by strong lineage-specific rate heterogeneity, suggesting a different evolutionary trajectory for each genus after its differentiation. It is possible, though in need of further study, that these differences in evolutionary patterns reflect adaptive divergence. This explanation warrants further investigation because geophagine cichlids possess remarkably diverse life history, ecological, and behavioral specializations. Geophagine reproductive strategies range from large-bodied, mouth-brooding, monogamous species with relatively large generation times (e.g. *Geophagus*) to small-bodied, polygynous substrate spawners that reach sexual maturity much earlier (e.g. *Apistogramma*). The importance of ecological specialization in the evolution of the group is also evident in the association between form and function in relation to trophic

biology and habitat use. Ecomorphological patterns range from deep bodied fishes with ventrally-oriented mouths that ingest and sift sandy substrates for invertebrates (e.g. *Geophagus*, *Satanoperca*), to elongate piscivores with terminal mouths (*Crenicichla*), and small species that inhabit highly structured habitats and feed mostly on epibenthic invertebrates (e.g. *Taeniacara*, *Biotoecus, Apistogramma*). Ecomorphology may determine both lineage-specific evolutionary trajectories and patterns of community assembly. Although inconclusive, these patterns strongly suggest a correlation between phenotype and environment, which is Schluter's third requisite to consider a clade as an adaptive radiation. At present, evidence of the fourth requisite, trait utility, is almost completely lacking. Explicit analyses of functional morphology and ecological performance of geophagines are needed. In conclusion, geophagine cichlids provide an outstanding group for the investigation of adaptive radiation of fishes in fluviatile habitats.

CHAPTER IV

MORPHOLOGY, MOLECULES AND CHARACTER CONGRUENCE IN THE TOTAL-EVIDENCE PHYLOGENY OF SOUTH AMERICAN GEOPHAGINE CICHLIDS (PERCIFORMES: LABROIDEI)

> The problems of phylogeny reconstruction in the face of muted morphological variation are manifold, yet without a sound phylogenetic framework our understanding of the behaviour, ecology and evolution of these fascinating fishes is greatly diminished. There is clearly great incentive to continue with phylogenetic studies of the family Cichlidae.
>
> —M. L. J. Stiassny 1991

INTRODUCTION

The subfamily Geophaginae constitutes an adaptive radiation of 18 genera and over 180 described species with remarkable morphological, ecological and reproductive diversity (Chapter III). Overall geophagine morphological and behavioral diversity strongly suggest ecomorphological specialization for feeding and habitat use (e.g. Winemiller 1995; Chapter III), and their reproductive versatility ranges from substrate spawning to mouth brooding, and from monogamy to polygyny in various combinations (e.g. Wimberger et al. 1998; Barlow 2000; Weidner 2000). Syntopy of genera and species in South American rivers indicates that ecomorphological specialization may also be related to niche partitioning in highly diverse ecological communities (e.g. Winemiller and Pianka 1990; Winemiller 1991; Arrington 2002).

Phylogenetic studies of cichlids have traditionally focused on higher-level relationships within the family Cichlidae, and have been based on morphological characters (e.g. Cichocki 1976; Stiassny 1981, 1987, 1991; Oliver 1984; Kullander 1998). However, limited morphological variation and extensive convergence among

cichlid taxa result in extensive homoplasy and decreased phylogenetic resolution (e.g. Stiassny 1987, 1991). Morphological convergence is rampant among cichlids due to the enormous ecological versatility of the group, which has undergone frequent adaptive modifications associated with trophic ecology, habitat use, reproductive biology, and behavior (e.g. Cichocki 1976; Winemiller et al. 1995; Rüber and Adams 2001). Ecologically significant variation in cichlids can be derived from relatively minor morphological modifications (see Stiassny 1991 for a review), leaving a relatively limited set of morphological characters to use in phylogenetics. Despite these drawbacks, morphological analysis frequently has provided a robust diagnosis of the higher-level evolutionary relationships (e.g. Stiassny 1991; Kullander 1998).

Recent molecular studies (e.g. Meyer 1993; Zardoya et al. 1996; Roe et al. 1997; Martin and Bermingham 1998; Farias et al. 1999; Verheyen et al. 2003), and some that employ total evidence analysis combining molecular and morphological data (Farias et al. 2000, 2001) have elucidated higher-level relationships within the Cichlidae. Furthermore, independently derived molecular data offer a broader context for the evaluation of underlying homology in morphological data. From the interaction of molecular and morphological datasets, congruence of homologous characters should emerge, allowing morphology to contribute to overall phylogenetic resolution (e.g. Chippindale and Wiens 1994; Wiens and Reeder 1995; Baker and DeSalle 1997; Baker et al. 1998; Hillis and Wiens 2000). Although incongruence is expected to occur among separate analyses of different data (e.g. Brower et al. 1996), it cannot be predicted a priori. Only combined analyses can uncover underlying homology from characters that appear homoplastic when examined separately (Cognato and Vogler 2001; Damgaard and Cognato 2003; Hodges and Zamudio 2004). Under these circumstances, homoplasy inherent to each partition is accommodated in the totality of the data, allowing the common phylogenetic signal to dominate the analysis, frequently producing better resolution and better supported trees (Chippindale and Wiens 1994; Wiens and Reeder 1995; Brower et al. 1996; Baker et al. 2001).

A total evidence approach, combining molecular and morphological data, should favor the emergence of congruent phylogenetic signal above the pervasive homoplasy of cichlid morphology, resulting in the "sound phylogenetic framework" needed to understand cichlid evolution. Building upon improved understanding of higher-level relationships, the next logical step is to clarify the phylogeny within groups of cichlids. Large numbers of morphological characters, derived from taxonomic and high-level phylogeny studies, are potentially available for the analysis of clades within the Cichlidae (e.g. Pellegrin 1904; Regan 1905a, 1905b, 1920; Cichocki 1976; Greenwood 1979; Stiassny 1981, 1987, 1991; Kullander 1983, 1998; Oliver 1984; Casciotta and Arratia 1993a, 1993b). These characters, however, need careful evaluation as high-level studies usually include reduced taxon sampling, and may overlook important variation essential for phylogenetic resolution at lower levels. The combination of diverse phylogenetic information, along with currently available molecular datasets (Chapter III), should provide resolved and well-supported hypotheses of relationships within groups of cichlids.

The subfamily Geophaginae was formally proposed by Kullander (1998) based on a morphological phylogenetic analysis of Neotropical taxa. In his classification, the subfamily included 16 genera divided into three tribes: Acarichthyini (genera *Acarichthys* and *Guianacara*), Crenicaratini (*Biotoecus, Crenicara*, *Dicrossus*, and *Mazarunia*), and Geophagini (*Geophagus*, *Mikrogeophagus, 'Geophagus' brasiliensis, 'Geophagus' steindachneri, Gymnogeophagus*, *Satanoperca*, *Biotodoma*, *Apistogramma*, *Apistogrammoides*, and *Taeniacara*). In Kullander's analysis, the subfamily was sister to the subfamily Cichlasomatinae, which included most of the remaining Neotropical cichlid diversity; the genera *Retroculus* (tribe Retroculinae), *Cichla* and *Crenicichla* (Cichlinae), *Astronotus* and *Chaetobranchus* (Astronotinae), and the African *Heterochromis*, were arrayed at the base of a paraphyletic Neotropical cichlid assemblage.

Molecular (Farias et al. 1998, 1999) and total evidence studies including Kullander's morphological data (Farias et al. 2000, 2001), however, have challenged the

above classification. Farias et al. (1999, 2000, 2001) repeatedly found the Neotropical Cichlidae to be monophyletic and *Heterochromis* to be basal to the African clade. The genera *Crenicichla* and *Teleocichla* were nested within Geophaginae, expanding the limits of the subfamily, and challenging a proposed relationship between *Crenicichla, Teleocichla* and the basal genus *Cichla* (Cichocki 1976; Stiassny 1987, 1991). Monophyly of Geophaginae *sensu* Farias *et al*. (2000) has been confirmed by an expanded molecular study of the group (Chapter III) with analysis of a molecular matrix of six loci including 16 genera and 30 species of geophagines and representatives of all other Neotropical clades. Chapter III's phylogeny significantly improved resolution of genus-level relationships within the subfamily, and revealed the existence of at least two well-defined clades within Geophaginae, but often with low support. The study also revealed the existence of extremely short branches at the base of the tree and significant heterogeneity of rates of molecular evolution among genes and taxa. Further resolution of geophagine relationships is a requisite for the study of the evolutionary biology of their adaptive radiation.

In this chapter, a new and extensive morphological dataset of geophagine cichlids is aimed at resolving the genus-level relationships within the subfamily. The morphological dataset includes characters described in previous studies, but most have been modified for better representation of morphological variation within the subfamily Geophaginae. Additionally, a number of characters are proposed here for the first time after examination of a large number of geophagine and other Neotropical taxa. The study includes a large amount of well-known osteological characters derived from previous studies of cichlid phylogenetics (e.g. Cichocki 1976; Oliver 1984; Kullander 1998). Additionally, an important amount of recently proposed characters of external morphology was added, including squamation and scale structure (Lippitsch 1993, 1995, 1998), squamation in the lateral line (Webb 1990), and color pattern (e.g. Kullander 1990; Kullander et al. 1992; López-Fernández and Taphorn 2004). The morphological dataset of 136 characters was combined with the six-loci molecular dataset of Chapter III in a total-evidence analysis of over 4,000 characters. The main goal is to improve

resolution and support for the genus-level phylogeny of geophagine cichlids by incorporating morphological information. Additionally, the topologies produced by molecular, morphological and combined data under parsimony and Bayesian paradigms are contrasted, congruence among different partitions of molecular and morphological data is analyzed, and the potential role that character incongruence and the pattern of geophagine evolution may have on the phylogenetic inference of relationships within the clade is discussed.

METHODS

Taxon sampling

DNA sequence data and morphological characters were collected for 21 genera and 38 species of Neotropical cichlids. Ingroup taxa included 30 species and 16 of the 18 genera of the subfamily Geophaginae (Farias et al. 1999, 2000, 2001; Chapter III). The genera *Teleocichla* and *Mazarunia* were not included in the study because specimens and tissue samples were not available. The genus *Geophagus* sensu lato was divided into *Geophagus* sensu stricto (Kullander 1986, and see López-Fernández and Taphorn 2004), '*Geophagus' brasiliensis* and '*Geophagus' steindachneri*. The latter two are undescribed genera, each including several species. One species of each of the genera *Cichlasoma*, *Mesonauta* and *Hoplarchus* were added to the ingroup to test geophagine monophyly against its sister group Cichlasomatinae (Kullander 1998, 2000, 2001). Outgroup taxa included three species of *Cichla* and one of *Astronotus* and *Retroculus*, respectively (Oliver 1984; Stiassny 1991; Kullander 1998; Farias et al. 1999, 2000, 2001). Throughout the paper, the terms ingroup and outgroup will refer to the above listing of taxa.

Molecular dataset

DNA data consisted of a combined supermatrix of three mitochondrial and three nuclear genes amounting to approximately 4,000 nucleotides (Chapter III). The

molecular dataset included sequences of the nuclear gene RAG2 for all species, and of the mitochondrial gene ND4 for 36 of the 38 species in this study. Additionally, it contained published sequences of the mitochondrial genes 16S and Cytochrome *b*, the microsatellite flanking region *Tmo-M27*, and the nuclear marker *Tmo-4C4* for most geophagine genera. Due to differences in taxon sampling among published studies and this one, sequences of different species were combined in order to increase resolution at the genus level. Details about DNA sequencing protocols, alignment, criteria to combine sequences into the supermatrix, and accession numbers are given in Chapter III (Table 3.1).

Morphological dataset

One hundred and thirty six characters of external morphology and osteology were analyzed both separately and in combination with the molecular supermatrix. Most external morphological characters were based on Lippitsch (1993). A few were added from the descriptions of lateral line configuration in Webb (1990), and previous descriptions of color pattern (Kullander 1986, 1990, 1998; Kullander and Ferreira 1988; Kullander and Nijssen 1989; Kullander and Silfvergrip 1991; Kullander et al. 1992). Osteological characters were based on a revision of the extensive literature on cichlid morphology, but were derived mostly from Cichocki (1976), Oliver (1984), Stiassny (1987, 1991), Casciotta and Arratia (1993a) and Kullander (1998). This study's revision of geophagine morphological diversity produced several additional characters used for the first time in this study. Descriptions of all morphological characters, illustrations, and detailed bibliographic references are given in Appendix II.

Most morphology-based efforts to elucidate cichlid phylogenies have focused on higher-level relationships within the family (e.g. Stiassny 1987, 1991), within specific African clades (e.g. Oliver 1984; Lippitsch 1993, 1995), Neotropical clades (e.g. Cichocki 1976; Casciotta and Arratia 1993), or a combination of the two (Kullander 1998). Additionally, an extensive description of characters has been published, but not included in formal phylogenetic analyses (e.g. Pellegrin 1904; Regan 1920; Kullander

1980, 1983, 1986, 1990; Kullander and Nijssen 1989). A significant portion of these studies was reviewed in search of previously proposed characters that could be of relevance for establishing the phylogeny of Geophaginae. Understandably, these studies present a diversity of approaches to character description, often lack uniformity in nomenclature, and sometimes have described characters in a way that does not allow their direct use in phylogenetics. Numerous characters were redescribed such that they could be used in the context of the present analysis. Characters that did not vary within the taxa examined were excluded, and in several cases, the original characters were split into several characters to facilitate coding or clarify the delimitation of character states. For example, Lippitsch's (1993) character 44 included both scale size and squamation pattern: lateral chest scales can be equal or smaller than flank scales; if they are smaller, they can be imbricating or not. The character was divided into size of lateral chest scales (character 16, Appendix II) and juxtaposition pattern of lateral chest scales (character 17, Appendix II).

Description and scoring of external morphology characters was based on direct observation of formalin-fixed, ethanol-preserved specimens. Meristic characters were evaluated on both sides of each specimen to account for variability. Osteological characters were analyzed in cleared and stained specimens (Dingerkus and Uhler 1977; Taylor and Van Dyke 1985) and/or dry, articulated skeletons. Whenever possible, observations were made on several individuals per species to account for intraspecific variability. A complete list of the material examined for morphological analysis is given in Appendix III, and cross-references to voucher specimens from which molecular data were obtained are given where appropriate. Detailed collection localities and other museum data for catalogued material are available from the NEODAT project website (www.neodat.org) and/or from HLF on request. Uncatalogued specimens used for morphological analysis and voucher specimens used for tissue sampling are or will be deposited at the American Museum of Natural History, New York.

All morphological characters were polarized using the outgroup method, keeping multistate characters unordered. Details on polarity decisions for each character are

given in the character description (Appendix II). The coded matrix of morphological characters is given in Appendix IV. Although the focus of the analysis is placed at the generic level, whenever possible several species per genus were analyzed, providing explicit tests of monophyly for the genera, and facilitating coding when genera are polymorphic for a character (see Wiens 2000).

Phylogenetic analyses

The molecular dataset was analyzed in a previous study (Chapter III), thus in this paper the morphological dataset was analyzed by itself and in combination with the molecular supermatrix. Both parsimony and Bayesian phylogenetic methods were performed on each dataset according to the following procedures.

Parsimony analyses. Parsimony analyses, both equally and successively weighted, were performed in PAUP* (Swofford 2002) using 100 replicates of heuristic search with random addition sequence and Tree Bisection and Reconnection branch swapping (TBR). In previous analyses of the molecular data (Chapter III) transition to transversion ratios were used to reweight characters under parsimony, but morphological data do not allow for an equivalent weighting rationale. Given this limitation, *a posteriori* differential weighting was performed (Chippindale and Wiens 1994: 286) by successive approximation (SA) analyses (Farris 1969), using the maximum value of the rescaled consistency index (rc) of each character as implemented in PAUP*. SA favors topologies in which homoplasy of the most consistent characters is minimized (Chase and Palmer 1997), thus helping reduce the effect of sequence saturation and rate heterogeneity in the molecular data, and assigning higher weights to the least homoplastic characters in the morphological dataset (Felsenstein 2004). Support for parsimony-derived topologies was estimated with non-parametric bootstrap (Felsenstein 1985) and Bremer support indices (Bremer 1988,1994) with searches performed in PAUP*. Bootstrap values were derived from 100 pseudoreplicates, each with 10 heuristic searches using random addition sequence and TBR. Bremer support was

estimated using topological constraints implemented in MacClade (Maddison and Maddison, 2000) under the same conditions of the original heuristic search in PAUP*.

Bayesian analyses. Bayesian analyses of the morphological and the total evidence datasets were performed in MrBayes 3.0b4 (Huelsenbeck and Ronquist 2001; Ronquist and Huelsenbeck 2003). This version of MrBayes incorporates a modified Metropolis coupled Markov Chain Montecarlo (MC^3) that allows the independent use of different models of evolution for each partition, including morphological characters (Ronquist and Huelsenbeck 2003). The inclusion of morphology is achieved through the implementation of Lewis' (2001) likelihood model for discrete morphological characters. This model assumes equal state frequencies, and can be combined with a gamma distribution to account for evolutionary rate heterogeneity among characters, but the model does not include an invariants estimate, because invariant characters are normally removed from morphological datasets (Nylander et al. 2004). Given these features of the model, the morphological partition was analyzed using a GTR + Γ substitution model that does not favor any particular direction of character change. This model approximates the conditions of a parsimony analysis with equal weights and unordered characters. More detailed and flexible models for morphological character evolution have been used (Nylander et al. 2004), but are not currently available in software packages. Nucleotide substitution models were the same as used in Chapter III. Parameters of substitution in all models and all partitions were unlinked and left to vary freely under MrBayes default priors, so that each model could accommodate several possible rate parameters (Huelsenbeck and Imennov 2002). Each Bayesian analysis was run for 2×10^6 generations, sampling every 100 generations for a total of 20,000 trees/samples per run. Log-likelihood values for each sample were plotted against the number of generations to determine whether the Markov chains had attained stationarity by reaching a stable likelihood value (Huelsenbeck and Ronquist 2001; Leaché and Reeder 2002). Samples with values below the stationarity level were discarded as burn-in. Three methods to avoid deriving phylogenies from suboptimal peaks of tree space were applied, including 1) the MC^3 algorithm of MrBayes; 2) the MC^3 searches repeated

with different starting trees, until not less than four independent searches converged to the same likelihood; and 3) for each of the four convergent runs, independently estimating 50% majority rule trees, and comparing the parameter values for each partition. Further details of each procedure are given in Chapter III.

Partitioned Bremer Support

To explore the effect of different partitions on the inferred phylogenies and to evaluate the degree of congruence between partitions, the local (node level) support for each topology was compared by calculating Partitioned Bremer Support (PBS) for each node (Baker and DeSalle 1997; Baker et al. 1998). PBS reveals if a partition in the simultaneous analysis supports the total evidence tree, and indicates how much each partition contributes to the overall Bremer support of each node. A positive value of PBS shows support for a particular node by a given partition, while a negative value indicates that the most parsimonious explanation of the data in that partition is not congruent with the combined tree. PBS values were calculated using 100 heuristic search replicates in TreeRot, version 2 (Sorenson 1999). The total tree length and each partition's length in the Bayesian total-evidence tree were calculated in PAUP* using the "describe trees" function, and subsequently entering the constraints file obtained from TreeRot. PBS values from the total-evidence analyses were also used to summarize the overall congruence between each partition using the method of Sota and Vogler (2001). PBS values obtained from each simultaneous analysis were compared using Spearman's ranked correlations. This procedure allows for a comparison of the support offered by each partition in the simultaneous and separate analyses. A positive correlation indicates congruent support between partitions, whereas a negative correlation indicates opposing support. Lack of correlation indicates that support is not associated with the partitions being tested (Cognato and Vogler 2001; Damgaard and Cognato 2003). Spearman's correlations were calculated in SPSS® version 11.0 for Windows®.

Internal Branch Tests

Internal Branch Tests (IBT) were used to determine whether the short basal branches in the geophagine phylogeny (Chapter III) represent credible relationships or a polytomy in which apparent relationships are spurious. IBTs are oriented to establish the reliability of a tree by determining whether the length of its internal branches is significantly different from zero (Nei and Kumar 2000). A bootstrap-based IBT was used, in which a distribution of internal branch lengths for the topology being tested is created, and used to determine whether the branches are significantly positive (Dopazo 1994; Sitnikova et al. 1995, Sitnikova 1996). The IBT was performed in MEGA2 version 2.1 (Kumar et al. 2001), using the combined molecular data set to build distance-based trees under Neighbor Joining (NJ) and Minimum Evolution (ME). Trees were produced under the Kimura-2-parameter (1980) and the Tamura-Nei (1993) models of nucleotide substitution, both with and without a gamma distribution to account for among-site rate heterogeneity (Swofford et al. 1996; Felsenstein 2004).

RESULTS

Phylogenetic relationships

Morphology. A total of 136 morphological characters were analyzed using both unweighted parsimony and successive approximation. The unweighted analysis resulted in eight most parsimonious (MP) trees of 638 steps and global consistency index (CI) of 0.34, retention index (RI) of 0.64 and rescaled consistency index (RC) of 0.22. The eight alternative trees differed in the position of the genera *Geophagus*, *Satanoperca*, and *Gymnogeophagus* with respect to each other, but were otherwise identical, as was the successive approximation tree. The strict consensus tree of the morphological analysis (Figure 4.1A) showed a monophyletic, but weakly supported, Geophaginae including *Crenicichla* at the base of the tree. Most intergeneric relationships had low or moderate support, except for three clades that grouped the genera *Acarichthys* and *Guianacara* (tribe Acarichthyini [Kullander 1998] from here on), *Apistogramma*

(including *Apistogrammoides*) and *Taeniacara*, and *Dicrossus* and *Crenicara* (crenicarine clade from here on, see Chapter III), respectively. Four independent Bayesian searches converged in the same likelihood after approximately 5 x 10^5 generations or 5,000 trees, and the first 10,000 trees were discarded as burn in. Fifty percent majority rule topologies and model parameters for each of four runs were identical, thus all trees were combined into the final topology (Figure 4.1B). The Bayesian analysis recovered a monophyletic Geophaginae, including *Crenicichla* at the base as in the MP analysis. The two trees were generally similar, but the Bayesian analysis placed the clade including *Acarichthys*, *Guianacara* and *Biotodoma* near the base of the tree, whereas it was part of the main clade in the MP analysis.

Combined analyses. The combined analysis (CA) of the morphological and molecular datasets included 4096 characters, of which 1292 were parsimony informative. The equal-weight parsimony analysis produced 2 MP trees of 6918 steps and CI = 0.33, RI = 0.42 and RC = 0.17. Both trees were completely resolved and showed a monophyletic Geophaginae, but the relationships within the subfamily were markedly different, showing incongruent intergeneric relationships, and rendering the strict consensus tree unresolved at the base (not shown). The successive approximation tree was identical to one of the equal weight topologies, but support was weak for most inter-generic nodes within Geophaginae (Figure 4.2A, Table 4.1).

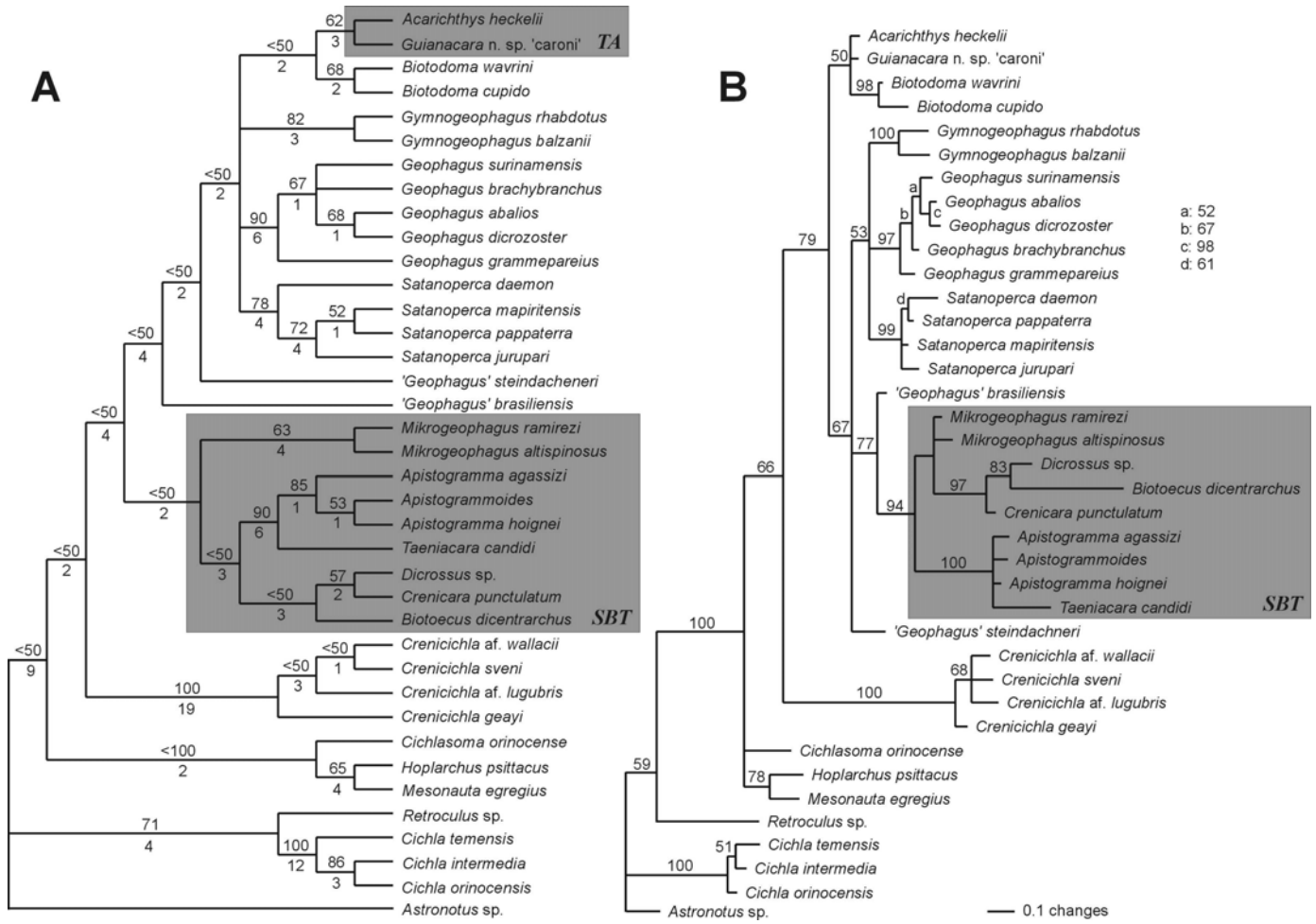

FIG. 4.1. Topologies derived from analysis of morphological data. A) Strict consensus of 8 MP topologies derived from 136 equally weighted morphological characters. Topologies differed in the position of the genera *Geophagus, Satanoperca* and *Gymnogeophagus*, but were otherwise identical, as was the successive approximation tree. Bootstrap support based on 100 pseudoreplicates is given above branches; Bremer support values based on 100 replicates of heuristic search are given below branches. See text for tree statistics. B) 50% majority rule Bayesian topology derived from morphological data analyzed under Lewis (2001) stochastic model of morphological evolution using a GTR model allowing for different rates among characters. The topology resulted from combining 40,000 trees from four independent runs of 2 x 10^6 generations sampling every 100 trees with burn in of 1 x 10^6 generations/10,000 trees for each analysis. Highlighted clades (see discussion): ***TA*** = tribe Acarichthyini, ***SBT*** = Small-bodied taxa.

In general, bootstrap and global Bremer support values were congruent with each other, and strongly supported the crenicarine clade and clades uniting *'Geophagus' steindachneri* with *Geophagus* sensu stricto, and *Apistogramma* with *Taeniacara*, respectively.

Four independent Bayesian searches with the combined data converged in the same likelihood value after approximately 100,000 generations; the first 2,000 trees were discarded as burn in. A fifty percent majority rule consensus was built with the combined trees from all four runs (Figure 4.2B, Table 4.1). The Bayesian topology was essentially identical to that obtained with the molecular data alone (Chapter III, Figure 3.6), with the exception that the Cichlasomatinae was grouped as sister to Geophaginae. The monophyletic Geophaginae had *Guianacara* at the base of the tree. The remainder of the subfamily was grouped in an unresolved tricotomy including a poorly supported clade uniting *Acarichthys*, *Biotoecus* and *Crenicichla*, the "*Satanoperca*" clade (*Satanoperca*, *Apistogramma* and *Taeniacara*), and the "Big clade," that included several subclades: The "*Mikrogeophagus'* clade (*Mikrogeophagus* and *'Geophagus' brasiliensis*), the "*Geophagus*" clade (*Gymnogeophagus*, '*Geophagus' steindachneri*, *Geophagus* sensu stricto), the crenicarine clade, and *Biotodoma*. Most posterior probabilities were high, but several nodes were weakly supported.

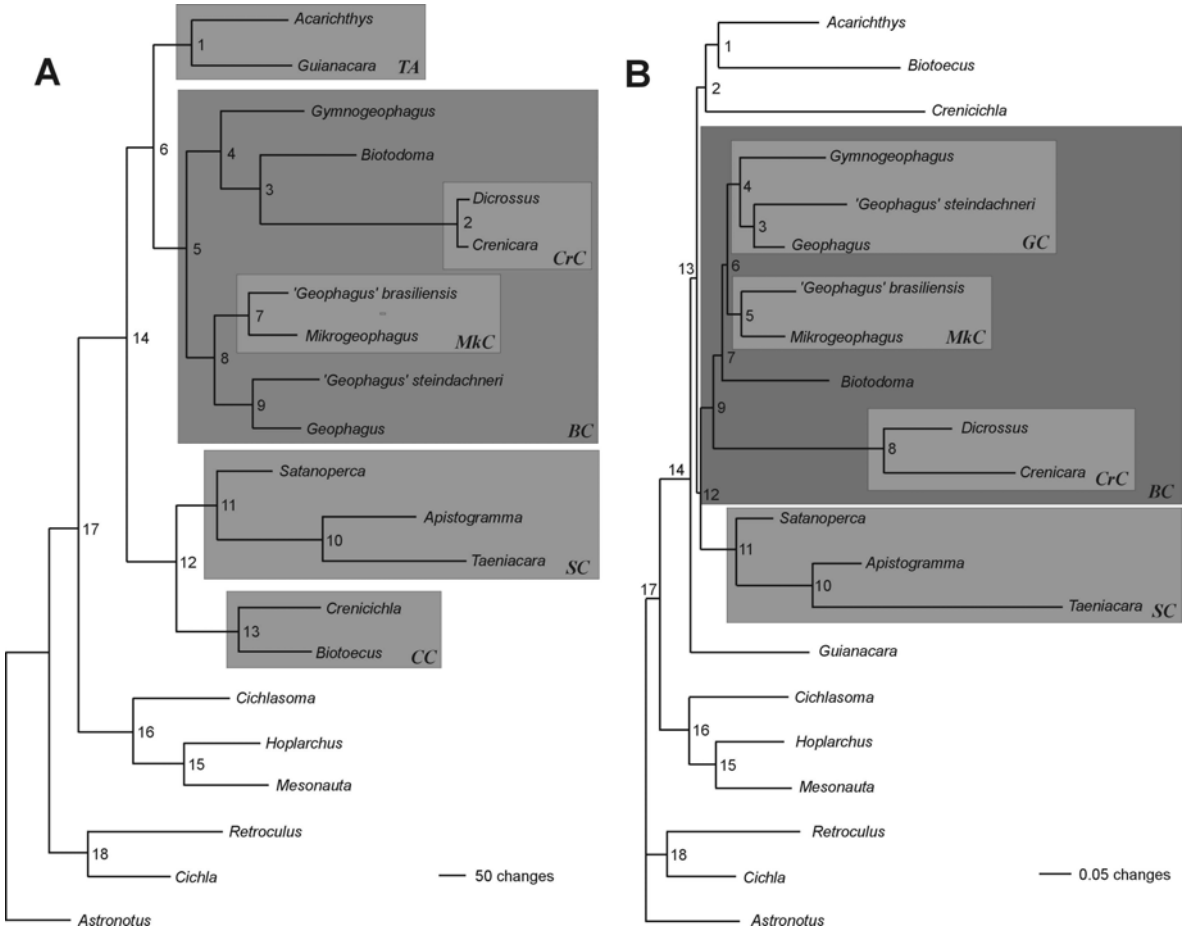

FIG. 4.2. Topologies derived from analysis of total-evidence dataset. A) Successive approximation topology from 2MP trees derived from 4096 characters of morphology and six molecular loci (nuclear: RAG2, *Tmo-M27*, *Tmo-4C4*; mitochondrial: ND4, cytochrome *b*, 16S). Bootstrap support based on 100 pseudoreplicates, Bremer decay indices, and Partitioned Bremer Support values based on 100 replicates of heuristic search for each partition are given in Table 1 for each numbered node on the tree. See text for tree statistics. B) 50% majority rule Bayesian topology derived from data analyzed using unlinked models of morphological evolution/nucleotide substitution for each partition. The topology resulted from combining 72,000 trees from four independent runs of 2 x 10^6 generations sampling every 100 trees with burn in of 200,000 generations/2,000 trees for each analysis. Posterior probabilities, Bremer decay indices, and Partitioned Bremer Support values based on 100 replicates of heuristic search for each partition are given in Table 1 for each numbered node on the tree. Highlighted clades (see discussion): ***TA*** = tribe Acarichthyini, ***BC*** = Big clade**,** ***SC*** = "*Satanoperca* clade"**,** ***CC*** = "*Crenicichla* clade"**,** ***GC*** = "*Geophagus* clade", ***CrC*** = "Crenicarine clade", ***MkC*** = "*Mikrogeophagus* clade".

TABLE 4.1. Support for genus-level trees obtained from the total matrix through A) successive approximation using parsimony (Figure 4.2A) and B) Bayesian analysis (Figure 4.2B). BS = Bootstrap values, DI = Bremer support values (Decay Index), PP = Posterior probabilities. Partitioned Bremer support values for each partition under both analysis methods are shown. Node numbers refer to node labels for the respective trees in Figure 4.2.

					Partitioned Bremer Support													
	Parsimony (A)		Bayesian (B)		Morphology		RAG2		Tmo-M27		Tmo-4C4		Cytochrome b		16S		ND4	
	BS	DI	PP	DI	A	B	A	B	A	B	A	B	A	B	A	B	A	B
Node 1	<50	1	52	-70	0	-25	7	4.5	0	1	0.5	-4.5	-17.5	-8.5	3	-10	8	-27.5
Node 2	96	12	67	-70	2.7	-25	11.8	4.5	0	1	3.2	-4.5	-9.7	-8.5	-2.2	-10	6.2	-27.5
Node 3	<50	0	98	-64	-7	-14.5	3.5	-0.5	0	1	-0.5	-3	-3.5	-5	3	-12.5	4.5	-29.5
Node 4	<50	0	100	-70	-7	-25	3.5	4.5	0	1	-0.5	-4.5	-3.5	-8.5	3	-10	4.5	-27.5
Node 5	<50	0	89	-67	-7	-16.5	3.5	8	0	1	-0.5	-2.5	-3.5	-16	3	-10.5	4.5	-30.5
Node 6	<50	3	59	-70	8.5	-25	3.5	4.5	0	1	2	-4.5	-7.5	-8.5	-0.5	-10	-3	-27.5
Node 7	<50	0	76	-70	-7	-18	3.5	1	0	1	-0.5	-4	-3.5	-5	3	-13	4.5	-32
Node 8	72	6	100	-58	10.5	-22.3	-5	16.3	0	1	1.5	-1.3	3.5	-18.2	-2.5	-12.2	-2	-21.3
Node 9	<50	0	100	-70	-7	-32	3.5	8	0	1	-0.5	-5	-3.5	-12	3	-7	4.5	-23
Node 10	97	20	100	-50	1	-24	16.5	21	3	4	9.5	5	-7.5	-16	5	-5	-7.5	-35
Node 11	<50	0	100	-70	-7	-32	3.5	8	0	1	-0.5	-5	-3.5	-12	3	-7	4.5	-23
Node 12	<50	0	72	-70	-7	-25	3.5	4.5	0	1	-0.5	-4.5	-3.5	-8.5	3	-10	4.5	-27.5
Node 13	<50	1	100	-52	0	-14	7	11	0	2	0.5	-5	-17.5	-24	3	-5	8	-17
Node 14	100	18	100	-48	11	-23	6.5	16	1	1	-0.5	-3	-15.5	-21	5	-6	10.5	-12
Node 15	99	22	100	-53	2	-30	11.5	19	0	0	1.5	-2	-12.5	-20	4	-7	15.5	-13
Node 16	98	17	100	-65	-5	-23	14.5	8	-1	2	2.5	-5	-11.5	-20	3	-7	14.5	-20
Node 17	77	5	100	-55	2	-29.5	3.5	12	1	1	-0.5	-4	-11.5	-12.5	3	-7	7.5	-15
Node 18	99	15	-	-	-4.5	-	7.5	-	0	-	0.5	-	-4	-	3	-	12.5	-
Total					***-20.8***	***-403.8***	***108.8***	***150.3***	***4***	***21***	***17.2***	***-57.3***	***-135.7***	***-224.2***	***44.8***	***-149.2***	***101.7***	***-408.8***

Partitioned Bremer Support and modified combined analyses

Evaluation of PBS values from the combined analyses revealed some incongruence among partitions (Table 4.1). Negative PBS values in at least some nodes of all partitions indicate that homoplasy is common across the data. Negative values were, not surprisingly, much more frequent in the Bayesian tree than in the parsimony topology. This is because the former is far removed from the most-parsimonious topology, and is derived using a method at odds with a parsimony-based measure of support. Although one might argue that using PBS on a topology not derived by parsimony is not informative, or is "unfair," the exercise produces some interesting results, as will be shown below. Pairwise comparisons of PBS values between partitions (Tables 4.2 and 4.3) showed both positive and negative values, which indicate that even though there is incongruence among partitions, there are also important elements of agreement in their phylogenetic information. Significantly positive correlations among several partitions, both in the parsimony and Bayesian analyses, indicate strong congruence within the data. Significantly negative correlations were all associated with the cytochrome *b* partition, in both the parsimony and Bayesian topologies. Cytochrome *b* was significantly incongruent with RAG2 and ND4 in both analyses, and additionally with morphology under parsimony and 16S under Bayesian analysis. Correlations to all other partitions also were negative, albeit non-significant. Since no other partition showed a systematic negative correlation with the remainder of the data, it seemed clear that the phylogenetic signal in cytochrome *b* was in strong conflict with the overall dataset, thus the partition was removed from the dataset and the simultaneous analysis repeated with a reduced total evidence matrix (RTE)

TABLE 4.2. Pairwise Spearman's correlation of Partitioned Bremer Support values for each partition in the successive approximation analysis of the total matrix. ** P < 0.01; * P< 0.05.

	Morphology	RAG2	*Tmo-M27*	*Tmo-4C4*	Cyt *b*	16S	ND4
Morphology	-	0.270	0.395	0.579*	-0.518*	-0.084	0.154
RAG2		-	0.026	0.647**	-0.696**	0.426	0.537*
Tmo-M27			-	-0.122	-0.186	0.473*	-0.213
Tmo-4C4				-	-0.375	-0.179	0.043
Cyt *b*					-	-0.362	-0.670**
16S						-	0.314
ND4							-

TABLE 4.3. Pairwise Spearman's correlation of Partitioned Bremer Support values for each partition in the Bayesian analysis of the total matrix. ** P < 0.01; * P< 0.05.

	Morphology	RAG2	*Tmo-M27*	*Tmo-4C4*	Cyt *b*	16S	ND4
Morphology	-	-0.121	0.434	0.285	-0.122	-0.283	-0.268
RAG2		-	0.165	0.373	-0.866**	0.675*	0.535*
Tmo-M27			-	-0.227	-0.285	0.424	-0.179
Tmo-4C4				-	-0.103	-0.224	-0.203
Cyt *b*					-	-0.689**	-0.675*
16S						-	0.531*
ND4							-

The RTE dataset included 2971 characters, of which 885 were parsimony informative. The parsimony analysis resulted in 2 MP trees of 4877 steps with CI = 0.38, RI = 0.46 and RC = 0.18. The MP trees differed only in the position of *'Geophagus' steindachneri*, which was alternatively placed as sister to *Gymnogeophagus* or *Geophagus* sensu stricto. The latter arrangement was supported by bootstrap analysis, but had no Bremer support (Figure 4.3). The parsimony topology was completely resolved and almost identical to the tree obtained by parsimony when all data were included, but for the majority of nodes, support was increased by the removal of the cytochrome *b* partition (Figures 4.2A and 4.3, Table 4.1). Geophaginae monophyly was strongly supported, and all genera were grouped into two large clades, although with low support. The first clade included the sister-group relationship between the tribe Acarichthyini and the "Big clade;" the second clade grouped the "*Satanoperca*" clade with a weakly supported group uniting *Crenicichla* and *Biotoecus* (the "*Crenicichla*" clade from here on). Bayesian analyses converged on the same likelihood after approximately 1 x 10^6 generations, thus the first 10,000 trees were discarded as burn in and a majority rule consensus tree was built by combining all remaining trees. Bayesian analysis without cytochrome *b* produced a topology very similar to the parsimony tree, although not as completely resolved (Figure 4.4). The strongly supported Geophaginae included a tricotomy of the Acarichthyini, the Big clade as sister to the "*Satanoperca*" clade, and finally the "*Crenicichla*" clade. Within the Big clade, the "*Geophagus*" clade was strongly supported, but the "*Mikrogeophagus*" clade was paraphyletic, including *Crenicara* and *Dicrossus*. All disagreement between the parsimony and Bayesian trees was located at deep branches of the phylogeny. PBS analysis of the RTE topologies (not shown) revealed the mitochondrial gene ND4 and the nuclear locus *Tmo-4C4* had most of the negative values in the parsimony analysis; the Bayesian tree showed a similar pattern, but in addition, all 16S values were negative. Despite this apparently large incongruence, no correlation was significantly negative in either analysis, and further removal of data was not deemed appropriate.

.

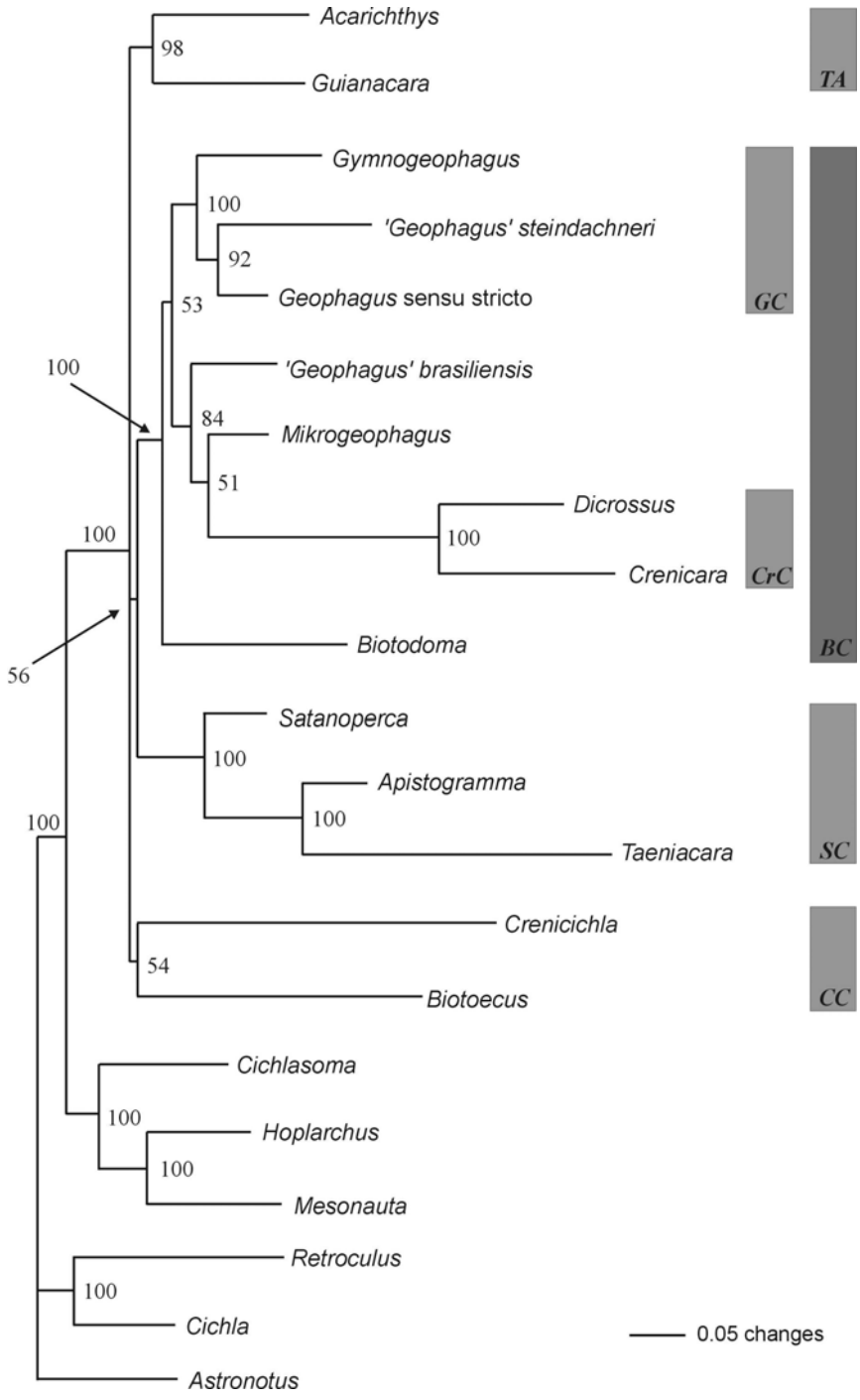

FIG. 4.3. 50% majority rule Bayesian topology derived from the reduced total evidence matrix (RTE) from which the cytochrome *b* partition was removed. Analysis consisted of 2971 characters of morphology and five molecular loci (nuclear: RAG2, *Tmo-M27*, *Tmo-4C4*; mitochondrial: ND4, 16S). The topology resulted from combining 40,000 trees from four independent runs of 2 x 10^6 generations sampling every 100 trees with burn in of 1 x 10^6 generations/10,000 trees for each analysis; posterior probabilities are given by each node. See text for tree statistics. Highlighted clades (see discussion): ***TA*** = tribe Acarichthyini, ***BC*** = Big clade**,** ***SC*** = "*Satanoperca* clade"**,** ***CC*** = "*Crenicichla* clade"**,** ***GC*** = "*Geophagus* clade", ***CrC*** = "Crenicarine clade".

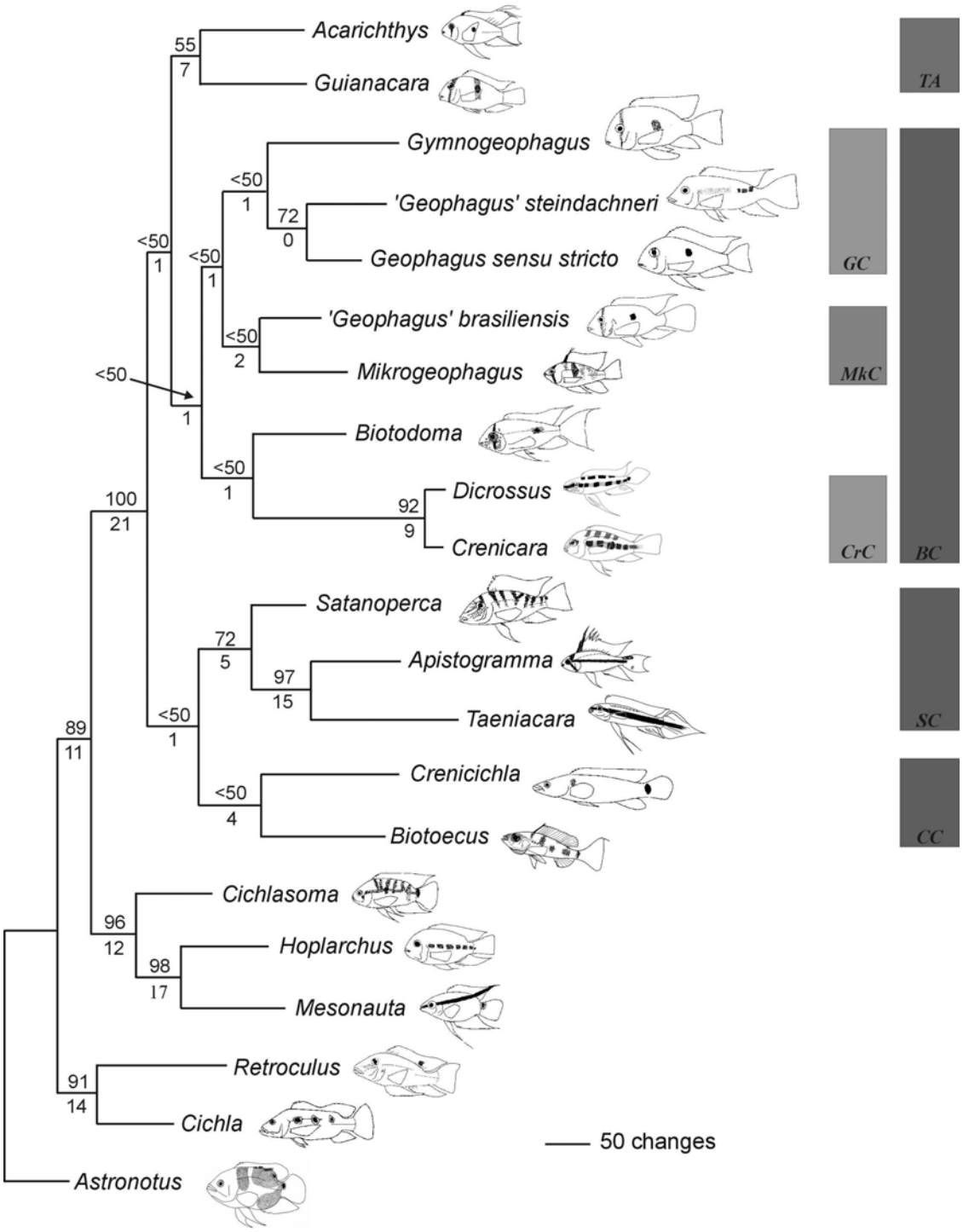

FIG. 4.4. Strict consensus topology from 2MP trees derived from the reduced total evidence matrix (RTE) from which the cytochrome *b* partition was removed. Analysis consisted of 2971 characters of morphology and five molecular loci (nuclear: RAG2, *Tmo-M27*, *Tmo-4C4*; mitochondrial: ND4, 16S). Bootstrap support based on 100 pseudoreplicates is given above branches; Bremer support values based on 100 replicates of heuristic search are given below branches. See text for tree statistics. Highlighted clades (see discussion): ***TA*** = tribe Acarichthyini, ***BC*** = Big clade**,** ***SC*** = "*Satanoperca* clade"**,** ***CC*** = "*Crenicichla* clade"**,** ***GC*** = "*Geophagus* clade", ***CrC*** = "Crenicarine clade", ***MkC*** = "*Mikrogeophagus* clade".

Internal Branch Tests

Although MEGA2 does not allow for the use of pre-defined trees, the topologies obtained by NJ and ME (not shown) were not radically different from those obtained by parsimony and Bayesian analyses using the molecular data. Under all models of nucleotide substitution, with and without a gamma distribution to account for among-site rate heterogeneity, the IBTs consistently found the length of basal branches non-significantly different from zero. With the exception of the branch at the base of the clade uniting *'Geophagus' steindachneri* and *Geophagus* sensu stricto, all intergeneric relationships showed branches with confidence probabilities much lower than 95% (Nei and Kumar, 2000; Kumar et al. 2001). These results clearly suggest that geophagine basal branches are extremely short, and explain the low support obtained for the deeper nodes in the tree.

DISCUSSION

Phylogenetic relationships of Geophaginae: Morphological analyses

Both morphology and total-evidence analyses produced a monophyletic Geophaginae, but relationships derived from the morphological and the combined analyses were markedly different. Monophyly of all genera was supported by the morphological data, except in the case of *Apistogrammoides*, which was grouped with *Apistogramma*, thus corroborating previous molecular results (Chapter III). When analyzed alone, the morphological dataset grouped all the small-bodied taxa, the so-called "dwarf cichlids," into a monophyletic clade (SBT in Figure 4.1A,B), and failed to recover most of the intergeneric groupings found under total evidence. The dwarf cichlid clade included *Mikrogeophagus*, *Apistogramma*, *Taeniacara*, *Dicrossus*, *Crenicara* and *Biotoecus*, and was poorly supported by six ambiguous synapomorphies (Characters 24, 51-54, 110). Neither the total evidence nor the molecular analyses supported a clade of small-bodied taxa. Morphological characters supporting this clade are probably correlated with body-size reduction, and do not represent true secondary

homologies (sensu de Pinna, 1991). Other studies have found that body-size reduction usually determines the parallel "miniaturization" of certain structures, creating non-homologous, convergent derived conditions (e.g. Buckup 1993). Perhaps the best illustration of the bias introduced by miniaturization is the grouping of *Dicrossus*, *Crenicara,* and *Biotoecus* (Figure 4.1A,B). This relationship was first found by Kullander (1998) in his morphological analysis, but has never been recovered from any molecular or total evidence analysis (Farias et al. 1999, 2000, 2001, Chapter III). Instead, the total evidence analyses suggest that *Biotoecus* is related to *Crenicichla* and has no close relationship with the crenicarine clade (Figures 4.3 and 4.4, and see below). The interaction of morphological characters with the molecular dataset produced different topologies than those obtained from morphology alone and heightened support for most clades. Numerous other studies have found that the combination of morphology and molecules often produces arrangements not recovered by either data type alone, and increases overall support (see Brower et al. 1996; Baker and DeSalle 1997; 1998; Wiley et al. 1998; Hodges and Zamudio 2004).

A remarkable difference between this study's morphological results and previous morphology-based analysis of Neotropical cichlids is the finding of *Crenicichla* being grouped with Geophaginae. In previous morphological analyses, Stiassny (1987, 1991), Casciotta and Arratia (1993a), and Kullander (1998) found *Crenicichla* to be sister to *Cichla*. Stiassny (1987) proposed the most comprehensive analysis of characters uniting the two genera, including both myological and osteological traits. Several of Stiassny's osteological characters were found to be more variable than expected, both in and outside *Cichla* and *Crenicichla* (e.g. urohyal morphology, Stiassny's character 2, was not included in this study because its high variability did not allow for a satisfactory coding scheme). In some cases, new character states were identified, with the consequence of reducing support for the former hypothesis (e.g. vomerine head morphology, Stiassny's character 5, this study's character 88). In this study, *Crenicichla* is unambiguously placed within Geophaginae by sharing the possession of a reduced number of concavities in the frayed zone of the fourth upper pharyngeal toothplate

(Character 113, state 1). This study is the first one to find congruence between morphological and molecular evidence regarding the relationships of *Crenicichla*. Finally, this study indicates that the genus *Teleocichla*, sister to *Crenicichla* (Stiassny 1987; Farias et al. 2000), also belongs in Geophaginae.

Phylogenetic relationships of Geophaginae: Total-evidence analyses

Total evidence analyses of morphological and molecular data produced similar topologies, differing only in the way the tribe Acarichthyini, *Crenicichla* and *Biotoecus*, and the grouping of some taxa within the "Big clade" (Figure 4.2A, B). Some of this disagreement disappeared with the removal of the cytochrome *b* partition, revealing that incongruence among the data was to an extent responsible for the lack of resolution in the phylogeny. The following paragraphs elaborate on the phylogenetic relationships of Geophaginae based on the RTE dataset (i.e. without cytochrome *b*). Clade nomenclature followed that used in Chapter III, but is expanded when necessary.

The "Big clade." Despite contradictory support (low on the MP tree and high on the Bayesian tree), the monophyly of the "Big clade" seems well established. Both parsimony and Bayesian analyses recovered the "*Geophagus* clade" (Figures 4.2B, 4.3 and 4.4), in which *Gymnogeophagus* is sister to a clade formed by *'Geophagus' steindachneri* and *Geophagus* sensu stricto. Among previous studies, only Kullander's (1998) included all these taxa, and he found *'G.' steindachneri* to group with *Satanoperca*, whereas *Gymnogeophagus* grouped with *Apistogramma*, and *Geophagus* sensu stricto remained unresolved at the base of the tribe Geophagini. Morphological analyses produced yet different arrangements (Figure 4.1), but none of the results suggested a relationship between *'Geophagus' steindachneri* and *Satanoperca* or between *Gymnogeophagus* and *Apistogramma*. The consistency of this study's molecular (Chapter III) and total evidence results (Figures 4.3 and 4.4) strongly suggests that the "*Geophagus* clade" is likely a monophyletic unit, even though support for its monophyly is not very high (see also next section of the discussion). The remaining relationships within the "Big clade" are less clear, although there is some evidence to

prefer the parsimony topology. Both MP and Bayesian analyses recovered the crenicarine clade, but the relationships of this group to other genera are not strongly resolved. The parsimony analysis grouped the crenicarines with *Biotodoma*, but with low bootstrap and marginal Bremer support values. Alternatively, the Bayesian tree showed the crenicarines grouped with *Mikrogeophagus*, placing *Biotodoma* at the base of the "Big clade," but with the lowest posterior probability in the tree. It seems favoring the parsimony results is cautious and advisable in this particular case for at least two reasons, including 1) it has been repeatedly suggested that support from posterior probabilities is inflated, misrepresenting the actual support that a dataset provides for clade monophyly (e.g. Suzuki et al. 2002; Douady et al. 2003; Simmons et al. 2004); and 2) the total-evidence parsimony topology (Figure 4.4) supports the monophyly of the "*Mikrogeophagus* clade" (*Mikrogeophagus* + *'Geophagus' brasiliensis*), which was repeatedly found in most of this study's analyses (Figures 3.3, 3.4 and 3.6). Although the parsimony topology is provisionally preferred, only additional data and taxon sampling could further clarify relationships within the "Big clade".

The tribe Acarichthyini, the "*Crenicichla* clade," and the "*Satanoperca* clade." Previous molecular analyses (Chapter III, Figures 4.5 and 6) suggested that these clades were located at the base of Geophaginae, but no clear relationships could be determined. Analysis of the RTE dataset recovered the tribe Acarichthyini (*Acarichthys* + *Guianacara*) both under parsimony and Bayesian analyses. Unlike previous molecular analyses (Chapter III), the Acarichthyini were not related to *Crenicichla* and *Biotoecus*, suggesting the morphological dataset had an effect on the results. Nonetheless, *Acarichthys* and *Guianacara* were grouped only by ambiguous morphological synapomorphies of squamation (character 31, reversal to state 0), color pattern (character 75, state 1) and osteology (character 114, state 2; character 122, state 1). Kullander (1998) formally proposed the tribe Acarichthyini based on characters of the first epibranchial bone (his character 14), the lower pharyngeal jaw (his character 20), the shared expansion of the basisphenoid and the parasphenoid wing (his character 36, and see also Kullander and Nijssen, 1989), and the infraorbital series (his character 44).

Evaluation of these characters revealed wide variation and perhaps ontogenetic variability as well. Particularly, the basisphenoid expansion varies among species of *Guianacara* (e.g. *Guianacara sphenozona*, *G*. n. sp. 'caroni'), and as interpreted here, the parasphenoid wing is expanded in several other taxa (e.g. *Geophagus*, and see Appendix III). Additionally, the basisphenoid shape varies independently from the parasphenoid. Differences between our character states and those of Kullander are probably due to differences in taxon sampling when evaluating morphological characters. However, regardless of the characters used the tribe Acarichthyini is frequently recovered in both morphological and molecular analyses (Kullander 1998; Farias et al. 1999, Farias et al. 2000, Chapter III). RTE parsimony and Bayesian analyses in this study consistently recovered the tribe (Figures 4.3 and 4.4), although with unclear resolution of its relation to other geophagines. The parsimony analysis placed it as sister to the "Big clade," but with low support, whereas the Bayesian analysis left it as part of a tricotomy at the base of Geophaginae.

Crenicichla and *Biotoecus* were grouped as a weakly supported clade by the parsimony total evidence (Figure 4.2A, Table 4.1) and by both RTE analyses. In contrast with the molecular dataset and the Bayesian total evidence analysis, genera in the Acarichthyini and the "*Crenicichla* clade" do not appear to be related. Despite its weak support, the "*Crenicichla* clade" is unambiguously defined by the absence of divergent ridges anterior to NLF0 (character 76, state 1), the lack of frontal crest (character 77, state 1), and the possession of a cartilaginous pharyngobranchial 1 (character 104, state 1). No other clade in this study is supported by three unambiguous morphological synapomorphies. Interestingly, the grouping of the two genera also was recovered by the parsimony analysis of the molecular supermatrix alone (Chapter III, Figure 3.5). Relationship of the "*Crenicichla* clade" to other geophagines is not clearly resolved, but some evidence supports its sister relationship with the "*Satanoperca* clade," instead of *Acarichthys*, as previously suggested by the molecular supermatrix analysis (Chapter III).

The "*Satanoperca* clade" (*Satanoperca*, *Apistogramma* and *Taeniacara*) is the most consistently recovered intergeneric arrangement among geophagines (see Chapter III, and figures in this paper), but recovered relationships to other geophagines are weakly supported. The parsimony RTE analysis grouped the "*Satanoperca*" and "*Crenicichla*" clades, and three ambiguous morphological apomorphies supported that arrangement. On the other hand, Bayesian analysis grouped it with the "Big clade," with weak support and no morphological apomorphies. Based on support, and presence of some morphological synapomorphies, the parsimony topology is provisionally preferred, but more evidence will be needed to corroborate whether the "*Satanoperca*" and "*Crenicichla*" clades are sister to each other.

In summary, the MP analysis of the reduced total evidence dataset produced the most resolved and supported hypothesis of relationships among geophagine cichlids (Figure 4.3). Monophyly of the subfamily was strongly supported by all analyses, and its sister-group relationship with the Cichlasomatinae was well supported (Figures 4.3 and 4.4), including five unambiguous morphological characters (43, 50, 55, 117, 119). In the MP topology, two large, sister clades encompassed all genera within Geophaginae. In the first of these, the tribe Acarichthyini (*Acarichthys* + *Guianacara*) was placed as sister to the "Big clade." Within the latter, the "*Geophagus* clade" ('*Geophagus' steindachneri* + *Geophagus* sensu stricto, and both sister to *Gymnogeophagus*) was sister to the "*Mikrogeophagus* clade" (*Mikrogeophagus* + '*Geophagus' brasiliensis*), and in turn, the "*Geophagus*" and "*Mikrogeophagus*" clades were sister to the crenicarine clade and *Biotodoma*. The second main clade within Geophaginae was formed by the sister relationship between the "*Satanoperca* clade" (*Satanoperca* + *Apistogramma* and *Taeniacara*) and the "*Crenicichla* clade" (*Crenicichla* + *Biotoecus*). Alternatively, but with very low support, the Bayesian analysis suggested the sister relationship of the "*Satanoperca* clade" and the "Big clade," leaving the Acarichthyini and the "*Crenicichla* clade" unresolved in a polytomy at the base of the tree (Figure 4.4).

Phylogenetic relationships recovered in this study were derived from the largest data set and taxon sample of geophagine cichlids analyzed to date. Some of these relationships have important implications for the definition and classification of the subfamily Geophaginae. The inclusion of the genus *Crenicichla* is justified both on molecular and morphological evidence, reconciling formerly opposed hypotheses of relationships (e.g. Stiassny 1987, 1991; Kullander 1998; Farias et al. 2000). These results confirm those of Farias (e.g. 1999, 2000) and justify the expansion of the subfamily from 16 to 18 genera by the addition of *Crenicichla* and its sister taxon *Teleocichla*. Likewise, the results refute the reality of the subfamily Cichlinae (*Cichla*, *Crenicichla*, *Teleocichla*) erected by Kullander (1998), thus leaving the relationships of *Cichla* in need of further study. The topologies suggest *Cichla* may be related to *Retroculus* (e.g. morphological characters 45 and 121, but see Farias et al. 2000), but that problem must be left for a study of basal relationships among cichlids, with proper taxon sampling. The tribe Acarichthyini (Kullander 1998) was well supported, and appears to be related to the "Big clade," but a more extensive analysis of morphology within *Guianacara* is needed to better understand the synapomorphies supporting the group (see above), as *Acarichthys* appears to be a monotypic genus. The relationship of *Crenicichla* with *Biotoecus*, and the monophyly of the "Big clade" suggest that the tribes Crenicaratini and Geophagini, as proposed by Kullander (1998), do not reflect actual relationships within Geophaginae. The Crenicaratini originally included *Dicrossus*, *Crenicara* and *Biotoecus*, but all combined data consistently grouped *Dicrossus* and *Crenicara* with the "Big clade." Kullander's Geophagini grouped all genera, with the exception of those in the Acarichthyini and Crenicaratini, but the inclusion of the crenicarine clade and the separation of *Satanoperca* and *Apistogramma* from the "Big clade", renders the Geophagini paraphyletic.

Finally, the arrangement of multi-generic lineages at the base of the geophagine tree is not entirely clear, and further data will be needed to offer stronger support for relationships. Likewise, a better-supported phylogeny of the subfamily will be needed before any definitive effort of revising geophagine classification is made. The

parsimony topology is provisionally accepted because it offers a more resolved hypothesis, supported by several morphological synapomorphies. In contrast, Bayesian relationships were less resolved ad supported by fewer morphological apomorphies. Additionally, because support for relationships at the base of the Bayesian tree (e.g. "Big clade" + "*Satanoperca* clade") is particularly weak, and posterior probabilities may represent inflated support (Suzuki et al. 2002; Douady et al. 2003; Simmons et al. 2004), basal relationships based on Bayesian analysis must be considered cautiously. Furthermore, the total-evidence parsimony analysis recovered relationships congruent with those from other analyses performed in this study, whereas the Bayesian topology did not. Nonetheless, both MP and Bayesian hypotheses showed weakly supported supra-generic arrangements at the base of the tree. The generality of this observation suggests that low support is not due to lack of data or potential problems associated with phylogenetic methods, but to the characteristics of the geophagine phylogeny itself. Several elements that characterize geophagine evolution appear to complicate the recovery of a well-supported phylogeny, and offer important insight into the evolutionary history of this group of Neotropical cichlids.

Limitations for the resolution of geophagine phylogeny

Incongruence. Removal of the cytochrome *b* partition determined a moderate but generalized increase in support for the parsimony topology, especially for nodes within Geophaginae (Figures 4.2A and 4.3, Table 4.1). The RTE dataset also produced very similar topologies under both parsimony and Bayesian analysis, which was not the case when cytochrome *b* was included in the dataset. It must be remembered that the cytochrome *b*, 16S, *Tmo-M27* and *Tmo-4C4* partitions are incomplete, and have important amounts of missing data. Although phylogenetic analyses have frequently shown great resistance to error due to missing data (Wiens and Reeder 1995), it is not possible to predict the effect of an incomplete matrix on a particular analysis. Under total-evidence, missing data may increase incongruence of a given partition if reduced

taxon sampling causes a biased representation of homoplasy and/or homology within the data.

Although parsimony seems to perform adequately even with large amounts of missing data (Wiens and Reeder 1995), the author is not aware of any study that has addressed the effect of missing data on maximum likelihood or Bayesian analyses. When cytochrome *b* is included, it appears that the parsimony analysis downplays the conflicting effect of this partition, favoring the interaction of the congruent signal from the other partitions. PBS values (Table 4.1) suggest that the topology is dominated by the congruent signal of most partitions, treating cytochrome *b* characters as non-informative homoplasy. This topological congruence is obtained at a cost, however, because support for nodes within Geophaginae is lower in the total evidence analysis than it is in the RTE. Ultimately, removal of cytochrome *b* does have a positive effect on the overall topology by increasing support for most of its nodes, even if the topology itself is not very different. In the Bayesian analysis, incongruence from cytochrome *b* is not being downplayed by the signal in other partitions, essentially because in the Bayesian analysis (as in Maximum Likelihood), topologies are not exclusively determined by synapomorphy, but by all characters (Felsenstein 1988, 2004; Lewis 2001). This interpretation seems appropriate, as the removal of cytochrome *b* causes an evident shift of Bayesian results towards the parsimony topology. Whether differences in support (under parsimony) or topology (under Bayesian analysis) are due to the cytochrome *b* partition having a different evolutionary history, to the effect of missing data, or to some other source of homoplasy cannot be determined until a complete data set is available for analysis. I prefer to provisionally accept the phylogeny obtained by removing cytochrome *b*, until a more complete dataset can be analyzed and the sources of incongruence can be studied.

Adaptive radiation. Support for the basal branches in the geophagine phylogeny, as measured by Bremer support, bootstrap and posterior probabilities, is lower than support for branches near the tips, and especially lower than support for clades outside the subfamily. The IBTs of the molecular data corroborate the weakness of the basal

geophagine relationships, and confirm the previous conclusion that basal branches are extremely short (Chapter III). Short branches at the base of a tree may be the consequence of lack of information for that particular level of the phylogeny, but are also the characteristic signature of a period of rapid differentiation associated with adaptive radiation (e.g. Hodges 1997; Jackman et al. 1997; Kontula et al. 2003). Even after removal of the cytochrome *b* partition, the analysis includes the majority of genera within Geophaginae, nearly 3,000 base pairs from five different loci, and a substantial morphological dataset. It is unlikely that low support for basal branches results from lack of data. Short, weak basal branches could result from reduced character fixation during a short, fast period of adaptive radiation that gave place to the geophagine genera. Furthermore, previous studies have repeatedly shown that geophagine cichlids evolve at significantly faster rates than other Neotropical cichlids, and that rate heterogeneity is pervasive at the molecular level (Farias et al. 1999, 2000; Chapter III). The group appears to have experienced extensive parallelisms at the morphological level (e.g. body size reduction, see above), adding to the extensive homoplasy within the clade. The combination of short branches, rate heterogeneity, and morphological homoplasy undoubtedly hinders the process of phylogenetic inference, and complicates the estimation of a well-supported phylogeny (e.g. Felsenstein 1978; Tateno et al. 1982; Hillis and Wiens 2000).

An evolutionary process with the characteristics of an adaptive radiation implies that complete phylogenetic resolution, if attainable, may not produce basal nodes with the strong statistical support found for more recent (e.g. species-level divergence) or slower diversification events (e.g. the cichlasomatine diversification, see Chapter III). It is evident that some relationships repeatedly found in the data, but with consistently low support are likely to represent real relationships for which not many characters are available (e.g. the "Big clade", "*Mikrogeophagus* clade"). Resolving uncertain relationships and establishing further support for weak relationships within the geophagine clade will require the addition of yet more data, and the improvement of taxon sampling (Graybeal 1998; Rannala et al. 1998; Zwickl and Hillis 2002). The

former should include slow-evolving, nuclear genes, which are more likely to contain informative characters for diversification events near the base of the tree (e.g. Springer et al. 2001). The latter should include better sampling of species-poor genera like *Guianacara*, *Biotoecus*, *Dicrossus* and *Crenicara*. Additionally, samples of the genus *Teleocichla* should help further resolve the relationship between *Crenicichla* and *Biotoecus*, and the position of these genera within Geophaginae. The current limitations of the geophagine phylogeny are essential for understanding the evolution of this clade of fluviatile cichlids. A phylogeny difficult to recover is part of a complex evolutionary puzzle in which ecological, behavioral and morphological diversity are also fundamental. Integrating phylogenetics with a clear understanding of the biology of these fishes should reveal the evolutionary processes behind this virtually unknown adaptive radiation.

CHAPTER V

CONCLUSION

Geophagine cichlids from South America constitute a species-rich clade of 18 genera with remarkable ecological, anatomical, and behavioral diversity. As such, this group of riverine Neotropical cichlids offers a unique opportunity for studying evolutionary processes and the origin of diversity in freshwater tropical fishes. The fundamental goal of this dissertation was to produce a sound phylogenetic hypothesis of geophagine relationships, and to this end, I used a total-evidence approach combining molecular and morphological data. Additionally, aspects of geophagine molecular evolution and generalities of the clade's evolutionary process were analyzed. The resulting total-evidence parsimony tree is the best estimate of geophagine relationships to date. Analysis of evolutionary patterns also supports monophyly of the subfamily Geophaginae and reveals a rapid diversification, providing further evidence for an adaptive radiation. The main findings of this study are summarized in the following paragraphs. Each section offers a brief discussion of remaining aspects on which research should focus in the future.

PHYLOGENETIC RELATIONSHIPS

DNA sequences of the mitochondrial ND4 and the nuclear RAG2 genes were analyzed separately, in combination, and as part of a super-matrix in which they were combined with published sequences of the mitochondrial 16S and cytochrome *b* genes, the microsatellite flanking region *Tmo-M27*, and the nuclear fragment *Tmo-4C4*. Molecular data were analyzed alone and in combination with a morphological matrix of 136 external and osteological characters. Molecular and morphological data were collected for 38 species of Neotropical cichlids from all major lineages, and included 16 of 18 genera and 30 species of Geophaginae, representing the largest and best

taxonomically sampled phylogenetic analysis of the group to date. All molecular, morphological, and total-evidence phylogenetic analyses performed in this study found the subfamily Geophaginae to be monophyletic. The generic composition and internal relationships within the subfamily differ from that proposed by Kullander (1998) based on morphological analysis. Resolution of relationships within the clade significantly expands the results of previous molecular and total-evidence studies by Farias et al. (2000, 1999, 2001) due to the expanded dataset and improved taxon sampling.

Parsimony analysis of the combined molecular and morphological data produced the most resolved and best supported topology (Figure 4.4), recovering relationships not found by analyses of the separate datasets. Although support for basal nodes is often low, this phylogeny is, for the time being, the best estimate of geophagine relationships. In this tree, a strongly supported, monophyletic Geophaginae includes two large clades, each in turn including two sister, multi-genus lineages. The first clade contains the tribe Acarichthyini (Kullander 1998), formed by the genera *Acarichthys* and *Guianacara*. The Acarichthyini is sister to the "Big clade," in which the "*Geophagus* clade" (genera *Gymnogeophagus*, *'Geophagus' steindachneri*, *Geophagus* sensu stricto) is sister to the "*Mikrogeophagus* clade" (*'Geophagus' brasiliensis*, *Mikrogeophagus*), and both are sister to a monophyletic group including the crenicarine clade (*Dicrossus*, *Crenicara*) and *Biotodoma*. The second large clade within Geophaginae includes the "*Satanoperca*" and "*Crenicichla*" clades; in the former, *Taeniacara* is sister to *Apistogramma* (including *Apistogrammoides*) and both are sister to *Satanoperca*; in the latter, *Crenicichla* and *Biotoecus* are sister to each other.

The phylogeny coincides with Kullander's (1998) and some of Farias et al.'s (1999, 2000) analyses in recovering a monophyletic tribe Acarichthyini, which was supported by both morphological and molecular synapomorphies. Other aspects of the tree differ from previous hypotheses. The best supported is the inclusion of *Crenicichla* within Geophaginae, a relationship previously found through molecular analysis, but never on the basis of morphological characters. In this analysis, both molecular and morphological datasets unambiguously place *Crenicichla* among the geophagines. By

implication, the genus *Teleocichla* is also included within Geophaginae, as its sister relationship to *Crenicichla* is well established on both molecular and morphological evidence. The relationship of *Biotoecus* and *Crenicichla*, supported by three unambiguous morphological synapomorphies, also was reported here for the first time. The remaining inter-generic relationships were not proposed before, and resulted from the increased taxon sampling in comparison to previous analyses. Despite low support (Figure 4.4.), the "Big clade" was consistently recovered by several analyses (see chapters III and IV), and its monophyly seems apparent, if not by support, at least by a criterion of repeatability (Chen et al. 2003). Within the "Big clade," the existence of three groups seems clear, but support for relationships among them is far from strong. The sister relationship of *Crenicara* and *Dicrossus* is well supported; the genus *Mazarunia* likely belongs in this clade, as its close relationship to both *Dicrossus* and *Crenicara* is well established (Kullander 1990). The sister relationship of the crenicarine clade to *Biotodoma* is weakly supported, and further analysis is be needed to confirm the position of that genus. The "*Geophagus*" and "*Mikrogeophagus*" clades also were repeatedly recovered. Despite low support, their consistent recovery suggests a monophyletic relationship, but this conclusion is more tentative. Relationships within the "*Satanoperca* clade" are among the best supported within Geophaginae, and the clade was recovered by all molecular and total evidence analyses. The sister-group relationship between the "*Crenicichla*" and "*Satanoperca*" clades is weakly supported, and the alternative arrangement as sister to the "Big clade" found by the Bayesian analysis (Figure 4.3) should not be discarded until an enlarged dataset is analyzed. In conclusion, relationships within Geophaginae are completely resolved by analysis of the present dataset, but basal relationships are less strongly supported. Complete resolution and high support for all basal nodes may not be attainable, due to the fast diversification process associated with an adaptive radiation at the base of the tree. Only a small amount of informative characters is available to resolve basal relationships, suggesting a low rate of character fixation during the diversification events at the base of the geophagine radiation. Further analysis, using both an enlarged dataset that includes

slow-evolving genes, informative at the base of the tree, and improved taxon sampling, is recommended.

TAXONOMIC IMPLICATIONS

Three new species of *Geophagus* sensu stricto were described from the Orinoco and Casiquiare drainages of Venezuela (Chapter II, López-Fernández and Taphorn 2004), raising the total number of species in the genus to 14. Although not explicitly stated in chapter II, the descriptions attempted to summarize current knowledge about the taxa. I believe that alpha-level taxonomic work is necessary for rapid and accurate identification of specimens, detecting lacunae of information about taxa, and the establishment of a starting point for studies of systematics, ecology, evolutionary biology, or biogeography (see also López-Fernández and Winemiller 2000, 2003). To this end, a series of steps were taken to describe the species. 1) As far as possible, descriptions included external morphological characters previously coded for use in phylogenetic analysis of geophagines (see Chapter IV and Appendix III). This approach allows ready expansion of the available phylogenetic matrix by standardizing characters used to describe new taxa. 2) Diagnoses of new species were complemented with illustrations of relevant diagnostic characters for all taxa in the genus, and keys were provided for all Venezuelan taxa. Ideally, this should be done for all taxa in the genus, but it was evident that such characters are not available from the scarce literature, and specimens of all species were not available for comparison. 3) Nomenclature for diagnostic characters was standardized with respect to previous studies or created when necessary. This is intended to create a standard for future taxonomic work, such that studies can be more easily integrated when expanding phylogenetic datasets and identification keys. 4) A summary of available information on geographic distribution was given in the form of maps complemented with lists of museum lots examined, to facilitate re-examination of collection material. 5) Finally, in a more informal way, all

available ecological and reproductive information was provided in the specific descriptions and in the discussion.

Above the species level, the phylogeny resulting from this study has some significant implications for the taxonomy of Geophaginae. At the broadest level, the inclusion of the genera *Crenicichla* and *Teleocichla* confirms Farias et al.'s findings (1999, 2000, 2001) and elevates the number of valid geophagine genera to 18 (but see below). The inclusion of *Crenicichla* within Geophaginae implies that Kullander's (1998) subfamily Cichlinae (*Cichla*, *Crenicichla*, and *Teleocichla*) is not a valid taxon, and the phylogenetic position of *Cichla* with respect to other Neotropical taxa remains unresolved (but see Farias et al. 2000, 2001; Stiassny 1987, 1991). Within Geophaginae, the tribe Acarichthyini (Kullander 1998) was relatively well supported, but the remainder of Kullander's geophagine classification is at odds with the phylogeny. The nesting of the crenicarine clade (*Crenicara* and *Dicrossus*) within the "Big clade" renders Kullander's tribes Crenicaratini and Geophagini paraphyletic. Paraphyly of these taxa was further indicated by the grouping of *Biotoecus* (formerly part of the Crenicaratini) with *Crenicichla*, and by the association of *Satanoperca* and *Apistogramma* outside of the "Big clade" (but see Figure 4.3 for an alternative arrangement). Finally, *Apistogrammoides pucallpaensis* was nested within *Apistogramma* in all phylogenetic analysis, indicating that the monotypic *Apistogrammoides* Meinken 1965 should be considered a junior synonym of *Apistogramma* Regan 1913. Other than including *Crenicichla* and *Teleocichla* in Geophaginae, recognizing the paraphyly of the Cichlinae, and synonymizing *Apistogrammoides*, it seems the most cautious course of action to wait until a more strongly supported phylogenetic hypothesis is available before proposing a new classification of Geophaginae.

CHARACTER CONGRUENCE AND MOLECULAR EVOLUTION

Character congruence among molecular and morphological partitions under total-evidence was examined in both parsimony and Bayesian topologies. The addition of morphology improved overall resolution and support for the phylogeny. When analyzed alone, the morphological dataset produced a topology significantly different from the molecular or total-evidence topologies. Disagreement was attributed to extensive morphological convergence among taxa that have undergone body-size reduction. When morphology was analyzed in the broader context of total-evidence, underlying homology emerged and the combined analysis produced the most resolved and supported topology.

The cytochrome *b* partition was found to be incongruent with all other partitions in the total-evidence analysis. Removal of this part of the molecular data did not change the parsimony topology, but increased support for several of its nodes. On the other hand, removal of cytochrome *b* data caused the Bayesian total-evidence tree to shift towards the parsimony topology. Convergence of the Bayesian tree towards the parsimony hypothesis suggests that cytochrome *b* contains significant homoplasy. Because Bayesian analysis uses all characters for topology reconstruction (Lewis 2001; Felsenstein 2004), homoplasy has a disproportionate effect on the result. Yet, parsimony accounts only for synapomorphic characters, thus downplaying the effect of homoplasy on the final topology. The cytochrome *b* partition has a large amount of missing data, thus it is not possible to know if incongruence is caused by the absence of characters or if it is due to some peculiarity associated with the evolution of this mitochondrial gene. Consideration of the above factors determined the provisional acceptance of the parsimony topology as the best estimate of geophagine phylogeny; additionally, Bayesian posterior probabilities are known to overestimate phylogenetic support, thus the parsimony topology provided a more conservative hypothesis of relationships.

Expanding on the results of Farias et al. (1999, 2000), Geophaginae were found to evolve significantly faster than other Neotropical cichlids. It also was found that rate heterogeneity within the group is extensive among and within genera, and among genes.

The fastest rates of evolution for the mitochondrial gene ND4 were found in *Crenicichla* and *Taeniacara*, but *Apistogramma* rates were fastest in the nuclear gene RAG2. ND4 was more extensively heterogeneous than RAG2, although some genera presented either significantly accelerated or decelerated rates of evolution in both genes. Statistical analysis of branch lengths under several models of molecular evolution showed that internal (basal) branches are, for the most part, not significantly different from zero. These results partially explain the weak support found for most basal branches, as they indicate that phylogenetic information associated with the base of the tree is scarce; they also are indicative of fast divergence of geophagine genera from their common ancestor.

ADAPTIVE RADIATION AND FUTURE RESEARCH

Short branches at the base of a phylogenetic tree may either result from lack of data or reflect rapid differentiation with reduced fixation of characters. The dataset from which the geophagine phylogeny was derived included 136 morphological characters and DNA sequences from five loci it is unlikely that a lack of data is the cause of short basal branches. Instead, the results suggest that Geophaginae radiated rapidly with limited character fixation during their initial burst of diversity, resulting in a phylogeny inherently difficult to recover due to scarcity of synapomorphies at the base of the tree. Origin of the geophagine genera is likely the result of adaptive radiation into unoccupied ecological space. Sudden ecological opportunity may appear through (1) development of novel phenotypic characters that open ecological niches previously unoccupied, (2) through the creation of new, ecologically unexploited habitat, or (3) a combination of these and other factors (see Schluter 2000). Geophagine cichlids fulfill the phylogenetic requirements of Schluter's (2000) definition of adaptive radiation, i.e. monophyly and rapid divergence. Future studies into geophagine evolution must address whether the diverse ecomorphological, life history, and behavioral traits of geophagine cichlids fulfill the requisites of correlation with the environment and of having adaptive value. A research program should focus on using the phylogeny as the appropriate evolutionary

context for discerning the historical circumstances and evolutionary trajectories of geophagine adaptive radiation.

The establishment of divergence dates for nodes in the phylogeny should provide a temporal anchor to place the geophagine radiation in the complex geological and hydrological history of South America (e.g. Lundberg et al. 1998). This task constitutes a significant challenge due to the pervasive heterogeneity of rates of molecular evolution, which complicates accurate estimation of divergence times based on molecular clocks (e.g. Kumar and Hedges 1998; Bromham et al. 2000). Additionally, the fossil record for cichlids in general and Neotropical clades in particular is scarce and poorly dated (Woodward 1898, 1939; Cockerell 1923; Schaeffer 1947; Bardack 1961; Casciotta and Arratia 1993), making it difficult to establish reliable calibration points for a molecular clock. Studies of evolutionary patterns in morphology and ecology probably hold the most promising prospects for future research. Ecological traits associated with feeding, habitat use, and life histories are remarkably diverse, and each of these elements of geophagine biology offers a distinct avenue for comparative research on geophagine evolution. Many geophagine cichlids feed by some form of substrate sifting to retain benthic invertebrates that constitute their diet. This pattern of feeding varies across genera, however, and some taxa are invertebrate pickers or piscivores. Although most geophagines inhabit clear or black waters with slow currents, habitats range from shallow, lentic waters with varying degrees of structural complexity to reophilic conditions. The generalized equilibrium life-history strategy of cichlids (Winemiller and Taphorn 1989; Winemiller and Rose 1993) underwent several modifications in geophagines, with reproductive modes approaching the versatility of those seen in cichlids from the African Great Lakes. Many communities harbor several genera and species of geophagine cichlids that reveal patterns of resource partitioning and niche differentiation. The origin of geophagine ecological diversity and the environmental conditions associated with its appearance are one of the most interesting aspects in the evolution of these cichlids. A great deal is known about functional morphology of cichlids and related fishes, particularly with regard to feeding (e.g. Barel 1983;

Wainwright 1988; Drucker and Jensen 1991) and locomotion. This knowledge provides a platform to develop better understanding of geophagine biomechanics and ecomorphological patterns of resource use in the wild (e.g. Winemiller 1989, 1991; Winemiller et al. 1995). Studies of biomechanics and functional morphology should be used to establish the adaptive value of morphological traits associated with feeding and habitat use (e.g. Wainwright 1987, 1994; Winemiller 1991; Westneat 1995, 1997). Phylogeny-based comparative methods should be used to remove similarity due to phylogenetic relatedness from studies of ecomorphological patterns. Covariation of ecological, behavioral, and morphological traits independently from phylogeny should indicate which character associations are adaptive and not simply ancestral traits (e.g. Felsenstein 1985; Coddington 1988; Harvey and Pagel 1991). Ecomorphological studies, of both geophagine taxa and fish communities, including geophagines, should clarify the ecological role of geophagine cichlids in the communities of which they are part. Furthermore, ecomorphological studies should elucidate mechanisms of resource partitioning and the basis of coexistence of syntopic geophagine genera and species in riverine environments of South America. Study of Geophaginae offers an exceptional opportunity to study adaptive radiation in riverine cichlids, and a unique view into the evolution of one of the most successful and diverse groups of vertebrates.

LITERATURE CITED

Arévalo, E., S. Davis, and J. Sites 1994. Mitochondrial DNA sequence divergence and phylogenetic relationships among eight chromosome races of *Sceloporus grammicus* complex (Phrynosomatidae) in Central Mexico. Syst. Biol. 43:387-418.

Arrington, D. A. 2002. Evaluation of the relationship between habitat structure, community structure, and community assembly in a Neotropical blackwater river. Ph.D. dissertation, Texas A&M University, College Station.

Arrington, D. A., and K. O. Winemiller. 2003. Diel changeover in sandbank fish assemblages in a neotropical floodplain river. J. Fish Biol. 63:442-459.

Axelrod, H. R. 1971. Expedition Río Aguaro, Venezuela 1971. Trop. Fish Hobby. XX:6-19,84-97.

Baker, R., and R. DeSalle. 1997. Multiple sources of character information and the phylogeny of Hawaiian drosophilids. Syst. Biol. 46:654-673.

Baker, R., G. Wilkinson, and R. DeSalle. 2001. Phylogenetic utility of different types of molecular data used to infer evolutionary relationships among stalked-eyed flies (Diopsidae). Syst. Biol. 50:87-105.

Baker, R., X. Yu, and R. DeSalle. 1998. Assessing the relative contribution of molecular and morphological characters in simultaneous analysis trees. Mol. Phylog. Evol. 9:427-436.

Bardack, D. 1961. New tertiary teleosts from Argentina. Am. Mus. Novi. 2041:1-27.

Barel, C. D. N. 1983. Towards a constructional morphology of cichlid fishes (Teleostei, Perciformes). Netherl. J. Zool. 33:357-424.

Barel, C. D. N., M. J. P. Van Oijen, F. Witte, and E. Witte-Maas. 1977a. An introduction to the taxonomy and morphology of the haplochromine Cichlidae from Lake Victoria. Netherl. J. Zool. 27:1-65.

---. 1977b. An introduction to the taxonomy and morphology of the Haplochromine Cichlidae from Lake Victoria. A manual to Greenwood's revision papers. Netherl. J. Zool. 27:333-389.

Barlow, G. W. 2000. The cichlid fishes: nature's grand experiment in evolution. Perseus publishing, Cambridge.

Bielawsky, J., A. Brault, and J. Gold. 2002. Phylogenetic relationships within the genus *Pimephales* as inferred from ND4 and ND4L nucleotide sequences. J. Fish Biol. 61:293-297.

Bremer, K. 1988. The limits of amino-acid sequence data in angiosperm phylogenetic reconstruction. Evolution 42:795-803.

---. 1994. Branch support and tree stability. Cladistics 10:295-304.

Bromham, L., D. Penny, A. Rambaut, and M. D. Hendy. 2000. The power of relative rates tests depends on the data. J. Mol. Evol. 50:296-301.

Brower, A. V. Z., R. DeSalle, and A. P. Vogler. 1996. Gene trees, species trees and systematics: a cladistic perspective. Ann. Rev. Ecol. Syst. 27:423-450.

Buckup, P. 1993. Phylogenetic interrelationships and reductive evolution in neotropical characidiin fishes (Characiformes, Ostariophysi). Cladistics 9:305-341.

Carruth, L. 2000. Freshwater cichlid *Crenicara punctulata* is a protogynous sequential hermaphrodite. Copeia 2000:71-82.

Casciotta, J. R., and G. Arratia. 1993a. Tertiary cichlid fishes from Argentina and reassessment of the phylogeny of New World cichlids (Perciformes: Labroidei). Kaupia 2:195-240.

---. 1993b. Jaws and teeth of American cichlids. J. Morph. 217:1-36.

Chase, M. W., and J. D. Palmer. 1997. Leapfrog radiation in floral and vegetative traits among twig epiphytes in the orchid subtribe Oncidiinae. Pp. 331-352 *in* T. J. Givnish and K. J. Sytsma, eds. Molecular evolution and adaptive radiation. Cambridge University Press, Cambridge.

Chen, W., C. Bonillo, and G. Lecointre. 2003. Repeatability of clades as a criterion of reliability: a case study for molecular phylogeny of Acanthomorpha (Teleostei) with larger number of taxa. Mol. Phylog. Evol. 26:262-288.

Chippindale, P., and J. A. Wiens. 1994. Weighting, partitioning, and combining characters in phylogenetic analysis. Syst. Biol. 43:278-287.

Cichocki, F. 1976. Cladistic history of cichlid fishes and reproductive strategies of the American genera *Acarichthys*, *Biotodoma* and *Geophagus*. Ph.D. dissertation, The University of Michigan, Ann Arbor.

---. 1977. Tidal cycling and parental behavior of the cichlid fish, *Biotodoma cupido*. Env. Biol. Fishes 1:159-169.

Cockerell, T. 1923. A fossil cichlid fish from the republic of Haiti. Proc. U. S. Nat. Mus 63:1-2.

Coddington, J. A. 1988. Cladistic tests of adaptational hypotheses. Cladistics 1988:3-22.

Cognato, A., and A. P. Vogler. 2001. Exploring data interaction and nucleotide alignment in a multiple gene analysis of *Ips* (Coleoptera: Scolytinae). Syst. Biol. 50:758-780.

Damgaard, J., and A. Cognato. 2003. Sources of character conflict in a clade of water striders (Heteroptera: Gerridae). Cladistics 19:512-526.

de Pinna, M. C. C. 1991. Concepts and tests of homology in the cladistic paradigm. Cladistics 7:367-394.

Dingerkus, G., and L. D. Uhler. 1977. Enzyme clearing of alcian blue stained whole small vertebrates for demonstration of cartilage. Stain Technol. 52:229-232.

Dopazo, J. 1994. Estimating errors and confidence intervals for branch lengths in phylogenetic trees by a bootstrap approach. J. Mol. Evol. 38:300-304.

Douady, C., F. Delsuc, Y. Boucher, W. Doolittle, and E. Douzery. 2003. Comparison of Bayesian and maximum likelihood bootstrap measures of phylogenetic reliability. Mol. Biol. Evol. 20:248-254.

Drucker, E. G., and J. S. Jensen. 1991. Functional analysis of a specialized prey processing behavior: winnowing by surfperches (Teleostei: Embiotocidae). J. Morph. 210:267-287.

Farias, I. P., G. Ortí, and A. Meyer. 2000. Total evidence: molecules, morphology, and the phylogenetics of cichlid fishes. J. exp. Zool. 288:76-92.

---. 2001. The Cytochrome *b* gene as a phylogenetic marker: the limits of resolution for analyzing relationships among cichlid fishes. J. Mol. Evol. 53:89-103.

Farias, I. P., G. Ortí, I. Sampaio, H. Schneider, and A. Meyer. 1999. Mitochondrial DNA phylogeny of the family Cichlidae: monophyly and fast molecular evolution of the Neotropical assemblage. J. Mol. Evol. 48:703-711.

Farias, I. P., H. Schneider, and I. Sampaio. 1998. Molecular phylogeny of Neotropical cichlids: the relationships of Cichlasomines and Heroines. Pp. 499-508 *in* L. R. Malabarba, R. E. Reis, R. P. Vari, Z. M. Lucena and C. A. S. Lucena, eds. Phylogeny and classification of Neotropical fishes. EDIPUCRS, Porto Alegre, Brazil.

Farris, J. S. 1969. A successive approximation approach to character weighting. Syst. Zool. 18:374-385.

Felsenstein, J. 1978. Cases in which parsimony or compatibility methods will be positively misleading. Syst. Zool. 27:401-410.

---. 1985a. Confidence limits on phylogenies: an approach using the bootstrap. Evolution 39:783-791.

---. 1985b. Phylogenies and the comparative method. Am. Nat. 125:1-15.

---. 1988. Phylogenies from molecular sequences: inference and reliability. Ann. Rev. Genet. 22:521-565.

---. 2004. Inferring phylogenies. Sinauer Associates, Inc., Sunderland, MA.

Fernández Yépez, A., and J. Anton. 1966. Estudio (análisis) ictiológico "Las Majaguas", Hoyas de los ríos Cojedes-Sarare, Edo. Portuguesa. Ministerio de Obras Públicas, Dirección de Obras Hidráulicas, Sistema de Riego "Las Majaguas", Caracas.

Gatesy, J., C. Matthee, R. DeSalle, and C. Hayashi. 2002. Resolution of a supertree/supermatrix paradox. Syst. Biol. 51:652-664.

Geyer, C., and E. Thompson. 1995. Annealing Markov Chain Montecarlo with applications to ancestral inference. J. Am. Stat. Assoc. 90:909-920.

Gosse, J. P. 1975. Révision du genre *Geophagus* (Pisces, Cichlidae). Mem. Acad. Royale des Sci. d'Outre-Mer. Classe des Sci. Nat. Med. XIX-3:1-172 + 18.

Goulding, M., M. Carvalho, and E. Ferreira. 1988. Rio Negro, rich life in poor waters. SPB Academic Publishing, The Hague, The Netherlands.

Graybeal, A. 1998. Is it better to add taxa or characters to a difficult phylogenetic problem? Syst. Biol. 47:9-17.

Greenwood, P. H. 1979. Towards a phyletic classification of the 'genus' *Haplochromis* (Pisces, Cichlidae) and related taxa. Part I. Bull.Br.Mus.Nat. Hist.(Zool) 35:265-322.

Harvey, P. H., and M. Pagel. 1991. The comparative method in evolutionary biology. Oxford University Press, Oxford.

Hasegawa, M., H. Kishino, and T. Yano. 1985. Dating the human-ape splitting by a molecular clock of mitochondrial DNA. J. Mol. Evol. 22:160-174.

Hillis, D. M., and J. J. Wiens. 2000. Molecules versus morphology in systematics: conflicts, artifacts, and misconceptions. Pp. 1-19 *in* J. J. Wiens, ed. Phylogenetic analysis of morphological data. Smithsonian Institution Press, Washington.

Hodges, S. 1997. Rapid radiation due to a key innovation in columbines (Ranunculaceae: *Aquilegia*). Pp. 391-406 *in* T. J. Givnish and K. J. Sytsma, eds.

Molecular evolution and adaptive radiation. Cambridge University Press, Cambridge.

Hodges, W., and K. Zamudio. 2004. Horned lizard (*Phrynosoma*) phylogeny inferred from mitochondrial genes and morphological characters: understanding conflicts using multiple approaches. Mol. Phylog. Evol. (In Press).

Holder, M., and P. Lewis. 2003. Phylogeny estimation: traditional and Bayesian approaches. Nature reviews genetics 4:275-284.

Huelsenbeck, J. P., and N. Imennov. 2002. Geographic origin of human mitochondrial DNA: accommodating phylogenetic uncertainty and model comparison. Syst. Biol. 51:155-165.

Huelsenbeck, J. P., and F. Ronquist. 2001. MRBAYES: Bayesian inference of phylogenetic trees. Bioinformatics 17:754-755.

Jackman, T., J. B. Losos, A. Larson, and K. de Queiroz. 1997. Phylogenetic studies of convergent adaptive radiations in Caribbean *Anolis* lizards. Pp. 535-558 *in* T. J. Givnish and K. J. Sytsma, eds. Molecular evolution and adaptive radiation. Cambridge University Press, Cambridge.

Kimura, M. 1980. A simple method for estimating evolutionary rate of base substitutions through comparative studies of nucleotide sequences. J. Mol. Evol. 16:111-120.

Kishino, H., and M. Hasegawa. 1989. Evaluation of the maximum likelihood estimate of the evolutionary tree topologies from DNA sequence data, and the branching order in Hominoidea. J. Mol. Evol. 29:170-179.

Kontula, T., S. Kirilchik, and R. Väinöla. 2003. Endemic diversification of the monophyletic cottoid fish species flock in Lake Baikal explored with mtDNA sequencing. Mol. Phylog. Evol. 27:143-155.

Kornfield, I., and P. Smith. 2000. African cichlid fishes: model systems for evolutionary biology. Ann. Rev. Ecol. Syst. 31:163-96.

Kullander, S. O. 1980. A taxonomical study of the genus *Apistogramma* Regan, with a revision of Brazilian and Peruvian species (Teleostei: Percoidei: Cichlidae). Bonner Zoologische Monographien 14:1-152.

---. 1983. A revision of the South American cichlid genus *Cichlasoma* (Teleostei: Cichlidae). Swedish Museum of Natural History, Stockholm.

---. 1986. Cichlid fishes of the Amazon River drainage of Peru. Swedish Museum of Natural History, Stockholm.

---. 1988. *Teleocichla*, a new genus of South American reophilic cichlid fishes with six new species (Teleostei: Cichlidae). Copeia 1988:196-230.

---. 1989. *Biotoecus* Eigenmann and Kennedy (Teleostei: Cichlidae): description of a new species from the Orinoco basin and revised generic diagnosis. J. Nat. Hist. 23:225-260.

---. 1990. *Mazarunia mazarunii* (Teleostei: Cichlidae),a new genus and species from Guyana, South America. Ichthyol. Explor. Freshwaters 1:3-14.

---. 1996. *Heroina isonycterina*, a new genus and species of cichlid fish from Western Amazonia, with comments on cichlasomine systematics. Ichthyol. Explor. Freshwaters 7:149-172.

---. 1998. A phylogeny and classification of the Neotropical Cichlidae (Teleostei: Perciformes). Pp. 461-498 *in* L. R. Malabarba, R. E. Reis, R. P. Vari, Z. M. Lucena and C. A. S. Lucena, eds. Phylogeny and classification of Neotropical fishes. EDIPUCRS, Porto Alegre, Brazil.

---. 2003. Family Cichlidae (Cichlids). Pp. 605-656 *in* R. RE, S. O. Kullander and C. J. Ferraris Jr, eds. Check list of the freshwater fishes of South and Central America. Museu de Ciências e Tecnologia - Pontifícia Universidade Católica do Rio Grande do Sul, Porto Alegre, Brazil.

Kullander, S. O., and E. J. G. Ferreira. 1988. A new *Satanoperca* species (Teleostei, Cichlidae) from the Amazon River basin in Brazil. Cybium 12:343-355.

Kullander, S. O., and H. Nijssen. 1989. The cichlids of Surinam. E.J. Brill, Leiden, The Netherlands.

Kullander, S. O., R. Royero, and D. Taphorn. 1992. Two new species of *Geophagus* (Teleostei: Cichlidae) from the Rio Orinoco Drainage in Venezuela. Ichthyol. Explor. Freshwaters 3:359-375.

Kullander, S. O., and A. M. C. Silfvergrip. 1991. Review of the South American cichlid genus *Mesonauta* Gunther (Teleostei, Cichlidae) with descriptions of two new species. Rev. Suisse Zool. 98:407-448.

Kullander, S. O., and W. Staeck. 1990. *Crenicara latruncularium* (Teleostei, Cichlidae), a new cichlid species from Brazil and Bolivia. Cybium 14:161-173.

Kumar, S., and S. B. Hedges. 1998. A molecular timescale for vertebrate evolution. Nature 392:917-920.

Kumazawa, Y., M. Yamaguchi, and M. Nishida. 1999. Mitochondrial molecular clocks and the origin of euteleostean biodiversity: familial radiation of perciforms may have predated the Cretaceous/Tertiary boundary. Pp. 35-52 *in* M. Kato, ed. The biology of biodiversity. Springer-Verlag, Tokyo.

Lamboj, A. 2004. *Pelvicachromis signatus* and *Pelvicachromis rubrolabiatus*, two new cichlid species (Teleostei, Perciformes) from Guinea, West Africa. Zootaxa 454:1-12.

Lamboj, A., and J. Snoeks. 2000. *Divandu albimarginatus*, a new genus and species of cichlid (Teleostei: Cichlidae) from Congo and Gabon, Central Africa. Ichthyol. Explor. Freshwaters 11:355-360.

Lamboj, A., and M. L. J. Stiassny. 2003. Three new *Parananochromis* species (Teleostei, Cichlidae) from Gabon and Cameroon, Central Africa. Zootaxa 209:1-19.

Laur, D., and A. Ebeling. 1983. Predator-prey relationships in surfperches. Env. Biol. Fishes 8:219-229.

Leaché, A., and T. Reeder. 2002. Molecular systematics of the Eastern Fence Lizard (*Sceloporus undulatus*): a comparison of Parsimony, Likelihood and Bayesian approaches. Syst. Biol. 51:44-68.

Lewis, P. 2001. A likelihood approach to estimating phylogeny from discrete morphological character data. Syst. Biol. 50:913-925.

Li, P., and J. Bousquet. 1992. Relative-rate test for nucleotide substitutions between two lineages. Mol. Biol. Evol. 9:1185-1189.

Linke, H., and W. Staeck. 1984. Amerikanische cichliden I. Kleine buntbarsche. Tetra Verlag, Berlin.

Lippitsch, E. 1990. Scale morphology and squamation patterns in cichlids (Teleostei, Perciformes): A comparative study. J. Fish Biol.:265-291.

---. 1993. A phyletic study on lacustrine haplochromine fishes (Perciformes, Cichlidae) of East Africa, based on scale and squamation characters. J. Fish Biol.:903-946.

---. 1995. Scale and squamation character polarity and phyletic assessment in the family cichlidae. J. Fish Biol. 47:91-106.

---. 1998. Phylogenetic studies of cichlid fishes in Lake Tanaganyica: a lepidological approach. J. Fish Biol. 53:752-766.

López-Fernández, H., and K. O. Winemiller. 2000. A review of Venezuelan species of *Hypophthalmus* (Siluriformes: Pimelodidae). Ichthyol. Explor. Freshwaters 11:35-46.

---. 2003. Morphological variation in *Acestrorhynchus microlepis* and *A. falcatus* (Characiformes: Acestrorhynchidae), reassessment of *A. apurensis* and distribution of *Acestrorhynchus* in Venezuela. Ichthyol. Explor. Freshwaters 14:193-208.

López-Fernández, H., and D. C. Taphorn. 2004. *Geophagus abalios*, *G. dicrozoster* and *G. winemilleri* (Perciformes: Cichlidae), three new species from Venezuela. Zootaxa 439:1-27.

Lovejoy, N. R., and B. B. Collette. 2001. Phylogenetic relationships of New World needlefishes (Teleostei: Belonidae) and the biogeography of transitions between marine and freshwater habitats. Copeia 2001:324-338.

Lowe-McConnell, R. H. 1969. The cichlid fishes of Guyana, South America, with notes on their ecology and breeding behaviour. Zool. J. Linn. Soc. 48:255-302.

---. 1991. Ecology of cichlids in South American and African waters, excluding the African Great Lakes. Pp. 62-85 *in* M. H. A. Keenleyside, ed. Cichlid fishes: behavior, ecology and evolution. Chapman Hall, London.

Lucena, C. A. S. d., and S. O. Kullander. 1992. The *Crenicichla* (Teleostei: Cichlidae) species of the Uruguai River drainage in Brazil. Ichthyol. Explor. Freshwaters 3:97-160.

Lundberg, J. G., L. G. Marshall, J. Guerrero, and M. C. Malabarba. 1998. The stage for Neotropical fish diversification: a history of tropical South American rivers. Pp. 13-48 *in* L. R. Malabarba , R. E. Reis, R. P. Vari , Z. M. Lucena and C. A. S. Lucena, eds. Phylogeny and classification of Neotropical fishes. EDIPUCRS, Porto Alegre, Brazil.

Machado-Allison, A. 1987. Los peces de los llanos de Venezuela. Un ensayo sobre su historia natural. Universidad Central de Venezuela, Caracas.

Machado-Allison, A., C. Lasso, and R. Royero. 1993. Inventario preliminar y aspectos ecológicos de los peces de los Ríos Aguaro y Guariquito (Parque Nacional), Estado Guárico, Venezuela. Mem. Soc. Cien. Nat. La Salle LIII:55-80.

Maddison, W., and D. R. Maddison. 2000. MacClade: Analysis of phylogeny and character evolution. Sinauer Associates, Sunderland, MA.

Mago-Leccia, F. 1970. Lista de los peces de Venezuela, incluyendo un estudio preliminar sobre la ictiogeografía del país. Ministerio de Agricultura y Cría, Oficina Nacional de Pesca, Caracas.

Martin, A. P., and E. Bermingham. 1998. Systematics and evolution of Lower Central American Cichlids inferred from analysis of cytochrome *b* gene sequences. Mol. Phylog. Evol. 9:192-203.

Meyer, A. 1993. Phylogenetic relationships and evolutionary processes in East African cichlid fishes. TREE 8:279-284.

Nei, M., and S. Kumar. 2000. Molecular evolution and phylogenetics. Oxford University Press, New York.

Nylander, J., F. Ronquist, J. P. Huelsenbeck, and J. Nieves-Aldrey. 2004. Bayesian phylogenetic analysis of combined data. Syst. Biol. 53:47-67.

Oliver, M. 1984. Systematics of African cichlid fishes: determination of the most primitive taxon, and studies on the haplochromines of lake Malawi. Ph.D. dissertation, Yale University, New Haven, CT.

Ortí, G., and A. Meyer. 1997. The radiation of characiform fishes and the limits of resolution of mitochondrial ribosomal DNA sequences. Syst. Biol. 46:75-100.

Pellegrin, J. 1904. Contribution à l'étude anatomique, biologique et taxonomique de poissons de la famille des Cichlidés. Mém. Soc. Zool. France 16:41-399.

Posada, D., and K. Crandall. 1998. Modeltest: testing the model of DNA substitution. Bioinformatics 14:817-818.

Rannala, B., J. P. Huelsenbeck, Z. Yang, and R. Nielsen. 1998. Taxon sampling and the accuracy of large phylogenies. Syst. Biol. 47:702-710.

Regan, C. T. 1905a. A revision of the fishes of the South-American cichlid genera *Acara*, *Nannacara*, *Acaropsis*, and *Astronotus*. Ann. Mag. Nat. Hist. 88:329-347.

---. 1905b. A revision of the South-American cichlid genera *Crenacara*, *Batrachops*, and *Crenicichla*. Proc. Zool. Soc. Lond. 1:152-168.

---. 1920. The classification of the fishes of the family Cichlidae. I. The Tanganyika genera. Ann. Mag. Nat. Hist. 9:33-53.

Reis, R., S. Kullander, and C. Ferraris Jr. 2003. Check list of the freshwater fishes of South and Central America. Pontifícia Universidade Católica do Rio Grande do Sul, Porto Alegre, Brazil.

Robinson, M., M. Gouy, C. Gautier, and D. Mouchiroud. 1998. Sensitivity of the relative rate test to taxonomic sampling. Mol. Biol. Evol. 15:1091-1098.

Rodríguez, M., and W. M. Lewis Jr. 1990. Diversity and species composition of fish communities of Orinoco floodplain lakes. Nat. Geo. Res. Expl. 6:319-328.

---. 1994. Regulation and stability in fish assemblages of Neotropical floodplain lakes. Oecologia 99:166-180.

Roe, K. J., D. Conkel, and C. Lydeard. 1997. Molecular systematics of Middle American Cichlid fishes and the evolution of trophic-types in '*Cichlasoma* (*Amphilophus*)' and '*C.*(*Thorichthys*)'. Mol. Phylog. Evol. 7:366-376.

Ronquist, F., and J. P. Huelsenbeck. 2003. MrBayes 3: Bayesian phylogenetic inference under mixed models. Bioinformatics 19:1572-1574.

Royero, R., A. Machado-Allison, B. Chernoff, and D. Machado-Aranda. 1992. Peces del Río Atabapo, Territorio Federal Amazonas, Venezuela. Acta Biol. Venez. 14:41-55.

Rüber, L., and D. Adams. 2001. Evolutionary convergence of body shape and trophic morphology in cichlids from Lake Tanganyika. J. Evol. Biol. 14:325-332.

Sanger, F., S. Nicklen, and A. Coulson. 1977. DNA sequencing with chain-termination inhibitors. Proc. Nat. Acad. Sci. USA 74:5463-5467.

Schaeffer, B. 1947. Cretaceous and tertiary actynopterygian fishes from Brazil. Bull. Am. Mus. Nat. Hist. 89:1-39.

Schindler, I. 1998. *Mesonauta guyanae*, spec. nov., a new cichlid fish from the Guyana Shield, South America (Teleostei: Cichlidae). Z. Fischk. 5:3-12.

Schluter, D. 2000. The ecology of adaptive radiation. Oxford University Press, New York.

Shimodaira, H., and M. Hasegawa. 1999. Multiple comparisons of Log-likelihoods with applications to phylogenetic inference. Mol. Biol. Evol. 16:1114-1116.

Simmons, M., K. Pickett, and M. Miya. 2004. How meaningful are Bayesian support values. Mol. Biol. Evol. 21:188-199.

Sitnikova, T. 1996. Bootstrap method of Interior-Branch test for phylogenetic trees. Mol. Biol. Evol. 13:605-611.

Sitnikova, T., A. Rzhetsky, and M. Nei. 1995. Interior-branch and bootstrap tests of phylogenetic trees. Mol. Biol. Evol. 12:319-333.

Sorhannus, U., and C. Van Bell. 1999. Testing for equality of molecular evolutionary rates: a comparison between a relative-rate test and a likelihood ratio test. Mol. Biol. Evol. 16:849-855.

Sota, T., and A. P. Vogler. 2001. Incongruence of mitochondrial and nuclear gene trees in the carabid beetles *Ohomopterus*. Syst. Biol. 50:39-59.

Springer, M., R. DeBry, C. Douady, H. Amrine, O. Madsen, W. de Jong, and M. Stanhope. 2001. Mitochondrial versus nuclear gene sequences in deep-level mammalian phylogeny reconstruction. Mol. Biol. Evol. 18:132-143.

Stiassny, M. L. J. 1981. The phyletic status of the family Cichlidae (Pisces: Perciformes): a comparative anatomical investigation. Netherl. J. Zool. 31:275-314.

---. 1987. Cichlid familial intrarelationships and the placement of the neotropical genus *Cichla* (Perciformes, Labroidei). J. Nat. Hist. 21:1311-1331.

---. 1991. Phylogenetic intrarelationships of the family Cichlidae: an overview. Pp. 1-35 *in* Keenleyside, ed. Cichlid Fishes: Behaviour, ecology and evolution. Chapman Hall, London.

---. 1992. Atavisms, phylogenetic character reversals, and the origin of evolutionary novelties. Netherl. J. Zool. 42:260-276.

Stiassny, M. L. J., and A. Meyer. 1999. Cichlids of the Rift Lakes. Sci. Am. 280:64-69.

Streelman, J., and S. Karl. 1997. Reconstructing labroid evolution with single-copy nuclear DNA. Proc. R. Soc. Lond. B 264:1011-1020.

Suzuki, Y., G. Glazko, and M. Nei. 2002. Overcredibility of molecular phylogenies obtained by Bayesian phylogenetics. Proc. Nat. Acad. Sci. USA 99:16138-16143.

Swofford, D. L. 2002. PAUP* Phylogenetic analysis using parsimony and other methods. Sinauer Associates, Inc., Sunderland, MA.

Swofford, D. L., G. Olsen, P. J. Waddell, and D. M. Hillis. 1996. Phylogenetic inference. Pp. 407-514 *in* D. M. Hillis, C. Moritz and B. K. Mable, eds. Molecular systematics. Sinauer Associates Inc., Sunderland, MA.

Tajima, F. 1993. Simple methods for testing the molecular evolutionary clock hypothesis. Genetics 135:599-607.

Takezaki, N., A. Rzhetsky, and M. Nei. 1995. Phylogenetic test of the molecular clock and linearized trees. Mol. Biol. Evol. 12:823-833.

Tamura, K., and M. Nei. 1993. Estimation of the number of nucleotide substitutions in the control region of mitochondrial DNA in humans and chimpanzees. Mol. Biol. Evol. 10:512-526.

Tang, K. 2001. Phylogenetic relationships among damselfishes (Teleostei: Pomacentridae) as determined by mitochondrial DNA data. Copeia 2001:591-601.

Taphorn, D. C., R. Royero, A. Machado-Allison, and F. Mago-Leccia. 1997. Lista actualizada de los peces de agua dulce de Venezuela. Pp. 55-100 *in* E. LaMarca, ed. Vertebrados actuales y fósiles de Venezuela. Museo de Ciencia y Tecnología de Mérida, Mérida, Venezuela.

Tateno, Y., M. Nei, and F. Tajima. 1982. Accuracy of estimated phylogenetic trees from molecular data. I. Distantly related species. J. Mol. Evol. 18:387-404.

Taylor, W., and G. Van Dyke. 1985. Revised procedures for staining and clearing small fishes and other vertebrates for bone and cartilage study. Cybium 9:107-119.

Thompson, J., D. Higgins, and T. Gibson. 1994. Clustal W: improving the sensitivity of progressive multiple sequence alignment through sequence weighting, position specific gap penalties and weight matrix choice. Nuc. Acid. Res. 22:4673-4680.

Verheyen, E., W. Salzburger, J. Snoeks, and A. Meyer. 2003. Origin of the superflock of cichlid fishes from Lake Victoria, East Africa. Science 300:325-329.

Wainwright, P. C. 1987. Biomechanical limits to ecological performance: mollusc-crushing by the Caribbean hogfish, *Lachnolaimus maximus* (Labridae). J. Zool.,Lond. 213:283-297.

---. 1988. Morphology and ecology: functional basis of feeding constraints in Caribbean labrid fishes. Ecology 69:635-645.

---. 1994. Functional morphology as a tool in ecological research. Pp. 42-59 *in* P. C. Wainwright and S. M. Reilly, eds. Ecological Morphology: Integrative Organismal Biology. University of Chicago Press, Chicago.

Webb, J. F. 1990. Ontogeny and phylogeny of the trunk lateral line system in cichlid fishes. J. Zool.,Lond. 221:405-418.

Weidner, T. 2000. South American Eartheaters. Cichlid Press, El Paso, TX.

Westneat, M. W. 1995. Feeding, function, and phylogeny: analysis of historical biomechanics in labrid fishes using comparative methods. Syst. Biol. 44:361-383.

Westneat, M. W., and J. A. Walker. 1997. Motor patterns of labriform locomotion: kinematic and electromyographic analysis of pectoral fin swimming in the labrid fish *Gomphosus varius*. J. exp. Biol. 200:1881-1893.

Wiens, J. J. 1998. Combining data sets with different phylogenetic histories. Syst. Biol. 47:568-581.

---. 2000. Coding morphological variation within species and higher taxa for phylogenetic analyses. Pp. 115-145 *in* J. J. Wiens, ed. Phylogenetic analysis of morphological data. Smithsonian Institution Press, Washington DC.

Wiens, J., and T. Reeder. 1995. Combining data sets with different numbers of taxa for phylogenetic analysis. Syst. Biol. 44:548-558.

Wiley, E., G. D. Johnson, and W. W. Dimmick. 1998. The phylogenetic relationships of lampridiform fishes (Teleostei: Acanthomorpha), based on total-evidence analysis of morphological and molecular data. Mol. Phylog. Evol. 10:417-425.

Wimberger, P. H., R. E. Reis, and K. R. Thornton. 1998. Mitochondrial phylogenetics, biogeography, and evolution of parental care and mating systems in *Gymnogeophagus* (Perciformes: Cichlidae). Pp. 509-518 *in* L. R. Malabarba , R. E. Reis, R. P. Vari , Z. M. Lucena and C. A. S. Lucena, eds. Phylogeny and classification of Neotropical fishes. EDIPUCRS, Porto Alegre, Brazil.

Winemiller, K. O. 1991. Ecomorphological diversification in lowland freshwater fish assemblages from five biotic regions. Ecol. Monogr. 61:343-365.

---. 1992. Ecomorphology of freshwater fishes. Nat. Geo. Res. Expl. 8:308-327.

Winemiller, K. O., L. C. Kelso-Winemiller, and A. L. Brenkert. 1995. Ecomorphological diversification and convergence in fluvial cichlid fishes. Env. Biol. Fishes 44:235-261.

Winemiller, K. O., and E. R. Pianka. 1990. Organization in natural assemblages of desert lizards and tropical fishes. Ecol. Monogr. 60:27-55.

Winemiller, K. O., and K. A. Rose. 1993. Why do most fish produce so many tiny offspring? Am. Nat. 142:585-603.

Winemiller, K. O., and D. C. Taphorn. 1989. La evolución de las estrategias de vida en los peces de los llanos occidentales de Venezuela. Biollania 6:77-122.

Woodward, A. 1898. Consideraçoes sobre alguns peixes terciarios dos schistos de Taubaté, estado de S. Paulo, Brazil. Revista do Museu Paulista 3:63-70.

---. 1939. Tertiary fishes from Maranhao, Brazil. Ann. Mag. Nat. Hist. 3:450-453.

Zardoya, R., D. Vollmer, C. Craddock, J. Streelman, S. Karl, and A. Meyer. 1996. Evolutionary conservation of microsatellite flanking regions and their use in the phylogeny of cichlid fishes (Pisces: Perciformes). Proc. R. Soc. Lond. B 263:1589-1598.

Zwickl, D., and D. M. Hillis. 2002. Increased taxon sampling greatly reduces phylogenetic error. Syst. Biol. 51:588-598.

APPENDIX I

CATALOGUE NUMBERS FOR DISTRIBUTION MAPS

Catalogue numbers from MCNG used to draw the distribution maps in Figures 2.9 and 2.13. Details on each locality are given with each species description and/or are available at the Neodat project website (http://www.neodat.org).

Geophagus abalios. MCNG 6111, 6660, 7023, 7681, 7827, 9390, 10118, 10195, 11413, 12359, 13220, 15892, 15979, 18643, 18652, 18684, 18734, 18767, 20060, 20238, 20300, 20631, 24241, 24303, 24757, 25952, 27197, 27962, 28076, 28081, 28139, 28158, 29781, 29866, 29880, 29939, 29959, 29987, 30680, 30714, 30728, 30745, 30769, 30801, 30855, 30882, 30921, 30939, 31010, 31018, 31027, 31061, 31073, 31096, 31182, 31221, 31231, 31255, 31288, 31326, 31342, 31349, 31364, 31366, 32668, 32682, 32836, 33153, 33157, 33173, 33197, 33211, 33269, 33851, 33976, 35209, 36769, 37650, 38232, 38317, 38707, 38735, 40385, 40591, 40878, 40976, 41368, 43979, 44865, 44866, 43825, 45028, 45029, 45034, 45040, 44690. *Geophagus dicrozoster*. 6219, 6278, 12135, 16388, 18156, 20143, 20191, 21422, 21598, 21599, 21783, 22013, 22300, 22356, 22460, 22874, 22904, 23012, 23750, 24387, 25902, 26343, 26454, 27130, 27792, 29582, 29714, 30010, 30020, 30040, 30045, 30054, 30062, 30462, 36629, 36682, 36770, 36790, 36808, 37858, 37975, 8225, 38423, 38503, 38785, 39240, 39271, 39334, 39355, 39364, 39406, 39531, 39545, 39550, 39572, 39591, 39613, 39633, 39671, 39692, 39735, 39777, 39822, 39853, 39872, 39910, 39924, 39952, 40007, 40022, 40068, 40219, 40343, 40383, 40414, 40453, 40482, 40776, 40815, 40839, 41019, 41111, 41124, 41127, 41145, 41151, 41158, 41170, 41176, 41208, 41226, 41284, 41318, 41352, 41363, 41384, 41389, 41422, 41428, 41442, 41445, 41487, 41502, 41533, 41565, 41668, 42424, 44862, 44863, 44864, 44589, 44600, 44607, 44612, 45030, 45033, 45035, 45037, 45039, 44699, 44762, 44773. *Geophagus winemilleri*. 12227, 12301, 35486, 37858, 42016, 42386. *Geophagus brachybranchus*. 1023, 13542, 16506, 29535, 45103. *Geophagus grammepareius*. 17247, 18096, 18183, 18243, 18263, 18296, 18310, 18318, 18349, 18407, 18408, 18553, 18571, 18598, 18755, 18792, 18921, 18922, 18943, 18945, 19330, 19476, 25480, 34396, 34413, 47545. *Geophagus taeniopareius*. 7631, 12461, 12541, 16389, 17719, 21512, 21603, 22168, 22367, 22428, 22459, 22506, 22509, 22578, 22723, 22875, 23013, 23199, 24304, 24397, 25700, 27168, 28862, 34814, 38523, 46033, 46395, 46420, 46467, 46521, 46543.

APPENDIX II

DESCRIPTION OF MORPHOLOGICAL CHARACTERS

References to the original papers where the characters were proposed are given when appropriate. To the best of our knowledge, characters without bibliographic reference are proposed here for the first time in a phylogenetic context. Numbers in brackets correspond to character states used in this paper. Refer to Appendix III for the coded matrix of characters states in the 38 taxa included in this study.

SQUAMATION PATTERNS

1 Operculum squamation (Lippitsch 1993: Ch. 1). Fully scaled [0], Kullander (1986: 190, Fig. 65); partially scaled [1]. State 1 does not include the naked "opercular spot" (Lippitsch 1993), which is characteristic of most African cichlids (Stiassny 1991), and was not observed in the taxa studied.

2 Opercular scales (Lippitsch 1993: Ch. 2, modified). Cycloid [0]; ctenoid [1]. Degrees of ctenoidi were considered as different character states by Lippitsch (1993); because we were unable to establish clear limits between degrees of ctenoidi, we have preferred to code the character as binary.

3 Subopercule squamation (Lippitsch 1993: Ch. 4). Fully scaled [0], Lippitsch (1993: 912, Fig. 2a); caudo-ventral rim naked [1], Lippitsch (1993: 912, Fig. 2a). State 1 restricted to cases in which the space left between the outermost row of scales and the edge of the subopercle is wide enough to contain another row of scales.

4 Subopercule scales (Lippitsch 1993: Ch. 5, modified as Ch. 2). Cycloid [0]; ctenoid [1].

5 Interopercule squamation (Lippitsch 1993: Ch. 6). Caudo-dorsally scaled [0]; caudally scaled [1], Lippitsch (1993: 913, Fig. 3b); fully scaled [2], Lippitsch (1993: 913, Fig. 3a); scaleless [3].

6 Interopercule scales (Lippitsch 1993: Ch. 7, modified as Ch. 2). Cycloid [0]; ctenoid [1].

7 Cheek squamation (Lippitsch 1993: Ch. 10). Fully scaled [0], Kullander (1986: 196, Fig. 68); rostral half naked [1]; rostro-ventrally naked [2], Kullander (1986: 130, Fig. 35); rostrally naked [3]; ventrally naked [4]; scaleless [5]. A rostral half naked (state 1) implies a straight, almost vertical line separating the caudal, scaled region from the rostral naked area. A rostrally naked cheek (state 3) lacks scales in the rostral-most portion of the cheek, but the naked area never reaches as much as half of the cheek, and the line separating the scaled from the naked portion is of irregular shape. A fully scaled

cheek was considered the plesiomorphic state based on *Astronotus* and two of the three species of *Cichla*.

8 Cheek scales (Lippitsch 1993: Ch. 11. modified as Ch. 2). Cycloid [0]; Ctenoid [1].

9 Postorbital squamation (Lippitsch 1993: Ch. 12). Single column [0], Lippitsch (1993: 915, Fig. 5a); more than 2 columns [1]; 2 columns [2] Lippitsch (1993: 915, Fig. 5b). Character restricted to scales immediately behind the orbit. The outgroup is highly variable, the plesiomorphic state was defined based on Lippitsch (1995).

10 Postorbital scales. Cycloid [0]; Ctenoid [1].

11 Size of occipital scales compared to dorsal scales (Lippitsch 1993: Ch. 17, modified). Smaller [0]; equal [1]. Dorsal scales refer to scales above the upper lateral line (ULL). Lippitsch's character was multistate, but we could not distinguish between her "not significant, significant, and extremely small scales".

12 Dorsal scales (Lippitsch 1993: Ch. 20, modified as Ch. 2). Cycloid [0]; ctenoid [1]. Polarity based on *Astronotus* and on basal cichlids and most labroids (Lippitsch, 1995).

13 Flank scales (Lippitsch 1993: Ch. 25). Circular [0]; ovoid, long axis vertical [1]; ovoid, long axis horizontal [2]. Evaluated on scales below the ULL and behind the caudal edge of the pectoral fin.

14 Lower median of caudal peduncle squamation (Lippitsch 1993: Ch. 41). 3 rows [0]; 2 rows [1]; 4 rows [2]; 5 rows [3]; 6 rows [4]; 7 rows [5]; 8 rows [6]; 11 rows [7]. Involves the number of scale rows between the lower lateral line (LLL, not included) and the row of scales posterior to the base of the anal fin (not included). Because the character was polymorphic among outgroup taxa, polarity was based on the Malagasy cichlid *Ptychochromis*. Cichlids from Madagascar are well established as the most basal members of the family (Stiassny 1991; Kullander 1998; Farias et al. 1999, 2000), and have been used before to determine plesiomorphic states (e.g. Lippitsch 1995).

15 Scales on lateral chest (Lippitsch 1993: Ch. 43, modified as Ch. 2). Ctenoid [0]; cycloid [1]. The lateral chest area is located caudal to the gill cover, ventral to the insertion of the pectoral fin, and rostral to the imaginary line between the pectoral and pelvic fin insertions.

16 Size of lateral chest scales compared to flank scales (Lippitsch 1993: Ch. 44, part, modified as Ch. 11). Smaller [0], Greenwood (1979: 271, Fig. 1); equal [1], Greenwood (1979: 272, Fig. 2).

17 Juxtaposition pattern of lateral chest scales (Lippitsch 1993: Ch. 44, part). Imbricating [0]; not imbricating [1].

18 Transition from chest to flank scales (Lippitsch 1993: Ch. 45). Gradual [0]; abrupt [1], Greenwood (1979: 272, Fig. 2). A gradual transition implies that scales in the chest and flank are the same size, or that change in size occurs across several rows of scales. An abrupt change implies two rows of differently sized scales lying next to each other, see also Lippitsch (1990: 280).

19 Ventral chest squamation (Lippitsch 1993: Ch. 46). Fully scaled [0]; scaleless [1]. Involves the area between the insertion of the pelvic fins and the ventral margin of the branchiostegal membrane.

20 Chest scales (Lippitsch 1993: Ch. 47, modified as Ch. 2). Cycloid [0]; Ctenoid [1].
21 Size of ventral chest scales compared to lateral chest scales (48). Smaller [0]; equal [1]. In state 0, ventral scales are less than half the size of the lateral chest scales.

22 Juxtaposition pattern of ventral chest scales (Lippitsch 1993: Ch. 48). Imbricating [0]; not imbricating [1].

23 Transition from ventral to lateral chest scales (Lippitsch 1993: Ch. 49). Gradual [0]; abrupt [1]. Evaluated as character 18.

24 Squamation between pelvic fins (Lippitsch 1993: Ch. 51). Irregular [0]; biserial [1]; uniserial [2]. Interpreted from Lippitsch (1993: 915) as the number of scale rows between the insertion of the pelvic fins. Irregular arrangement involves a variable number of scales not arranged in a clear pattern, usually with several scales between the pelvics. Uniserial and biserial involve one or two rows of scales between the pelvic fins, respectively.

25 Large interpelvic scale (Lippitsch 1993: Ch. 52). Absent [0]; present [1].

26 Scales on belly (Lippitsch 1993: Ch. 54, modified as Ch. 2). Ctenoid [0]; cycloid [1]. Involves the area caudal to the base of the pelvic fins and rostral to the anus.

27 Size of belly scales compared to flank scales (Lippitsch 1993: Ch. 55). Smaller [0]; equal [1]. Evaluated as character 16.

28 Transition from belly to flank scales (Lippitsch 1993: Ch. 56). Gradual [0]; abrupt [1]. Evaluated as character 18.

29 Scales on anal-genital region (Lippitsch 1993: Ch. 58, modified as Ch. 2). Ctenoid [0]; cycloid [1]. See comments on character 2. Restricted to scales immediately surrounding the anus and the urogenital papilla.

30 Caudal fin squamation (Lippitsch 1993: Ch. 65). Fully scaled [0]; partially scaled [1].

31 Scales on caudal fin (Lippitsch 1993: Ch. 66, modified as Ch. 2). Cycloid [0]; Ctenoid [1].

32 Pattern of caudal fin squamation (Lippitsch 1993: Ch. 67, modified). Rays densely covered [0]; single rows on inter-radial membranes [1]; staggered rows on inter-radial membranes [2].

33 Squamation of pectoral fin (Lippitsch 1993: Ch. 73). Scaleless [0]; partially scaled [1]. Polarity based on *Astronotus, Cichla intermedia,* and Lippitsch (1993).

34 Squamation of dorsal fin (Lippitsch 1993: Ch. 60, part, modified as Ch. 11). Scaled [0]; scaleless [1].

35 Scaled portion of dorsal fin (Lippitsch 1993: Ch. 60, part). Soft portion only [0]; both soft and spinous portions [1]. Characters 35 to 37 are inapplicable for taxa with naked dorsal fin.

36 Scales on dorsal fin (Lippitsch 1993: Ch. 61, modified as Ch. 2). Ctenoid [0], cycloid [1].

37 Squamation pattern of dorsal fin (Lippitsch 1993: Ch. 62). Double or multiple rows on inter-radial membranes [0]; single rows on inter-radial membranes [1].

38 Squamation pattern on base of dorsal fin (Lippitsch 1993: Ch. 63). With scaly pad [0]; without pad or sheath [1], (Kullander *et al.* 1992: 363, Fig. 2); with vestigial sheath [2]; with well developed sheath [3], (Kullander *et al.* 1992: 363, Fig. 2). In our interpretation of Lippitsch (1993) character, a scaly pad refers to a distinct area at the base of the dorsal fin, with scales smaller than those on the flanks. Contrary to a sheath, the pad does not cover any portion of the fin.

39 Scales on pad or sheath of dorsal fin (Lippitsch 1993: Ch. 64, modified as Ch. 2). Ctenoid [0]; cycloid [1].

40 Squamation of anal fin (Lippitsch 1993: Ch. 68, part). Scaled [0]; scaleless [1].

41 Scaled portion of anal fin (Lippitsch 1993: Ch. 68, part). Soft portion only [1]; both soft and spiny portions [1]. Characters 41 to 43 inapplicable for taxa with naked anal fin. Polarity based on *Astronotus*.

42 Scales on anal fin (Lippitsch 1993: Ch. 69, modified as Ch. 2). Ctenoid [0]; cycloid [1].

43 Squamation pattern of anal fin (Lippitsch 1993: Ch. 70). Multiple rows on inter-radial membranes [0]; single rows on inter-radial membranes [1].

44 Squamation pattern on base of anal fin (Lippitsch 1993: Ch. 71). With scaly pad [0]; without pad or sheath [1]; with vestigial sheath [2]; with well developed sheath [3].

45 Scales on pad or sheath of anal fin (Lippitsch 1993: Ch. 72, modified as Ch. 2). Cycloid [0]; Ctenoid [1].

DERMAL BONES

46 Preopercular edge. Smooth [0]; serrated [1]. Serration of dermal bones has been used as a taxonomic character (e.g. Kullander 1980, 1990; Kullander & Staeck 1990), but not used in phylogenetic analysis (but see Kullander 1990).

47 Supracleithral edge. Smooth [0]; serrated [1].

48 Post-temporal edge. Smooth [0]; serrated [1].

LIPS

49 Lower lip fold at the symphyseal zone. Discontinuous [0]; continuous [1].

50 Type of lip fold (Stiassny 1987). [0] Type I, African; [1] type II, American. See also Kullander (1983, 1986).

LATERAL LINE SYSTEM AND ASSOCIATED SQUAMATION

51, 52, 53, 54 Opening of the frontal pores. Multiple [0]; single [1]. The opening of the frontal pores NLF0 (50), NLF1 (51), NLF2 (52) and NLF3 (53) (see Barel *et al.* 1977: 91, Fig. 8) at the skin surface can have single or multiple openings. Generally, the four openings share the same state, except in *Biotodoma*, *Gymnogeophagus* and *Cichlasoma*, which suggest there is independence between pores.

55 Number of preopercular lateralis canal foramina (Stiassny 1987; 1991: Ch. 17). [0] 7; [1] 6; [2] 5. See also Kullander (1998: Ch. 47).

56 Number of lateralis canals on the dentary (Casciotta and Arratia 1993a: Ch. 15). [0] 5; [1] 4. See also Kullander (1983: Ch, 3; 1998, Ch. 45, 46).

57 Trunk canal pattern of the lateral line. D4 [0]; D1 [1]; D2 [2]; D3 [3]; D8 [4]; D8.5 [5]; D9 [6]; continuous lateral line [7]. Characters 54 to 59 refer to the original analysis of lateral line configuration and ontogeny of Webb (1990: 412-413, Fig. 4 and Table 1)

and are explained in detail in that paper. Condition D8.5 (State 5) is described from *Apistogrammoides pucallpaensis*; it consists of a lower lateral line with pored scales as in Webb's condition D9, and an upper lateral line with only a few tubed scales rostrally as in Webb's condition D8. The continuous lateral line condition (State 7) has been amply discussed regarding the phylogenetic position of *Cichla* (Stiassny 1981, 1987, 1991); we have considered it autapomorphic, regardless of whether it has truly arisen *de novo,* or is an atavistic expression of a basal percomorph condition (Stiassny 1992).

58 Number of overlapping tubed scales. 4 or less [0]; 7 or more [1]. Overlapping refers to scales in the ULL and LLL that are located in the same column. Scales are normally not arranged in straight columns, but forming a zigzag pattern. Scales were considered to be in the same column when located in the same dorso-ventral zigzagging line.

59 Number of ULL pitted scales caudally from last tubed ULL scale. 7 or less [0]; 15 or more [1]. Scale types were evaluated following descriptions in Webb (1990: 409).

60 Number of scale rows between ULL and LLL. 2 or 3 [0]; 4 or 5 [1]. Although there is no apparent discontinuity between the two states, we did not find any taxon with an intermediate condition. Specimens of some species may have 2 or 3 (*Retroculus*), or 4 or 5 rows of scales (*Cichla intermedia*), but we did not find any taxon with 3 or 4 rows.

61 Number of scale rows between ULL and dorsal origin. 6-7 rows [0]; 1 row [1]; 2 rows [2]; 3 rows [3]; 4 rows [4]; 5 rows [5]; 8-11 rows [6]; 12 rows [7]; 14 rows [8]; 18 rows [9]. See comments on character 57. States including a range of counts represent taxa with individuals presenting any of the numbers included in the range; states with a single number of scales rows represent taxa in which we did not observe individual variation.

62 Number of scale rows between last ULL tubed scale and base of the dorsal fin. 2-5 rows [0], 0.5 rows [1], 1 row [2], 11 or more [3]. See comments on character 58. A 0.5 row is determined by the presence of a single scale approximately half the size of a normal flank scale.

63 Dorsal caudal ramus (Kullander 1998: Ch. 78). Absent [0]; present between caudal rays D3 and D4 [1]; present between caudal rays D2 and D3 [2].

64 Ventral caudal ramus. Present between caudal rays V4 and V5 [0]; present between caudal rays V3 and V4 [1]; absent [2].

COLOR PATTERN

65 Caudal spot (Kullander 1998: Ch. 88, part). Present [0]; absent [1]. Involves a dark mark, ocellated or not, on the base of the caudal peduncle. Characters 63 and 64 inapplicable if caudal spot is absent.

66 Caudal spot position. Dorsal [0]; medial [1].

67 Caudal spot type. Ocellus [0]; blotch [1]; *Dicrossus* band [2]. The "*Dicrossus* band" refers to a single, faint, vertical band only present in *Dicrossus* and *Biotoecus*.

68 Dorsal spot. Absent [0]; present [1]. The so-called "*Tilapia* spot" (Trewavas 1983 in Kullander 1998); among Neotropical taxa, an equivalent dark blotch at the base of the soft portion of the dorsal fin is found only in *Retroculus*. Kullander indicates its presence in *Heros* (Kullander 1998) and we have observed a comparable character in some specimens of *Hoplarchus* and *Mikrogeophagus altispinosus*. It is difficult to ascertain whether the spot observed in these derived Neotropical taxa is homologous with the dorsal spot found in many African and Madagascan taxa.

69 Suborbital stripe. Absent [0]; complete, extending from the lower edge of the orbit to the interopercule [1]; from the lower edge of the orbit to the preopercule (inclusive) [2]; limited to the cheek [3]; limited to the preopercule [4]; complete except for the preopercule [5].

70 Supraorbital stripe. Absent [0]; directed caudad [1]; directed rostrad [2].

71 Postorbital stripe. Absent [0]; present [1]; present, *Dicrossus* type [2]. The "*Dicrossus* type" consists of an isosceles triangular shaped blotch with its base on the caudal edge of the orbit and its tip pointing caudad.

72 Preorbital stripe (Kullander 1998: Ch. 89, modified). Absent [0]; present, *Apistogramma* type [1]; present, *Dicrossus* type [2]. The *Apistogramma* stripe is thin, dark with smooth or irregular edges, directed rostrally but slightly inclined ventrally; the *Dicrossus* stripe is broad, sharp-edged and directed rostrally.

73 Lateral band. Present [0]; absent [1]. A lateral band is a more or less distinguishable, frequently spotted, dark band running from behind the opercle to the base of the caudal fin; it is sometimes continued on the head by the postorbital and preorbital stripes. Character evaluation in some taxa can be confounded by ontogenetic stage, for example, in *Cichla*, the band is present in juveniles, but disappears (*C. orinocensis, C. temensis*) or is modified (*C. intermedia*) in the adults. We have coded *Cichla* based on adult specimens.

74 Body bars. Faint [0]; forming a spotted, interrupted midline [1]; camouflage-like [2]; barred [3]; forming a checkerboard pattern [4]. Most cichlids present a faint pattern of vertical bars on the flanks, and generally, the spots forming the lateral band coincide with the body bars.

75 First dorsal ray membranes. Immaculate [0]; black or dark colored [1].

NEUROCRANIUM

76 Presence of divergent frontal ridges anterior to NLF0 (Cichocki 1976: Ch. 3, modified). Present [0]; absent [1]. See also Stiassny (1991:12-13) (Figure II.1).

77 Presence of medial frontal crest. Present [0]; absent [1]. (Figure II.1).

78 Composition of the pharyngeal apophysis of the basicranium (Regan 1920). Consisting of parasphenoid only [0]; consisting of both the parasphenoid and the basioccipital [1]. See also Cichocki (1976: Ch. 6) and Kullander (1998: Ch. 28) for a discussion of the pharyngeal apophysis in Neotropical cichlids.

79 Expansion of the dorsal parasphenoid wing (Kullander and Nijssen 1989). Absent [0]; present [1]. Kullander & Nijssen (1989, Fig. 47) indicated that an expansion in both the parasphenoid wing and the basisphenoid were synapomorphic for *Acarichthys* and *Guianacara* (see also Kullander 1998: Ch. 36). We found an expanded parasphenoid wing is common among geophagines, and not necessarily associated with a basisphenoid expansion (see character 5) (Figure II.1).

80 Basisphenoid expansion. Present [0]; absent [1]. Kullander and Nijssen (1989) (Figure II.1).

81 Caudal expansion of the mesethmoid. Absent [0]; present [1]. In lateral view, the mesethmoid covers less than 1/5 of the orbit diameter (e.g. *Cichla*, *Retroculus*); in the derived condition, it can cover up to ¼ of the total orbital diameter (Figure II.1).

82 Sphenotic foramen and canal, borne on the anterodorsal region of the expanded postorbital process of the neurocranium (Stiassny 1987, Fig. 6). Absent [0]; present [1].

83 Opening of NLF4. Single pore [0]; 2 opposed pores at the end of the tubes formed by a broken canal [1]. (Figure II.1).

84 Opening of NLF5. Single pore [0]; double pore [1]; NLF5 absent [2]. (Figure II.1).

85 Line of the sphenotic-pterotic canal. [0] moderately angled (140-160 degrees); [1] sharply angled (120 degrees or less); [2] approximately straight (180 degrees) (Figure II.1).

86 Suture between the vomerine wing and the parasphenoid bar (Stiassny 1991: Ch. 8, Fig. 1.12). [0] interdigitating; [1] straight.

87 Mesethmoid-Vomer interaction (Casciotta and Arratia 1993: Ch. 2). [0] sutured; [1] not sutured.

88 Shape of the rostral margin of the vomerine head (Stiassny 1987: Ch. 5, Fig. 5, modified). [0] Ridged; [1] indented; [2] flat. (Figure II.1).

SUSPENSORIUM

89 Foramen on the lateral face of the ascending process of the premaxilla (Cichocki 1976: Ch. 15). [0] absent; [1] present.

90 Development of the dermal splint of the palatine shaft (Kullander 1998: Ch. 50). [0] Long, largely contiguous with the rostral edge of the ectopterygoid; [1] Short, reaching the ectopterygoid, but not contiguous with it; [2] Absent, the caudal end of the palatine is lined across the ectopterygoid. (Figure II.2).

91 Shape of the maxillary process of the palatine (Kullander 1998: Ch. 51). [0] flattened dorsoventrally; [1] cylindrical.

92 Morphology of the posteroventral palatine laminar expansion (Cichocki 1976: Ch. 20, modified). [0] narrow, thick, and largely contiguous with the anterodorsal margin of the endopterygoid; [1] approximately triangular, with a gap between the lamina and the anterodorsal edge of the endopterygoid; [2] well developed, largely contiguous with the anterodorsal margin of the endopterygoid; [3] thin and narrow, contiguity with the endopterygoid restricted to its extreme ventral margin or not contacting it at all; [4] lamina absent, the palatine and the endopterygoid are not contiguous. (Figure II.2).

93 Axial lateral palatine ridge (Cichocki 1976: Ch. 21, modified). [0] present; [1] absent.

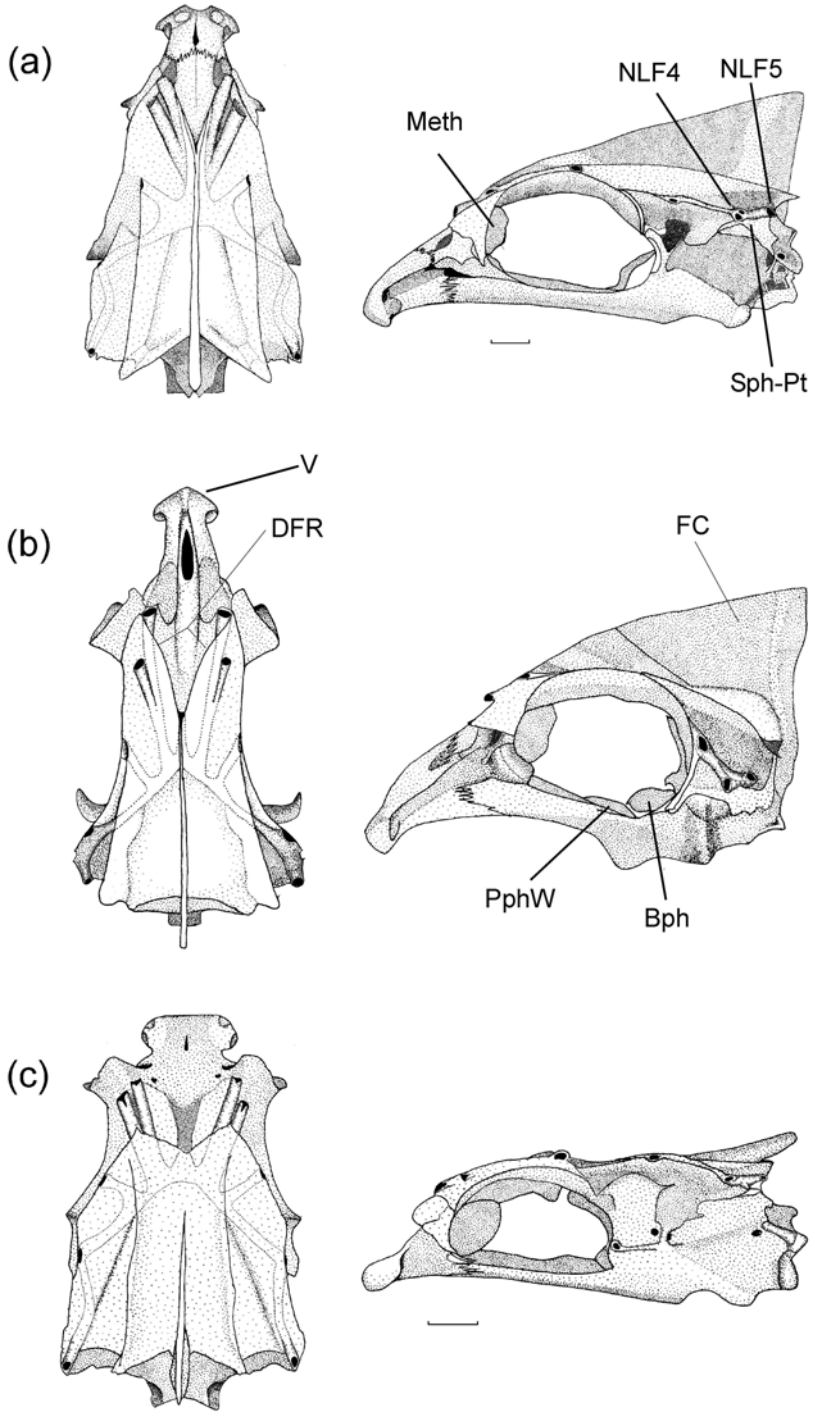

FIG. II.1. Semi-diagrammatic illustration of dorsal (left) and lateral (right) view of the neurocrania of a) *Cichla intermedia* (AMNH, Uncatalogued); b) *Geophagus dicrozoster* (MCNG 40623); c) *Crenicichla* af. *lugubris* (AMNH, Uncatalogued). Scale bar = 5 mm. Abbreviations: Bph = basisphenoid; DFR = divergent frontal ridges; FC = frontal crest; Meth = mesethmoid; NLF4-5 = neurocranial lateral line foramina; PphW = parasphenoid wing; Sph-Pt = sphenotic-pterotic canal; V = vomerine head.

94 Structure of the axial lateral palatine ridge. [0] single, reduced ridge separating the maxillary process of the palatine from the posteroventral expansion; [1] single, well developed ridge in the same position as in state 0; [2] bifurcated, well developed ridge with an axial arm as in states 0 and 1, and an additional maxillary or anteriorly directed ridge following the caudo-rostral direction of the maxillary process; [3] lack of medial ridge, but presence of a reduced ridge following the contour of the maxillary process. (Figure A.2).

95 Suture between hyomandibular and metapterygoid (Oliver 1984: Ch. 24). [0] present; [1] absent. See also Stiassny (1987, Fig. 7).

96 Pointy extension in the anterodorsal corner of the interoperculum, in medial view. [0] absent; [1] present.

PHARYNGEAL OSTEOLOGY

97 Relative direction of the uncinate process of the first epibranchial in relation to the anterior arm (Cichocki 1976: Ch. 30, modified). [0] caudally directed; [1] approximately parallel. See also Stiassny (1991: 26-27) and Kullander (1998: Ch. 3).

98 Relative lengths of the anterior arm and uncinate process of first epibranchial (Oliver 1984: Ch. 1). [0] approximately equal; [1] uncinate process longer than the anterior arm; [2] uncinate process shorter than anterior arm. See also Oliver (1984: Ch. 9), Stiassny (1991: Ch. 1, 24) and Kullander (1998: Ch. 1).

99 Deep indentation in the dorsal margin of the uncinate process of the first epibranchial (Kullander 1998: Ch. 3). [0] Absent; [1] present. Mentioned by Kullander (1998: Ch. 3, special condition of state 2) for *Satanoperca*, but he did not offer a detailed description. We interpreted a fold, forming a sharp angle at the base of the uncinate process, as the indentation referred to by Kullander.

100 Relative widths of the uncinate process and anterior arm of epibranchial 1 (Kullander 1998: Ch. 4). [0] uncinate process wider; [1] both processes approximately equal. See Kullander (1986, Fig. 37 and 107).

101 Development of an anterior laminar expansion (lobe) of epibranchial 1 (Cichocki 1976: Ch. 32). [0] absent; [1] present, fully developed; [2] present, reduced; [3] present, deep instead of laminar. (Figure II.3)

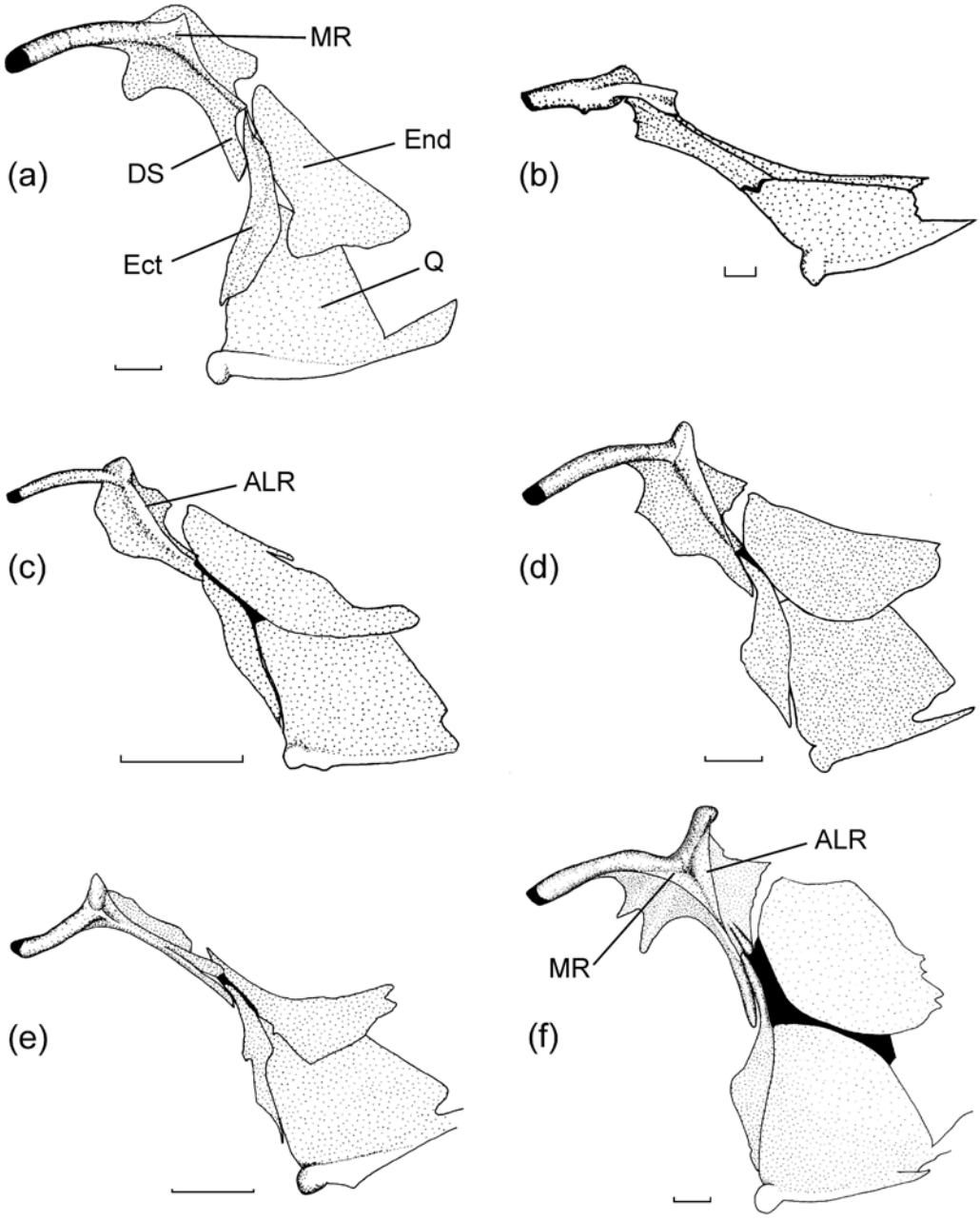

FIG. II.2. Semi-diagrammatic illustration of the anterior portion of the suspensorium in left lateral view, highlighting features of the palatine and associated dermal bones. a) *Retroculus lapidifer* (MNRJ, Uncatalogued); b) *Crenicichla* af. *lugubris* (AMNH, Uncatalogued); c) *Crenicara latruncularium* (AMNH 39751); d) *Biotodoma cupido* (AMNH 39940); e) *Apistogramma hoignei* (AMNH, Uncatalogued); f) *Geophagus dicrozoster* (MCNG 40623). Scale bar = 1 mm. Abbreviations: ALR = axial lateral ridge of the palatine; DS = dermal splint of the palatine; Ect = ectopterygoid; End = endopterygoid; MR = maxillary ridge of the palatine; Q = quadrate.

.

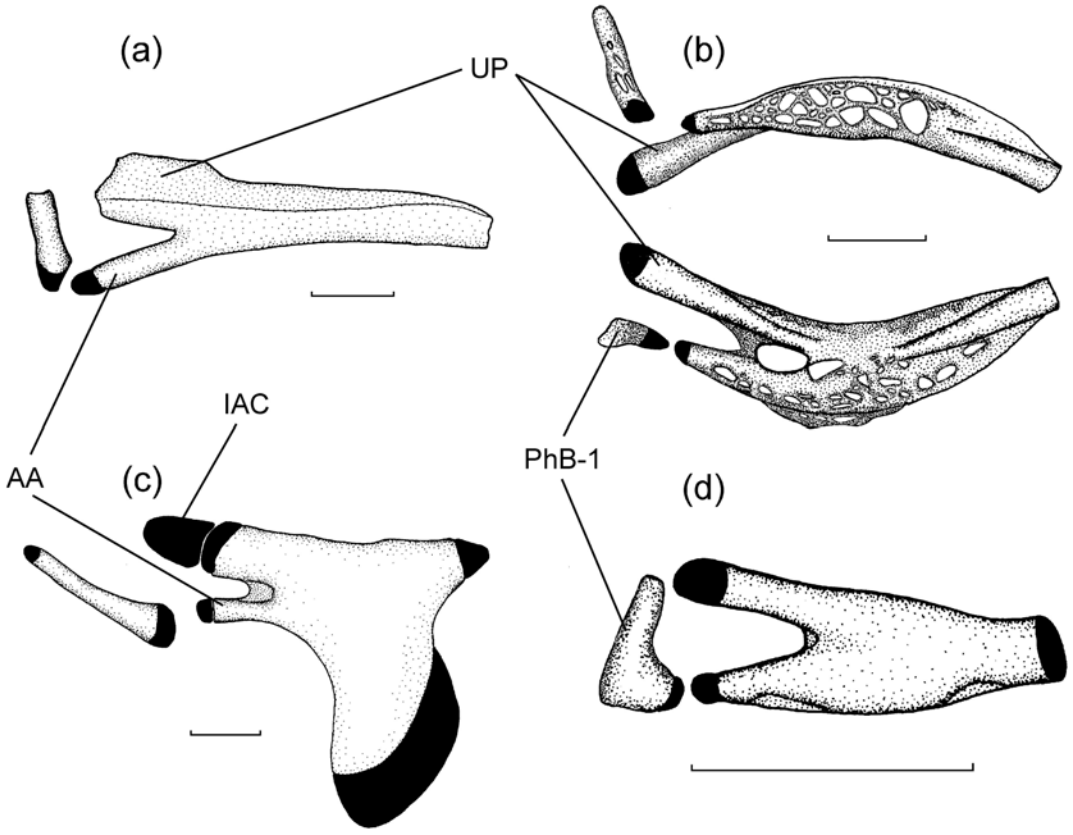

FIG. II.3. Semi-diagrammatic illustration of the first epibranchial and the associated pharyngobranchial in right, approximately antero-dorsal view. Position of the pharyngobranchial is not necessarily natural. a) *Cichla temensis* (AMNH, uncatalogued); b) *Retroculus lapidifer* (MNRJ, Uncatalogued), above: approximately rostral view, below: anterodorsal view; c) *Geophagus dicrozoster* (MCNG 40623); d) *Crenicara latruncularium* (AMNH 39751). Scale bar = 1 mm. Abbreviations: AA = anterior arm of epibranchial 1; IAC = interarcual cartilage; PhB-1 = pharyngobranchial 1; UP = uncinate process (posterior arm) of epibranchial 1.

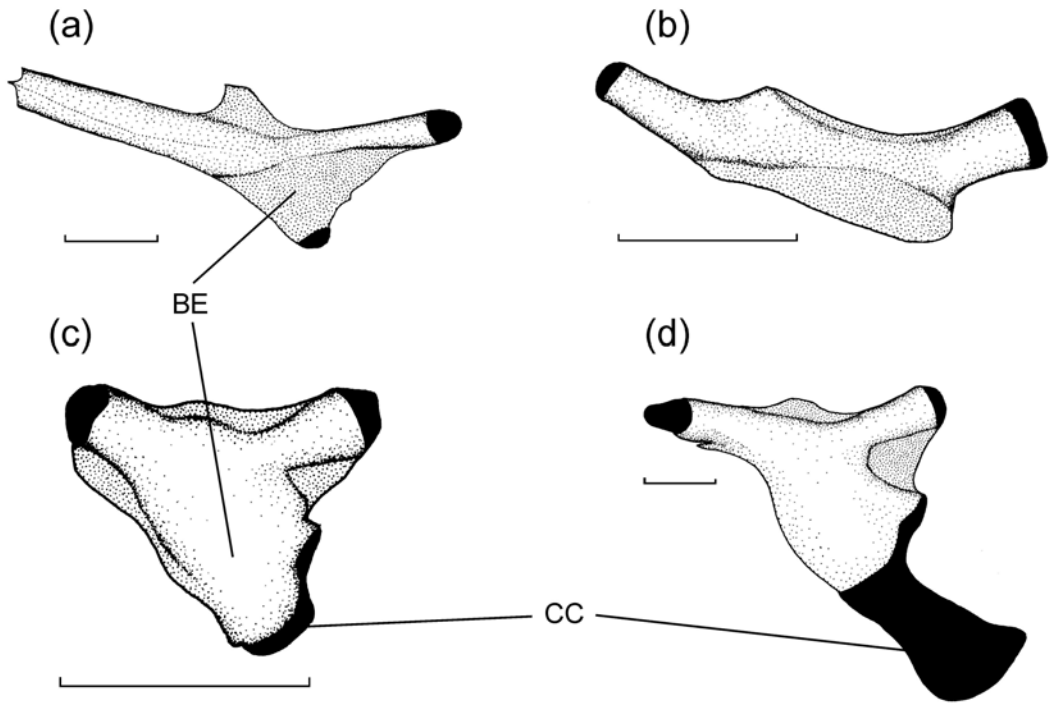

FIG. II.4. Semi-diagrammatic illustration of second epibranchial in left, approximately antero-dorsal view. a) *Cichla temensis* (AMNH, Uncatalogued); b) *Crenicichla* af. *lugubris* (AMNH, Uncatalogued); c) *Mikrogeophagus ramirezi* (AMNH, Uncatalogued); d) *Geophagus dicrozoster* (MCNG 40623). Scale bar = 1 mm. Abbreviations: BE = bony expansion of the second epibranchial; CC = cartilage cap.

102 Rostral margin of epibranchial 2 bearing an antero-ventral laminar expansion. [0] expansion present, with reduced cartilage cap; [1] expansion present without cartilage cap; [2] expansion and cartilage reduced; [3] expansion present with fully developed, axe-shaped cartilage cap. (Figure II.4).

103 Presence and shape of the interarcual cartilage (Kullander 1998: Ch. 22). [0] Present, globular; [1] present, elongate; [2] absent.

104 Condition of the first pharyngobranchial. [0] Bony, [1] cartilaginous.

105 Lateral expansion at the base of pharyngobranchial 1. [0] Absent, [1] present.

106 Rostrocaudal flattening of pharyngobranchial 1. [0] Absent, [1] present.

107 Gill rakers on ceratobranchials. [0] Present; [1] absent.

108 Shape of expansion of EB4. [0] Expansion large, giving an approximately square shape to inner half of epibranchial 4; [1] expansion triangular; [2] expansion follows the contour of epibranchial 4. (Figure II.5)

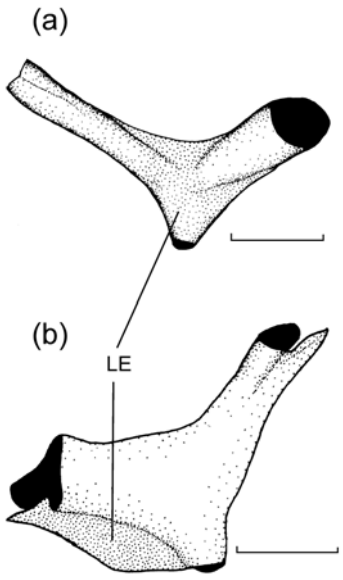

FIG. II.5. Semi-diagrammatic illustration of fourth epibranchial in left, approximately antero-dorsal view. a) *Cichla temensis* (AMNH, Uncatalogued); b) *Geophagus dicrozoster* (MCNG 40623). Scale bar = 1 mm. Abbreviations: LE = laminar expansion of the fourth epibranchial.

109 Fourth ceratobranchial toothplates (Cichocki 1976: Ch. 39). [0] Absent; [1] present, separated from the outer gill rakers. See also Stiassny (1991: Ch. 3).

110 Unicuspid teeth on external gill rakers of ceratobranchial 4. [0] Present; [1] absent.

111 Lateral gill rakers on ceratobranchial 5 (Cichocki 1976: Ch. 40, Fig. 1.21). [0] Absent; [1] present, attenuate, ossified at least at the base and lacking teeth; [2] present, forming low, rounded, and heavily ossified tooth plates.

112 Suture of the lower pharyngeal jaws (Casciotta and Arratia 1993a: Ch. 16). [0] Fully sutured along the saggital axis; [1] not fully sutured. Kullander (1998) indicates that this character may change ontogenetically.

113 Number of concavities in the frayed zone at the caudal edge of the fourth upper pharyngeal toothplate (Casciotta and Arratia 1993a: Ch. 17, Fig. 24A,B). [0] 3 or more; [1] 2; [2] 1. See also Casciotta and Arratia (1993, Fig. 12-13).

PECTORAL GIRDLE

114 Anteriorly directed spinous process on the distal postcleithrum (Stiassny 1987: Ch. 3, Fig. 2). [0] Absent; [1] present; [2] present, reduced to short, blunt process directed anteriorly. Kullander (1998, Ch: 49) added state 2.

115 Relative length of the medial process of the proximal extrascapula. [0] about 2 times in distal process; [1] of approximately equal length as the distal process; [2] at least 4.5-5.0 times in distal process. (Figure II.6).

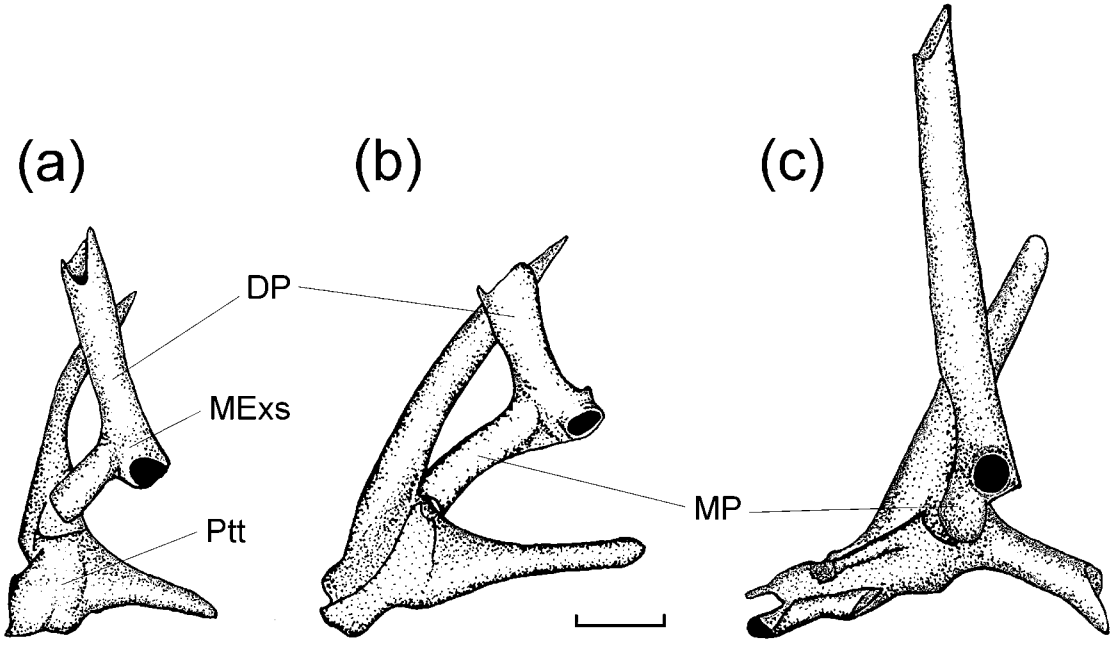

FIG. II.6. Semi-diagrammatic illustration of the post-temporal and proximal extrascapula in left, lateral view. a) *Retroculus lapidifer* (MNRJ, Uncatalogued); b) *Cichla temensis* (AMNH, Uncatalogued), c) *Satanoperca mapiritensis* (MCNG 37262). Scale bar =1 mm. Abbreviations: DP = distal process of the medial extrascapula; MExs = medial extrascapula; MP = medial process of the medial extrascapula; Ptt = post-temporal.

INFRAORBITAL SERIES

Nomenclature used to identify the elements of the infraorbital series is generally not comparable among the work of different authors. Following outgroup analysis, we have adopted the nomenclature used by Kullander (1986). The plesiomorphic condition among Neotropical cichlids is the possession of seven infraorbitals, including two lacrimal ossicles, as found in *Cichla*, *Astronotus*, and *Retroculus* (e.g. see Kullander 1998; Farias et al. 1999, 2000, 2001). The nomenclature of individual ossicles is as follows (and see Fig. 11a): 1 = anteriormost lacrimal, 2 = second lacrimal, (1+2) = the fused lacrimals, 3 to 6 = infraorbitals beyond lachrymal, 7 = dermosphenotic. Any combination of numbers in parentheses indicates fusion of the corresponding elements (Figure II.7).

The following infraorbital characters are derived and modified from Cichocki (1976, characters 45, 46 and 48, Figs. 1.24 to 1.26), Oliver (1984, character 17, Fig. 5), and Kullander (1998, character 3). See also Kullander (1986, Fig. 102) and Kullander (1996, Fig. 13A-C).

116 Infraorbitals 4, 5 and 6. [0] All unfused; [1] (4+5), 6; [2] (4+5+6).

117 Lacrimals. [0], unfused; [1] fused.

118 Infraorbital 3. [0] present, [1] absent.

119 Number of canals in the lacrimal. [0] 3+1 (three on 1, one on 2), [1] 4, [2] 3.

120 Direction of the posterior canal of the lacrimal. [0] posteroventrally directed, [1] posterodorsally directed.

121 Posterior canal of the lacrimal. [0] Extensively open along the caudal margin, forming a half tube; [1] canal terminates in a single pore.

122 Ratio of depth to length of the lacrimal. [0] longer than deep; [1] deeper than long; [2] approximately as long as deep.

123 Notch in the anterodorsal edge of the lachrymal. [0] present, [1] absent. See also Oliver (1984: Fig. 5) and Cichocki (1976: Fig. 1.24).

124 Shape of infraorbital 3. [0] Tubular; [1] tubular, with a ventrally directed laminar expansion; [2] tubular, with ventral and dorsally directed laminar expansions.

125 Association between lacrimal (1+2 or 2) and infraorbital 3. [0] contiguous, but not overlapping; [1] overlapping.

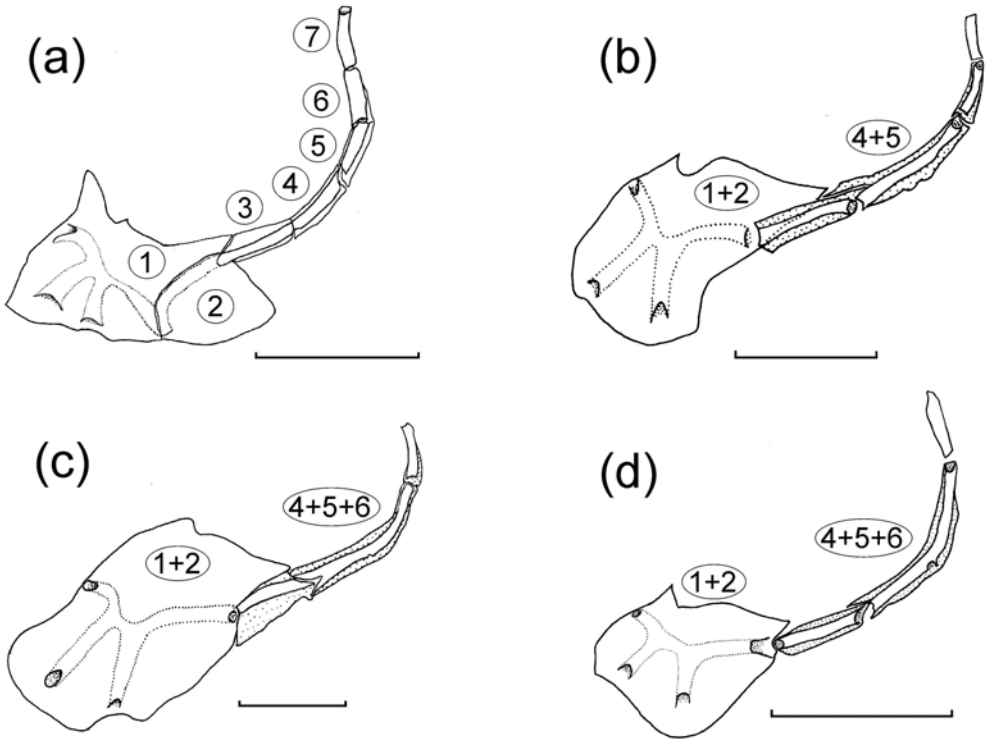

FIG. II.7. Semi-diagrammatic illustration of infraorbital series in left, lateral view. a) *Cichla temensis* (AMNH, Uncatalogued); b) *Geophagus dicrozoster* (MCNG 40623); c) *Satanoperca mapiritensis* (MCNG 37262); d) *Biotodoma cupido* (AMNH 39940). Scale bar = 5 mm. Nomenclature: 1-7 = plesiomorphic number of infraorbital ossicles, where 1 and 2 are separate lacrimals, and 7 is the dermosphenotic; 1+2 = derived, "fused" lacrimals; 4+5 = fusion of ossicles 4 and 5; 4+5+6 = fusion of ossicles 4, 5, and 6.

126 Pointed dorso-caudal laminar expansion of the lacrimal contiguous with the anterodorsal edge of infraorbital 3. [0] Absent; [1] present.

AXIAL SKELETON

127 Number of predorsal bones (Cichocki 1976: Ch. 50). [0] 2, [1] 1, [2] 0. See also Stiassny (1991: Ch. 25) and Kullander (1998: Ch. 67).

128 Procurrent spinous process on the anterodorsal margin of the first dorsal fin pterygiophore (Cichocki 1976: Ch. 51). [0] Absent; [1] present.

129 Total vertebral number (Cichocki 1976: Ch. 57, modified). [0] 32 or more, [1] 26-29, [2] 23-24. See also Stiassny (1987: Ch. 4).

130 Number of anterior vertebrae (Cichocki 1976: Ch. 57, modified). [0] 10-15, [1] 18-24.

131 Number of anterior vertebrae with centra exhibiting relative frontal compression (Cichocki 1976: Ch. 58). [0] 3, [1] 4, [2] 2, [3] 1, [4] 0.

132 Development of parhypurapophysis (Cichocki 1976: Ch. 60). [0] Well developed, terminating at about the mid-longitudinal axis of the vertebral; [1] absent; [2] reduced, terminating not more than one half the distance from its base to mid-vertebral axis.

133 Number of epihemal caudal ribs (Kullander 1998: Ch. 75). [0] 0, [1] 7 or more.

134 Development of vertebral hypapophyses (Pellegrin 1904, Fig. 8). [0] Short, paired; [1] long, co-ossified distally; [2] absent. See also Kullander (1998: Ch. 77).

135 Vertebrae bearing expanded hypapophyses (Pellegrin 1904). [0] 4; [1] 3.

136 Parapophyses of first 2 caudal vertebrae fused, and in turn fused to first anal pterygiophore. [0] Absent; [1] present.

APPENDIX III

MATERIAL EXAMINED

List of material examined for morphological analysis and vouchers specimens for tissue samples used for DNA sequencing. For each genus the following information is given: species name, museum acronym and catalogue number; collection year; preparation mode and number of exemplars (A = alcohol, CS = cleared and stained, DS = dry skeleton, numbers in parentheses indicate number of voucher specimens from which tissue samples for DNA sequencing was taken); country of collection, drainage or state/county, collection locality. Catalogue numbers starting with an H are cross-referenced with museum numbers, and indicate the samples used for DNA sequencing from the tissue collection, Laboratory of Wildlife Genetics, Department of Wildlife and Fisheries Sciences, Texas A&M University. Museum abbreviations are as follows: AMNH – American Museum of Natural History, New York, USA; BM (NH) = British Museum (Natural History), London, UK; MCNG = Museo de Ciencias Naturales de Guanare, Guanare, Venezuela; MNHN = Muséum National d'Histoire Naturelle, Paris, France; MNRJ = Museu Nacional do Rio de Janeiro, Brazil; NLU = North Eastern Louisiana University, Monroe, USA; TCWC = Texas Cooperative Wildlife Collection, College Station, USA. Uncatalogued material will be deposited at the Department of Ichthyology of the American Museum of Natural History, unless otherwise indicated. More detailed locality data, if available, can be found at the Neodat project's website (www.neodat.org), on the websites of each museum, or on request from HLF.

OUTGROUP TAXA

Astronotus crasspinnis: (AMNH 221982); 1987; A = 1, CS = 1; Argentina, no further data.

Astronotus sp.: (TCWC 7502.28); 1993; A = 1; Venezuela, Portuguesa, Caño Maraca at Finca Urriola. - (AMNH Uncatalogued, H6297-6298); 2001; A = 2(2); Aquarium trade.

Cichla intermedia: (AMNH Uncatalogued); 2002; DS = 1; Venezuela, Apure, Río Cinaruco, Pica Raya reef. - (AMNH Uncatalogued); 2002; DS = 1; Venezuela, Apure, Río Cinaruco. - (AMNH Uncatalogued); 2001; A = 1; Venezuela, Apure, Río Cinaruco. - (MCNG 39581); 1999; CS = 1; Venezuela, Apure, Río Cinaruco. - (MCNG 41117); 1999; CS = 1; Venezuela, Apure, Río Cinaruco. - (H6238, No voucher); 2000; Venezuela, Apure, Río Cinaruco at Payara hole (reef point).

Cichla orinocensis: (AMNH Uncatalogued); 2002; DS = 1; Venezuela, Apure, Río Cinaruco, Laguna Larga N shore. - (AMNH Uncatalogued); 2002; DS = 1; Venezuela, Apure, Río Cinaruco. - (TCWC 8312.08); 1994; A = 2, CS = 3; Venezuela, Bolívar, Río Caroní, NE Guri reservoir near dam F. - (TCWC 7500.37); 2001; A = 1; Venezuela,

Apure, Río Apure at Laguna Larga. - (H6237, No voucher); 2000; Venezuela, Apure, Río Cinaruco at Payara hole (reef point).

Cichla temensis: (AMNH Uncatalogued); 2002; DS = 1; Venezuela, Apure, Río Cinaruco, Laguna Larga. - (AMNH Uncatalogued); 1994; A = 7, CS = 3; Venezuela, Apure, Río Cinaruco. - (AMNH Uncatalogued); 2000; A = 1; Venezuela, Apure, Río Cinaruco, Laguna Larga at mouth of Caño Largo. - (AMNH Uncatalogued); 2000; A = 1; Venezuela, Apure, Río Cinaruco at Laguna Larga. - (H6239, No voucher); 2000; Venezuela, Apure, Río Cinaruco at Payara hole (reef point).

Retroculus lapidifer: (BM(NH) 1970.10.28:59); 1968; A = 1; Brazil, Mattogrosso, Rio das Mortes, Xaventina Island. - (MNRJ Uncatalogued); 1999; A = 3, CS = 2; Brazil, Goiás, Rio Maranhão, at Cachoeria do Macadinho. - (MNRJ SM 21-521 E. P. Caramaschi); 1999; A = 1; Brazil, Rio Tocantins, Serra da Mesa reservoir at dam.

Retroculus sp.: (H6293, No known voucher); No date; Brazil, Macapá.

CICHLASOMATINAE

Cichlasoma orinocense: (AMNH Uncatalogued, H6209-6210); 2000; CS, T = 2; Venezuela, Apure, road from La Pedrera (Táchira State) to Guasdualito, a few minutes after Las Guacas. - (AMNH Uncatalogued, H6211); 2000; A = 2(2); Venezuela, Apure, Caño Maporal at iron bridge on road to UNELLEZ modulo.

Hoplarchus psittacus: (AMNH Uncatalogued); 2002; DS = 1; Venezuela, Apure, Río Cinaruco. - (AMNH Uncatalogued); 2002; DS = 1; Venezuela, Apure, Río Cinaruco. - (MCNG 39961); 1999; A = 7, CS = 2; Venezuela, Apure, Río Cinaruco, Laguna Oheros. - (MCNG Uncatalogued, H6241); 2000; A = 1(1); Venezuela, Apure, Río Cinaruco, Caño at mouth of Laguna Larga.

Mesonauta egregius: (AMNH Uncatalogued, H6226-6227); 2000; A = 3(3), CS = 1(1); Venezuela, Apure, Caño Maporal at iron bridge on road to UNELLEZ modulo.

GEOPHAGINAE

Acarichthys heckelii: (AMNH 14352); 1937; A = 3, CS = 2; Guyana, Essequibo, Essequibo river at Rockstone. - (AMNH 221358); 1977; A = 1; Brazil, Amazonas, branch of the Rio Janauacá at mouth of Lago do Castanho. - (AMNH Uncatalogued, H6288-6289); 2000; A = 2(2); Aquarium trade.

Apistogrammoides pucallpaensis: (AMNH Uncatalogued, H6203-6204); 1999; A = 8(4), CS = 2; Perú, Río Orosa, Pacaurillo and/or Madre Selva reserve.

Apistogramma hoignei: (AMNH Uncatalogued); 2000; A = 1; Venezuela, Apure, road from La Pedrera (Táchira State) to Guasdualito, a few minutes after Las Guacas. - (AMNH Uncatalogued, H6223); 2000; A = 4(3); Venezuela, Apure, Caño Maporal at iron bridge on the road to UNELLEZ modulo.

Apistogramma agassizi: (AMNH 21582); No date; CS = 1; Peru, Amazon basin. - (AMNH Uncatalogued, H6199-6200); 1999; A = 3(3); Perú, Río Orosa, Pacaurillo and/or Madre Selva reserve.

Biotodoma cupido: (AMNH 40148); 1964; A = 1; Bolivia, Beni, Arroyo Grande, 2 km W Guayamerín, ca. 1.5 km above mouth. - (AMNH 215177); No date; A = 47; Guyana, Demerara, Malali. - (AMNH 39940); 1964; A = 10, CS = 2; Bolivia, Beni, Río Iténez, 2 km SE Costa Marques, Brazil. - (AMNH 43359); 1935; CS = 1; Guyana, Demerara, Malali. - (AMNH Uncatalogued; H6195-6196); 1999; A = 3, T = 3; Perú, Río Orosa, Pacaurillo reserve.

Biotodoma wavrini: (AMNH Uncatalogued); 1999; A = 17, CS = 2; Venezuela, Apure, Río Cinaruco at Laguna Larga. - (MCNG 41367, H6202); 1999; A = 1(1); Venezuela, Apure, Río Cinaruco at Laguna Larga. - (AMNH Uncatalogued, H6230); 2000, A = 6(6); Venezuela, Apure, Río Cinaruco at Payara hole (reef point). - (AMNH Uncatalogued); 2000, A = 2; Venezuela, Apure, Río Cinaruco, Laguna Larga at mouth of Caño Largo.

Biotoecus dicentrarchus: (AMNH 221350); 1977; A = 1; Brazil, Amazonas, Ilha de Marchantaria. - (NLU 75944); 1999; A = 20; Venezuela, Apure, Rio Cinaruco at Laguna Larga. - (AMNH Uncatalogued); 1999; A = 1; Venezuela, Apure, Río Cinaruco. - (AMNH Uncatalogued, H6249-6250); 2000; A = 12(6), CS = 4; Venezuela, Apure, Río Cinaruco at Laguna Larga.

Crenicara punctulatum: (AMNH 78126); 1987; A = 1; Peru, Loreto, Rio Tahuayo, tributary of Rio Amazonas, at Huasi village. - (AMNH 39917); 1964; CS = 2; Bolivia, Beni, Pond in arroyo below lower campo of Pampa de Meio, ca. 12 km SE Costa Marques, Brazil.

Crenicara latruncularium: (AMNH 39751); 1964; A = 13, CS = 2; Bolivia, Beni, Río Iténez, 2 km SE Costa Marques, Brazil. - (AMNH Uncatalogued, H6301-6302); 2003; A = 2(2); Aquarium trade.

Crenicichla geayi: (AMNH Uncatalogued, H6207-6208); 2000; A = 1(1), CS = 1(1); Venezuela, Portuguesa, Río Las Marías at Quebrada Seca.

Crenicichla af. *lugubris*: (AMNH Uncatalogued); 2002; DS = 1; Venezuela, Apure, Río Cinaruco, Caño Largo. - (AMNH Uncatalogued); 2002; DS = 1; Venezuela, Apure, Río Cinaruco. - (AMNH Uncatalogued); 2002; DS = 1; Venezuela, Apure, Río Cinaruco. -

(MCNG 40225); 1999; A = 1; Venezuela, Apure, Río Cinaruco at Laguna Larga. - (MCNG 41034); 1999; A = 1; Venezuela, Apure, Río Cinaruco at Laguna Estrechura. - (MCNG 40122); 1999; CS = 1; Venezuela, Apure, Río Cinaruco at Laguna Las Guayabas. - (H6230, No voucher); 2000; Venezuela, Apure, Río Cinaruco at Payara hole (reef point). - (H6242, No voucher); 2000; Venezuela, Apure, Río Cinaruco at Laguna Larga.

Crenicichla sveni: (AMNH Uncatalogued, H6213-6214); 2000; A = 2(2), CS = 2(2); Venezuela, Apure, road between Guasdualito and Elorza.

Crenicichla af. *wallacii*: (AMNH Uncatalogued, H6244-6245); 2000; A = 2(2), CS = 2(2); Venezuela, Apure, Río Cinaruco at Laguna Larga. - (AMNH Uncatalogued); 2000; A = 2; Venezuela, Apure, Río Cinaruco, Laguna Larga at mouth of Caño Largo.

Dicrossus filamentosus: (MCNG 12190); 1985; A = 12, CS = 5; Venezuela, Amazonas, Caño Iguarapo, aprox. 1 km above mouth, near Piedra de Culimacare of Río Casiquiare.

Dicrossus sp.: (H6285, Sample is voucher); 2000; Aquarium trade.

Geophagus abalios: (AMNH Uncatalogued); 2002; DS = 1; Venezuela, Apure, Río Cinaruco. - (AMNH Uncatalogued); 2002; DS = 1; Venezuela, Apure, Río Cinaruco. - (MCNG 40636); 1999; CS = 1; Venezuela, Apure, Río Cinaruco. - (H6259-6260, No vouchers); 2000; Venezuela, Apure, Río Cinaruco at Laguna Larga.

Geophagus brachybranchus: (AMNH 72130); 1982; A = 2; Guyana, Essequibo, sandbar on N bank of Cuyuní river, just W of Caowrie creek mouth. - (AMNH 215202); No date; A = 19; Guyana, Demerara, Demerara river at Wismar. - (AMNH 72098); 1982; A = 2; Guyana, Essequibo, Kartabo point, between Cuyuní river mouth and Mazaruni river mouth. - (AMNH 54944); 1979; CS = 3; Surinam, Nickerie, Camp Hydro, ca. km 370, ca. 30 km N Tiger Falls. - (AMNH 54881); 1979; A = 26; Surinam, Nickerie, Toeboeroe creek, km 220, 300-900 m from mouth. - (AMNH Uncatalogued, H6271-6272); 2000; A = 3(3); Surinam, Nickerie, Toeboeroe creek, km 220, 300-900 m from mouth.

Geophagus dicrozoster: (AMNH Uncatalogued); 2002; DS = 1; Venezuela, Apure, Río Cinaruco, Caño Largo. - (AMNH Uncatalogued); 2002; DS = 1; Venezuela, Apure, Río Cinaruco. - (AMNH Uncatalogued, H6255-6256); 2000; A = 5(4); Venezuela, Apure, Río Cinaruco at Laguna Larga. - (AMNH Uncatalogued); 2000; A = 1; Venezuela, Apure, Río Cinaruco at Payara hole (reef point).

Geophagus grammepareius: (MCNG 34396); 1994; A = 2, CS = 3; Venezuela, Bolívar, Río Caroní near Río Claro. - (AMNH Uncatalogued, H6265); 2000; A = 1(1); Venezuela, Bolívar, Río Claro at bridge on the road to Guri.

Geophagus surinamensis: (MNHN 2001.2275); 2001; A = 2; French Guiana, Antécume Pata, Upper Maroni river. - (MNHN 2001.2279, H6299); 2001; A = 2(1); French Guiana, Antécume Pata, Upper Maroni river. - (MNHN 2001.2280, H6300); 2001; A = 2(1); French Guiana, Antécume Pata, Upper Maroni river. - (MNHN 2001.2281); 2001; A = 3, CS = 2; French Guiana, Antécume Pata, Upper Maroni river.

'Geophagus' brasiliensis: (AMNH 222386); 1991; A = 7, CS = 3; Brazil, Sâo Paulo, Rio Pardo at Riberão Preto. - (AMNH Uncatalogued, H6286-6287); 2000; A = 2(2; Aquarium trade.

'Geophagus' steindachneri: (MCNG 758); 1976; A = 11, CS = 2; Venezuela, Trujillo, Río Motatán at Puente 3 de febrero. - (AMNH Uncatalogued, H6283-6284); 2001; A = 2(2); Aquarium trade.

Guianacara n. sp. 'caroni': (AMNH 91068); 1990; CS = 1; Venezuela, Bolívar, Río Paragua above second rapids above Río Carapo mouth. - (AMNH Uncatalogued, H6266-6267); 2000; A = 27(5), CS = 2; Venezuela, Bolívar, Río Claro, at bridge on the way to Guri.

Gymnogeophagus balzanii: (AMNH 1278); 1901; A = 1, CS = 1; Paraguay, Río Paraguay at Asunción. – (AMNH Uncatalogued, H6296); 2001; Aquarium trade.

Gymnogeophagus rhabdotus: (AMNH Uncatalogued, H6296); 2001; A = 1(1). Aquarium trade. - (AMNH 12348); 1933; A = 5, CS = 3; Argentina, Buenos Aires. - (AMNH Uncatalogued, H6294-6295); 2001; A = 2(2). Aquarium trade.

Mikrogeophagus altispinosus: (AMNH Uncatalogued, H6278-6279); 2000; A = 5(5), CS = 2; Aquarium trade.

Mikrogeophagus ramirezi: (AMNH Uncatalogued); 2000; A = 1; Venezuela, probably Monagas State, no other data available. - (AMNH Uncatalogued, H6217-6218); 2000; A = 4(4), CS = 2(2); Venezuela, Apure, Caño Maporal at iron bridge on the way to UNELLEZ modulo.

Satanoperca daemon: (AMNH Uncatalogued); 2002; DS = 1; Venezuela, Apure, Río Cinaruco. - (AMNH Uncatalogued); 2002; DS = 1; Venezuela, Apure, Río Cinaruco. - (AMNH Uncatalogued); 2002; DS = 1; Venezuela, Apure, Río Cinaruco. - (AMNH Uncatalogued); 2000; A = 5; Venezuela, Apure, Río Cinaruco, Laguna Larga at mouth of Caño Largo. - (AMNH Uncatalogued); 1999; A = 6, CS =1; Venezuela, Apure, Río Cinaruco at Laguna Larga. - (MCNG 37255); 1997; A = 1, CS = 1; Venezuela, Guárico, Aguaro-Guariquito National Park, Caño Charcotico. - (AMNH Uncatalogued, H6261-6261); 2000; A = 2(2); Venezuela, Apure, Río Cinaruco at Laguna Larga. - (MCNG Uncatalogued, H6248); 2000; A = 1(1); Venezuela, Apure, Río Cinaruco at Laguna Larga.

Satanoperca jurupari: (AMNH 12752); 1934; A = 8, CS = 1; Brazil, Amazonas, Rio Livramento, tributary of Rio Madeira. - (AMNH Uncatalogued, H6198); 1999; A = 1(1); Perú, Río Orosa at Yanashi. - (H6198, No voucher); 1999; Perú, Caño Santa Rita, Nanay drainage.

Satanoperca mapiritensis: (AMNH Uncatalogued, H6263-6264); 2000; A = 2(2); Venezuela, Bolívar, Río Pao at the most E cross with road between Maripa and Ciudad Bolívar. - (AMNH Uncatalogued, H6274-6275); 2000; A = 4(4); Venezuela, Anzoátegui, Río Morichal Largo. - (AMNH Uncatalogued); 1999; CS =1; Venezuela, Apure, Río Cinaruco at Laguna Larga.

Satanoperca pappaterra: (AMNH 40103); 1964; A = 8, CS = 2; Brazil, Rondonia, Overflow pond of Rio Guaporé 1 km W Costa Marques. (H6309-6310, No vouchers);2000; Brazil, Rio Paraná.

Taeniacara candidi: (AMNH Uncatalogued, H6290-6291); 2000; A = 2(2), CS = 1; Aquarium trade.

ADDITIONAL MATERIAL EXAMINED

African taxa

Paratilapia mellandi: (AMNH 9011); 1925; A = 4; Angola, Cunene river at Capelongo.

Paratilapia polleni: (AMNH 217760); 1988 or 1990; CS = 1; No further data.

Ptychochromis oligacanthus: (AMNH 97028); 1990; A= 3, CS = 2; Madagascar, Tamatave, Bay Lake, 1 km S of turnoff from Marolambo-Mananjary road.

Ptychochromoides katria: (AMNH 93700); 1990; CS = 5; Madagascar, River Novosivolo below Zule's village, large side-pool off mainstream.

Tylochromis leonensis: (AMNH 59650); 1990; A = 11; Sierra Leone, River Taia, Taiama Bridge.

Tylochromis variabilis: (AMNH 57162); 1915; CS = 1; Congo, Stanleyville.

Outgroup

Cichla ocellaris: (AMNH 97396); No date; CS = 1; No further data.

Cichlasomatinae

Heros n. sp. ‘common’ (AMNH Uncatalogued); 2002; DS = 1; Venezuela, Apure, Río Cinaruco. - (AMNH Uncatalogued); 2002; DS = 1; Venezuela, Apure, Río Cinaruco.

Mesonauta festivum: (AMNH 40053); 1964; CS = 3; Bolivia, Beni, Río Baures, 500 miles above mouth, on left.

Geophaginae

Biotodoma af. *cupido*: (AMNH 12751); 1934; A = 2; Brazil, Amazonas, Rio Livramento, tributary of Rio Madeira.

Guianacara sphenozona: (AMNH 54857); 1979; A = 5; Surinam, Nickerie, Kabelebo river, 1 km S Avanavero falls. - (AMNH 54763); 1979; A = 18; Surinam, Nickerie, Kapoeri creek, ca. 7 km from junction of Corintijn [Corantijn] river. - (AMNH 17635); 1938; A = 4; Guyana, Essequibo, blackwater creek at Essequibo river headwaters. - (AMNH 54939); 1979; CS = 5; Surinam, Nickerie, Camp Hydro, ca. km 370, ca. 30 km N Tiger Falls.

Gymnogeophagus gymnogenys: (AMNH 57055); 1985; A = 2, CS = 1; Brazil, Rio Grande do Sul, near Porto Alegre.

Geophagus harreri: (AMNH 16434); 1939; A = 2; Surinam, Marowijne, Litani river near Tapoute.

Geophagus megasema: (AMNH 39936); 1964; A = 1; Bolivia, Beni, Río Iténez 5 km SW Costa Marques, Brazil.

Geophagus taeniopareius: (AMNH 56180); 1981; A = 2, CS = 2; Venezuela, Amazonas, Río Cataniapo, ca. 800 m from mouth, near Puerto Ayacucho.

Satanoperca leucosticta: (AMNH 215096); 1935; A = 8; Guyana, Demerara, Demerara river at Wismar. - (AMNH 7090); 1908; A = 3; Guyana, Demerara, Maduni creek.- (AMNH 214849); 1934; A = 2; Guyana, Demerara, Demerara river at Malali. - (AMNH 215206); No date; Guyana, Demerara, Demerara river at Wismar.

APPENDIX IV

CODED MATRIX OF MORPHOLOGICAL CHARACTERS

	1	2	3	4	5	6	7	8	9	10	11	12	13	14	15	16	17	18	19	20	21	22	23	24	25	26	27	28	29	30	31	32	33	34	35	36	37	38	39	40
Acarichthys heckelii	0	0	0	0	0	0	0	0	0	0	0	1	1	0	0	0	0	0	0	0	0	0	1	2	1	0	0	0	0	1	0	1	0	1	-	-	-	1	-	1
Apistogramma agassizi	0	1	0	1	2	0	4	0	0	1	0	1	1	0	0	0	0	0	0	0	1	0	1	2	1	0	0	0	0	1	0	1	0	1	-	-	-	1	-	1
Apistogramma hoignei	0	1	0	0	2	0	0	0	0	1	0	1	1	0	0	0	0	0	0	0	1	0	0	2	1	0	0	0	0	1	0	1	0	1	-	-	-	1	-	1
Apistogrammoides pucallpaensis	0	1	0	0	2	0	0	0	0	1	0	1	1	0	0	0	0	0	0	1	1	0	0	2	1	0	0	0	0	1	0	1	0	1	-	-	-	1	-	1
Astronotus sp.	0	0	0	0	0	0	0	0	2	0	1	0	0	5	1	0	0	0	0	0	1	0	0	0	0	0	0	0	0	1	0	1	0	0	0	0	0	0	0	0
Biotodoma cupido	0	0	0	0	3	-	2	0	0	0	0	1	1	2	0	0	0	0	0	0	0	0	1	0	1	0	1	0	0	1	1	1	0	1	-	-	-	1	-	1
Biotodoma wavrini	0	0	1	0	3	-	3	0	0	0	0	1	1	2	0	0	0	0	0	0	0	0	1	2	1	0	0	0	0	1	0	1	0	1	-	-	-	1	-	1
Biotoecus dicentrarchus	1	0	1	0	3	-	2	0	0	0	0	1	1	0	1	0	1	1	1	-	-	-	-	2	0	1	0	0	0	1	0	1	0	1	-	-	-	1	-	1
Cichla intermedia	0	0	0	1	1	0	0	0	1	1	0	1	0	7	0	0	0	0	0	0	0	0	1	0	0	0	1	0	1	1	0	0	0	1	-	-	-	0	1	0
Cichla orinocensis	0	0	0	1	1	1	0	0	1	1	0	1	0	6	0	0	0	0	0	0	0	0	0	0	0	0	1	0	1	0	1	0	1	0	0	1	0	0	1	0
Cichla temensis	0	0	0	0	0	0	2	0	1	1	0	1	2	7	0	0	0	0	0	0	0	0	0	0	0	0	0	0	0	0	1	0	1	0	0	1	0	0	1	0
Cichlasoma orinocense	0	1	0	1	2	1	0	1	0	1	0	1	1	0	0	1	0	0	0	1	0	0	1	0	1	0	0	0	0	1	1	1	0	0	0	0	1	2	0	0
Crenicara punctulatum	1	1	1	1	0	1	0	1	0	1	0	1	1	0	0	0	0	0	0	1	1	0	0	2	1	0	0	0	0	1	1	1	0	1	-	-	-	1	-	1
Crenicichla geayi	0	0	0	0	0	0	0	0	0	0	0	1	1	0	0	1	0	1	0	0	1	0	0	0	0	1	0	1	1	1	0	1	0	1	-	-	-	1	-	1
Crenicichla af. *lugubris*	0	0	0	0	0	0	0	0	1	0	0	0	2	8	1	0	0	1	0	0	1	0	0	0	1	1	0	1	1	1	0	1	0	1	-	-	-	1	-	1
Crenicichla sveni	0	0	0	0	0	0	0	0	1	0	0	0	1	4	1	0	0	0	0	0	0	0	1	1	0	1	0	0	1	1	0	2	0	1	-	-	-	1	-	1
Crenicichla af. *wallacei*	0	0	0	0	0	0	0	0	1	0	0	0	1	4	1	0	0	1	0	0	1	0	0	0	1	1	0	1	1	1	0	1	0	1	-	-	-	1	-	1
Dicrossus sp.	1	1	1	0	0	0	?	?	0	?	0	1	1	0	0	0	0	0	0	1	1	0	0	2	1	0	1	0	0	1	0	1	0	1	-	-	-	1	-	1
Geophagus abalios	0	1	0	1	1	1	1	1	0	1	0	1	1	2	0	0	0	0	0	0	0	0	1	0	0	0	0	0	0	0	1	0	0	0	1	0	0	0	0	0

	1	2	3	4	5	6	7	8	9	10	11	12	13	14	15	16	17	18	19	20	21	22	23	24	25	26	27	28	29	30	31	32	33	34	35	36	37	38	39	40
Geophagus brachybranchus	0	1	0	1	0	0	1	1	0	1	1	1	1	2	0	0	0	0	0	0	0	0	1	0	0	0	0	0	0	0	1	0	0	0	1	0	0	0	0	1
Geophagus dicrozoster	0	1	1	1	1	0	1	1	0	0	0	1	1	3	0	0	0	0	0	0	0	0	1	0	0	0	0	0	0	0	1	0	0	0	1	0	0	0	0	1
Geophagus grammepareius	1	1	0	0	0	0	1	0	0	0	1	1	1	2	0	0	0	0	0	0	0	0	1	0	0	0	0	0	0	1	0	1	0	0	1	-	-	-	1	-	1
Geophagus surinamensis	0	1	0	1	0	1	1	1	0	0	0	1	1	2	0	0	0	0	0	0	0	0	1	0	1	0	1	0	0	0	1	0	0	0	1	0	0	1	-	0
'Geophagus' brasiliensis	0	0	1	0	1	0	0	0	0	0	0	1	1	0	0	0	0	0	0	0	1	0	0	0	1	0	0	0	0	1	1	1	0	1	-	-	-	1	-	1
'Geophagus' steindachneri	0	1	0	1	3	-	0	0	0	1	0	1	1	0	0	0	0	0	0	0	0	0	1	0	1	0	0	0	0	1	1	1	0	0	0	0	1	3	0	1
Guianacara n. sp. 'caroni'	0	0	0	0	0	0	0	0	0	0	0	1	1	0	0	0	0	0	0	0	0	0	0	2	1	0	0	0	0	1	0	1	0	1	-	-	-	1	-	1
Gymnogeophagus balzanii	1	0	1	0	0	0	0	0	0	0	0	1	1	2	0	0	0	1	0	1	1	0	0	0	1	0	0	0	0	1	1	1	0	0	1	0	1	1	-	0
Gymnogeophagus rhabdotus	1	0	1	0	3	-	1	0	0	0	0	1	1	1	0	0	0	0	0	0	0	0	1	0	1	0	0	0	0	1	1	1	0	1	-	-	-	1	-	1
Hoplarchus psittacus	0	0	0	0	1	0	0	0	0	0	0	1	1	3	0	0	0	0	0	0	0	0	1	0	0	0	0	0	0	1	1	1	1	0	0	0	1	1	0	1	0
Mesonauta egregius	0	0	0	0	2	0	0	0	0	0	0	0	1	1	0	0	1	0	0	0	1	0	0	0	0	0	0	0	0	0	-	1	1	1	0	0	0	0	1	0	0
Mikrogeophagus altispinosa	0	1	0	1	1	0	0	1	0	1	0	1	1	0	0	0	0	0	0	1	1	0	0	2	0	0	0	0	0	1	1	1	0	1	-	-	-	1	-	1
Mikrogeophagus ramirezi	0	1	0	1	1	0	0	0	0	1	0	1	1	0	0	0	0	0	0	1	1	0	0	2	1	0	0	0	0	1	1	1	0	1	-	-	-	1	-	1
Retroculus sp.	0	1	1	1	0	1	1	0	0	1	0	1	1	3	0	0	0	0	0	0	0	1	1	0	0	1	0	1	1	0	1	0	1	0	1	0	1	0	0	1
Satanoperca daemon	1	0	0	0	0	0	0	0	0	0	0	1	1	2	0	0	0	0	0	0	0	0	1	0	1	0	1	0	1	1	0	1	0	1	-	-	-	1	-	1
Satanoperca jurupari	1	1	1	1	0	1	0	1	0	1	0	1	1	6	0	0	0	0	0	1	1	0	0	0	1	0	0	0	0	1	1	1	0	1	-	-	-	1	-	1
Satanoperca mapiritensis	1	1	0	1	0	0	0	1	0	1	0	1	1	0	0	1	0	0	0	0	1	0	0	0	1	0	1	0	0	1	1	1	0	1	-	-	-	1	-	1
Satanoperca pappaterra	1	1	0	1	0	0	0	1	0	1	0	1	1	0	0	0	0	0	0	0	1	0	0	0	1	0	1	0	0	1	1	1	0	1	-	-	-	1	-	1
Taeniacara candidi	0	0	?	?	1	0	0	0	0	0	0	1	1	1	1	0	0	0	0	0	1	0	0	2	1	0	0	0	0	1	1	1	0	1	-	-	-	1	–	1

	4 1	4 2	4 3	4 4	4 5	4 6	4 7	4 8	5 9	5 0	5 1	5 2	5 3	5 4	5 5	5 6	5 7	5 8	5 9	6 0	6 1	6 2	6 3	6 4	6 5	6 6	6 7	6 8	6 9	7 0	7 1	7 2	7 3	7 4	7 5	7 6	7 7	7 8	7 9	8 0
Acarichthys heckelii	-	-	-	1	-	0	0	0	0	1	0	0	0	0	0	1	0	0	0	0	0	5	0	1	2	1	-	-	0	1	1	0	0	0	0	1	0	0	0	1	0
Apistogramma agassizi	-	-	-	1	-	0	0	0	1	1	1	1	1	1	1	1	4	0	0	0	2	1	1	2	0	1	1	0	1	0	1	1	1	0	1	0	0	0	0	1
Apistogramma hoignei	-	-	-	1	-	0	0	0	1	1	1	1	1	1	1	?	4	0	0	0	2	1	1	2	0	1	1	0	1	1	1	1	0	1	1	0	0	0	0	1
Apistogrammoides pucallpaensis	-	-	-	1	-	0	0	0	1	1	1	1	1	1	1	1	5	0	1	0	2	1	1	2	0	1	1	0	1	1	1	1	1	0	1	0	0	0	0	1
Astronotus sp.	0	0	0	0	1	0	0	0	0	0	0	0	0	0	0	0	0	0	0	0	0	0	0	0	0	0	0	0	0	0	0	0	0	2	?	0	0	0	0	1
Biotodoma cupido	-	-	-	1	-	0	0	1	0	1	0	0	1	0	1	0	3	0	0	0	0	0	0	2	1	-	-	0	1	1	0	0	1	0	0	0	0	0	0	1
Biotodoma wavrini	-	-	-	1	-	0	0	0	0	1	0	0	0	0	1	0	0	0	0	0	5	0	1	2	1	-	-	0	1	1	0	0	0	0	0	0	0	0	0	1
Biotoecus dicentrarchus	-	-	-	1	-	0	0	0	0	1	1	1	1	1	2	1	6	-	-	0	1	2	1	2	0	1	2	0	0	0	2	0	0	1	1	1	1	0	0	0
Cichla intermedia	1	1	0	0	0	0	0	0	0	0	0	0	0	0	0	0	7	-	0	-	8	3	1	0	0	0	0	0	0	0	0	0	1	0	0	0	0	1	0	0
Cichla orinocensis	1	1	0	0	0	0	0	0	0	0	0	0	0	0	0	0	0	0	0	1	7	3	1	0	0	0	0	0	0	0	0	0	1	1	0	0	0	1	0	0
Cichla temensis	1	1	0	0	0	0	0	0	0	0	0	0	0	0	0	0	7	-	-	-	8	-	0	0	0	0	0	0	0	0	1	1	1	3	0	0	0	1	0	0
Cichlasoma orinocense	0	0	1	2	1	0	?	?	0	1	0	1	0	0	1	1	1	0	0	0	3	0	1	2	0	0	0	0	0	0	0	0	1	1	0	?	0	0	0	1
Crenicara punctulatum	-	-	-	1	-	1	0	1	0	1	1	1	1	1	1	1	2	0	0	0	3	2	1	2	0	1	-	0	0	3	0	1	0	4	0	0	0	0	1	1
Crenicichla geayi	-	-	-	1	-	1	0	0	0	1	0	0	0	0	1	0	1	0	0	1	6	0	0	2	0	0	0	0	0	0	1	1	1	0	0	1	1	0	0	1
Crenicichla af. *lugubris*	-	-	-	1	-	1	0	0	0	1	0	0	0	0	1	0	1	0	0	1	9	3	0	2	0	0	1	0	3	0	1	1	1	0	0	1	1	0	0	1
Crenicichla sveni	-	-	-	1	-	1	0	0	0	1	0	0	0	0	1	0	1	0	0	0	0	0	1	2	0	0	0	0	0	0	1	1	1	0	0	1	1	0	0	1
Crenicichla af. *wallacei*	-	-	-	1	-	1	1	0	0	1	1	1	1	1	1	?	1	0	0	0	6	0	0	2	0	0	0	0	0	0	1	1	0	0	0	1	1	0	0	1
Dicrossus sp.	-	-	-	1	-	1	1	1	0	1	1	1	1	1	1	1	4	0	0	0	3	2	1	2	0	1	2	0	0	0	2	2	0	4	0	0	0	0	1	1
Geophagus abalios	0	0	1	0	1	0	0	0	0	1	0	0	0	0	1	0	0	0	0	0	6	0	0	0	1	-	-	0	0	0	0	0	1	0	0	0	0	0	1	1

	41	42	43	44	45	46	47	48	49	50	51	52	53	54	55	56	57	58	59	60	61	62	63	64	65	66	67	68	69	70	71	72	73	74	75	76	77	78	79	80
Geophagus brachybranchus	-	-	-	1	-	0	0	0	0	1	0	0	0	0	0	1	0	0	0	0	0	0	0	2	1	0	1	-	-	0	0	0	0	0	1	0	0	0	0	0	1	1
Geophagus dicrozoster	-	-	-	1	-	0	0	0	0	1	0	0	0	0	0	1	0	0	-	0	0	6	0	0	0	1	-	-	0	4	0	0	0	1	0	0	0	0	0	1	1
Geophagus grammepareius	-	-	-	1	-	0	0	?	0	1	0	0	0	0	0	1	0	0	0	0	0	0	0	2	1	1	1	-	-	0	2	0	0	0	1	0	0	0	0	0	1	1
Geophagus surinamensis	0	0	1	1	-	0	0	0	0	1	0	0	0	0	0	1	0	0	0	0	0	0	0	0	1	0	0	-	-	0	0	0	0	0	1	0	0	0	0	0	1	1
'Geophagus' brasiliensis	-	-	-	1	-	0	0	0	0	1	0	0	0	0	0	1	0	0	0	0	0	3	2	1	0	0	1	1	0	2	1	0	0	0	0	0	0	0	0	1	1
'Geophagus' steindachneri	-	-	-	3	1	0	0	0	0	1	0	0	0	0	0	1	0	0	0	0	0	4	2	0	0	0	1	1	0	3	1	0	0	0	0	0	0	0	0	1	0
Guianacara n. sp. 'caroni'	-	-	-	1	-	0	0	0	0	1	0	0	0	0	0	1	0	0	0	0	0	4	2	1	2	1	-	-	0	1	1	0	0	0	0	1	0	0	0	1	1
Gymnogeophagus balzanii	0	0	1	1	-	0	0	0	0	1	0	0	1	1	1	0	0	0	0	0	5	0	0	0	1	-	-	0	3	2	0	0	1	0	0	0	0	0	1	1
Gymnogeophagus rhabdotus	-	-	-	1	-	0	0	0	0	1	1	1	1	1	1	?	?	?	?	0	4	2	?	?	1	-	-	0	3	1	0	0	1	0	0	0	0	0	1	1
Mesonauta egregius	0	0	1	3	1	0	0	0	0	1	1	1	1	1	1	1	1	0	0	0	4	0	2	1	1	0	0	0	0	0	1	1	1	0	0	0	0	0	0	0
Hoplarchus psittacus	0	0	1	3	1	0	0	0	0	1	0	0	0	0	0	1	1	0	0	0	1	6	0	1	2	0	0	1	1	0	0	1	1	1	1	0	0	0	0	0	0
Mikrogeophagus altispinosa	-	-	-	1	-	1	0	0	0	1	1	1	1	1	1	0	2	0	0	0	3	2	1	0	1	-	-	1	2	1	0	0	1	0	1	0	0	0	1	1
Mikrogeophagus ramirezi	-	-	-	1	-	0	0	0	0	1	1	1	1	1	1	?	1	0	0	0	3	2	0	0	0	1	1	0	2	1	0	0	0	0	1	0	0	0	0	1
Retroculus sp.	-	-	-	0	0	0	0	?	0	0	0	0	0	?	0	1	0	1	0	0	0	0	0	0	1	1	-	-	1	0	1	0	0	0	0	0	0	0	0	0	0
Satanoperca daemon	-	-	-	1	-	0	1	0	0	1	0	0	0	0	0	1	0	0	0	0	0	5	0	1	0	0	0	0	0	0	2	0	0	1	0	0	0	0	0	0	1
Satanoperca jurupari	-	-	-	1	-	0	0	0	0	1	0	0	0	0	0	1	0	0	0	0	0	4	2	0	0	0	0	1	0	0	2	0	0	0	0	0	0	0	0	0	1
Satanoperca mapiritensis	-	-	-	1	-	0	0	0	0	1	0	0	0	0	0	1	0	0	0	0	0	4	2	1	0	0	0	1	0	0	0	0	0	1	0	0	0	0	0	1	1
Satanoperca pappaterra	-	-	-	1	-	0	1	0	0	1	0	0	0	0	0	1	0	0	0	0	0	5	2	1	0	0	0	1	0	0	0	0	0	1	1	0	0	0	0	0	?
Taeniacara candidi	-	-	-	1	-	0	?	?	1	1	1	?	1	1	2	1	4	0	0	0	1	1	1	2	0	1	1	0	1	0	1	1	1	0	0	0	0	0	0	1

	81	82	83	84	85	86	87	88	89	90	91	92	93	94	95	96	97	98	99	100	101	102	103	104	105	106	107	108	109	110	111	112	113	114	115	116	117	118	119	120
Acarichthys heckelii	0	0	0	0	0	0	0	0	1	0	1	2	0	1	?	0	1	0	0	0	0	3	0	0	1	1	0	0	1	1	0	0	1	2	2	1	1	0	1	1
Apistogramma agassizi	1	0	0	0	0	0	1	0	0	0	0	3	0	0	1	0	1	0	0	0	1	0	1	0	0	0	0	0	0	1	1	0	2	0	0	1	1	1	1	1
Apistogramma hoignei	1	0	0	0	0	1	1	0	0	0	0	3	0	1	1	1	1	1	0	0	1	0	1	0	0	1	0	0	0	1	1	0	2	0	2	1	1	1	1	1
Apistogrammoides pucallpaensis	1	0	0	0	0	0	1	0	0	0	0	3	1	-	1	1	1	1	0	0	1	0	1	0	1	1	0	0	0	1	1	0	2	0	0	1	1	1	1	1
Astronotus sp.	0	0	0	0	0	0	0	0	0	0	0	0	0	0	0	0	1	0	0	0	0	0	0	0	0	1	0	0	0	0	0	0	0	0	0	1	0	0	0	0
Biotodoma cupido	1	0	0	0	0	0	0	0	0	0	1	1	0	1	1	1	1	1	0	1	1	3	1	0	1	0	0	0	1	1	0	0	1	2	2	2	1	0	1	1
Biotodoma wavrini	0	0	0	0	0	0	0	0	0	0	1	1	0	1	1	1	1	1	0	0	1	3	1	0	1	1	0	0	1	1	0	0	1	2	2	2	1	0	1	1
Biotoecus dicentrarchus	1	0	0	0	0	1	0	0	0	1	1	1	0	1	1	?	1	1	0	1	0	3	0	1	0	0	1	0	0	1	0	0	?	?	?	-	1	1	2	0
Cichla intermedia	1	1	0	1	0	0	0	1	0	0	0	0	0	1	0	0	0	0	0	0	0	2	0	0	0	0	0	0	1	0	0	0	1	0	1	1	0	0	0	0
Cichla orinocensis	1	1	0	1	0	0	0	1	0	0	0	0	0	1	0	0	0	0	0	0	0	2	0	0	0	0	0	0	1	0	0	0	1	0	1	1	0	0	0	0
Cichla temensis	1	1	0	1	0	0	0	1	0	0	0	0	0	1	0	0	0	0	0	0	0	2	0	0	0	0	0	0	1	1	0	0	1	0	1	1	0	0	0	0
Cichlasoma orinocense	1	0	0	0	0	0	0	0	1	0	1	1	0	1	1	1	1	2	0	0	0	?	0	0	0	1	0	0	1	0	0	0	0	0	0	1	1	0	1	1
Crenicara punctulatum	1	0	0	0	0	1	1	0	1	1	1	1	0	1	1	0	0	1	0	1	2	0	0	0	1	1	0	0	0	1	0	0	1	0	0	2	1	0	1	1
Crenicichla geayi	1	1	1	0	2	1	0	2	0	2	0	4	1	0	?	0	1	1	0	1	0	1	0	1	1	1	0	2	1	0	1	0	1	1	?	?	?	0	?	?
Crenicichla af. *lugubris*	1	0	1	0	2	0	0	2	0	2	0	4	1	-	1	0	1	1	0	1	0	1	0	1	0	0	0	2	1	0	2	0	1	1	0	0	1	0	1	1
Crenicichla sveni	1	1	1	0	2	0	0	1	0	2	0	4	1	-	1	0	1	1	0	1	0	1	0	1	1	1	0	2	1	0	2	0	1	1	1	0	1	0	1	1
Crenicichla af. *wallacei*	1	1	1	0	0	0	0	2	0	2	0	4	1	-	1	?	1	1	0	1	0	1	?	?	?	?	0	2	1	0	2	0	1	?	1	0	1	0	1	1
Dicrossus sp.	1	0	0	0	0	1	0	0	1	1	1	1	0	1	1	?	0	1	0	0	2	0	2	0	0	0	1	0	0	1	0	0	1	0	0	2	1	0	1	1
Geophagus abalios	0	0	0	0	1	0	0	0	1	0	1	2	0	2	0	1	1	0	0	0	1	3	1	0	1	1	0	0	1	1	0	0	1	0	2	1	1	0	1	1

	81	82	83	84	85	86	87	88	89	90	91	92	93	94	95	96	97	98	99	100	101	102	103	104	105	106	107	108	109	110	111	112	113	114	115	116	117	118	119	120
Geophagus brachybranchus	0	0	0	0	1	0	0	0	1	0	1	2	0	2	0	1	1	0	0	0	1	3	1	0	1	1	0	0	1	1	0	0	1	0	0	1	1	0	1	1
Geophagus dicrozoster	0	0	0	0	1	0	0	0	1	0	1	2	0	2	0	1	1	0	0	0	1	3	1	0	1	0	0	0	1	1	0	0	1	0	2	1	1	0	1	1
Geophagus grammepareius	0	0	0	0	0	0	0	0	1	0	1	2	0	2	0	1	1	0	0	0	1	3	1	0	1	1	0	0	1	1	0	0	1	0	2	1	1	0	1	1
Geophagus surinamensis	0	0	0	0	1	0	0	0	1	0	1	2	0	2	0	1	1	0	0	0	1	3	1	0	1	1	0	0	1	1	0	0	1	2	2	1	1	0	1	1
'Geophagus' brasiliensis	1	0	0	0	0	0	0	0	1	0	1	1	0	1	0	1	1	1	0	0	1	0	1	0	1	1	0	0	1	0	1	0	1	0	2	1	1	0	1	1
'Geophagus' steindachneri	0	0	0	0	0	0	0	0	0	0	0	2	0	2	0	1	1	1	0	0	1	0	1	0	1	1	0	0	1	0	1	0	1	0	1	1	1	0	1	1
Guianacara n. sp. 'caroni'	1	0	0	0	1	0	0	0	1	0	1	1	0	1	0	0	1	1	0	0	0	0	0	0	0	1	1	0	0	1	0	0	0	1	2	2	1	1	0	1	1
Gymnogeophagus balzanii	0	0	0	0	1	0	0	0	0	0	0	2	0	1	1	1	1	0	0	0	1	0	0	0	0	0	0	0	1	1	0	0	1	0	2	2	1	0	1	1
Gymnogeophagus rhabdotus	0	0	0	0	2	0	0	0	0	0	1	?	0	1	0	1	1	0	0	0	1	1	0	0	1	1	0	0	1	1	0	0	1	0	2	2	1	0	1	1
Hoplarchus psittacus	0	0	0	0	1	0	0	0	0	0	1	1	0	1	0	1	1	0	0	0	0	1	0	0	0	1	0	0	1	0	0	0	0	2	2	2	1	0	1	1
Mesonauta egregius	1	0	0	0	1	0	0	0	0	1	1	1	0	1	0	1	1	0	0	0	0	3	0	0	1	1	0	0	1	0	0	0	0	0	2	2	1	0	1	1
Mikrogeophagus altispinosa	1	0	0	0	0	0	0	0	1	0	0	1	0	1	0	0	1	1	0	0	1	0	0	0	1	1	0	0	1	1	1	0	1	2	0	1	1	0	1	1
Mikrogeophagus ramirezi	1	0	0	0	0	1	0	0	1	0	0	1	0	1	0	0	1	1	0	0	1	0	0	0	1	1	0	0	1	1	0	0	1	2	0	1	1	0	1	1
Retroculus sp.	0	0	0	0	1	0	0	0	0	0	0	1	0	3	0	1	0	1	0	1	3	1	0	0	0	0	0	0	1	0	0	0	0	2	0	0	0	0	0	0
Satanoperca daemon	1	0	0	0	0	0	0	0	0	0	0	2	0	0	1	1	0	1	1	0	1	3	1	0	1	1	0	0	0	1	0	0	1	0	2	2	1	0	1	1
Satanoperca jurupari	0	0	0	0	0	0	0	0	0	0	0	2	0	0	1	1	0	1	1	0	1	3	1	0	1	1	0	0	0	1	0	0	1	0	2	2	1	0	1	1
Satanoperca mapiritensis	0	0	0	0	1	0	0	0	0	0	0	2	0	0	1	1	0	1	1	0	1	3	1	0	0	1	0	0	0	1	0	0	1	0	2	2	1	0	1	1
Satanoperca pappaterra	?	0	0	0	1	0	0	0	0	0	0	2	0	0	?	1	0	1	1	0	1	3	1	0	1	1	0	0	0	1	0	0	1	0	2	2	1	0	1	1
Taeniacara candidi	1	0	0	2	2	1	0	0	0	0	1	3	1	-	1	1	0	1	0	0	2	1	1	0	0	0	0	0	0	?	1	0	2	0	1	-	1	1	?	?

	1 1 1 1 1 1 1 1 1 1 1 1 1 1 1 1
	2 2 2 2 2 2 2 2 2 3 3 3 3 3 3 3
	1 2 3 4 5 6 7 8 9 0 1 2 3 4 5 6
Acarichthys heckelii	1 1 0 ? 1 1 1 0 1 0 0 0 0 0 1 0
Apistogramma agassizi	1 0 1 0 1 1 1 0 2 0 2 1 0 2 – 0
Apistogramma hoignei	? 0 ? 0 1 ? 1 0 2 0 2 1 0 2 – 0
Apistogrammoides pucallpaensis	1 0 1 1 1 1 1 0 2 0 2 1 0 2 – 0
Astronotus sp.	1 0 0 0 0 0 0 0 0 0 0 1 0 1 0 0
Biotodoma cupido	1 2 0 2 0 1 0 0 1 0 0 0 0 0 1 0
Biotodoma wavrini	1 2 0 2 0 1 0 0 1 0 0 0 0 0 1 0
Biotoecus dicentrarchus	? 0 0 - - 0 1 0 1 0 2 2 0 0 1 0
Cichla intermedia	0 0 0 2 1 0 0 0 0 0 2 0 0 0 1 0
Cichla orinocensis	0 0 0 2 1 0 0 0 0 0 2 0 0 0 1 0
Cichla temensis	0 0 0 2 1 0 0 0 0 0 2 0 0 0 1 0
Cichlasoma orinocense	1 0 1 0 1 0 0 0 1 0 1 2 0 0 0 0
Crenicara punctulatum	1 0 0 0 0 0 1 0 1 0 0 2 0 0 1 0
Crenicichla geayi	? 0 0 ? ? ? 2 0 0 1 4 1 0 2 – 0
Crenicichla af. *lugubris*	1 0 0 0 1 0 2 0 0 1 2 1 0 2 – 0
Crenicichla sveni	? 0 ? 0 ? 0 2 0 0 1 3 1 0 2 – 0
Crenicichla af. *wallacei*	? 0 0 0 ? 0 2 0 0 1 3 1 0 2 – 0
Dicrossus sp.	1 0 0 0 0 1 1 0 1 0 2 2 0 2 – 0
Geophagus abalios	1 1 0 1 1 1 1 0 1 0 0 0 1 1 1 0

	1 1 1 1 1 1 1 1 1 1 1 1 1 1 1 1 2 2 2 2 2 2 2 2 2 3 3 3 3 3 3 3 1 2 3 4 5 6 7 8 9 0 1 2 3 4 5 6
Geophagus brachybranchus	1 1 0 1 1 1 1 0 1 0 0 0 1 1 1 0
Geophagus dicrozoster	1 1 0 1 1 1 1 0 1 0 0 0 1 1 1 0
Geophagus grammepareius	1 1 0 1 1 1 1 0 1 0 0 0 1 1 1 0
Geophagus surinamensis	1 1 0 1 1 1 1 0 1 0 0 0 1 1 1 0
'Geophagus' brasiliensis	? 2 0 0 0 1 1 0 1 0 2 2 0 0 1 0
'Geophagus' steindachneri	1 1 0 1 1 1 1 0 1 0 2 0 0 1 1 0
Guianacara n. sp. 'caroni'	1 1 0 2 1 1 0 0 1 0 0 0 0 0 1 0
Gymnogeophagus balzanii	1 1 0 1 1 1 2 1 1 0 0 0 0 1 1 0
Gymnogeophagus rhabdotus	1 2 0 1 1 1 2 1 1 0 0 2 0 1 1 0
Hoplarchus psittacus	1 2 0 0 1 0 0 0 1 0 0 2 0 1 1 1
Mesonauta egregius	1 2 0 0 1 0 0 0 1 0 0 1 0 1 1 1
Mikrogeophagus altispinosa	1 0 0 2 1 0 1 0 1 0 0 2 0 0 1 0
Mikrogeophagus ramirezi	1 0 0 0 0 0 1 0 1 0 0 2 0 0 1 0
Retroculus sp.	0 1 0 1 0 1 0 0 0 0 0 0 0 0 0 0
Satanoperca daemon	1 1 0 0 1 1 1 0 1 0 1 0 0 1 1 0
Satanoperca jurupari	1 1 0 1 1 1 1 0 1 0 1 0 0 1 1 0
Satanoperca mapiritensis	1 1 0 1 1 1 1 0 1 0 1 0 0 1 1 0
Satanoperca pappaterra	1 1 0 ? 1 1 1 0 1 0 1 0 0 1 1 0
Taeniacara candidi	? 0 0 - - 0 1 0 2 0 2 1 0 2 – 0

VITA

Hernán López Fernández

Apartado Postal 506, Mérida 5101, Edo. Mérida, Venezuela

Education

2004 PhD. Wildlife and Fisheries Sciences, Texas A&M University

1998 B.S. Biology, Universidad de Los Andes, Venezuela

Honors, Awards & Fellowships

2004 Ph.D. Student Award. Wildlife and Fisheries Sciences, Texas A&M University

2003 Best Oral Presentation, Neotropical Ichthyological Association

2001, 2003 Axelrod Fellowship, Department of Ichthyology, American Museum of Natural History

1991-1996 "Award to Talent" Program, Undergraduate Scholarship, Fundación Gran Mariscal de Ayacucho (Venezuelan Government)

Peer Reviewed Publications

López-Fernández, H. & D.C. Taphorn. 2004. *Geophagus abalios*, *G. dicrozoster* and *G. winemilleri* (Perciformes: Cichlidae), three new species from Venezuela. Zootaxa, 439: 1-27.

López-Fernández, H. & K. O. Winemiller. 2003. Morphological variation in *Acestrorhynchus microlepis* and *A. falcatus* (Characiformes: Acestrorhynchidae), reassessment of *A. apurensis* and distrinution of *Acestrorhynchus* in Venezuela. Ichthyological Exploration of Freshwaters, 14: 193-208.

López-Fernández, H. & K. O. Winemiller. 2000. A review of Venezuelan species of *Hypophthalmus* (Siluriformes: Pimelodidae). Ichthyological Exploration of Freshwaters, 11:35-46.